A typical microscopy experiment

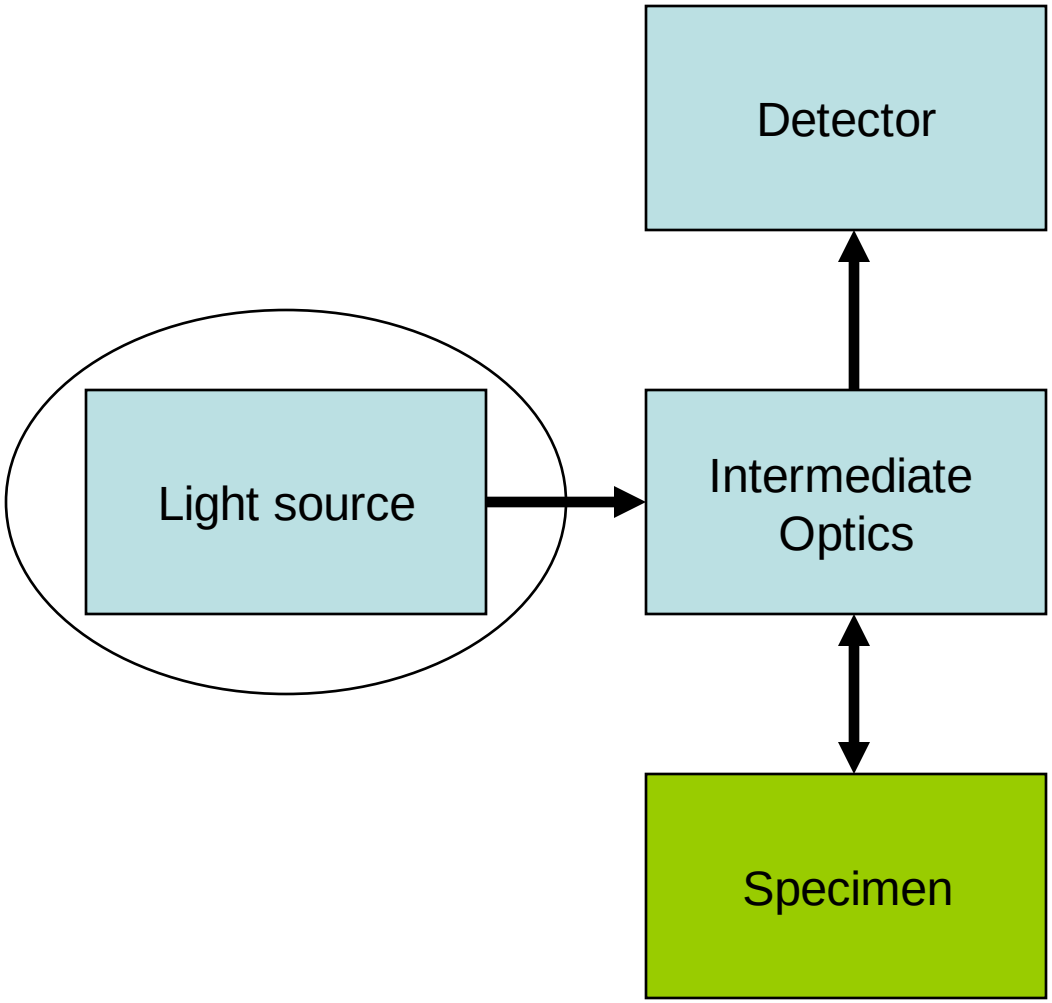

Lasers – A Coherent Light Source

Laser = Light amplification of stimulated emission of radiation

Invented in 1950s by Charles Townes, Alexandr Prokhorov, & Nikolai Basov

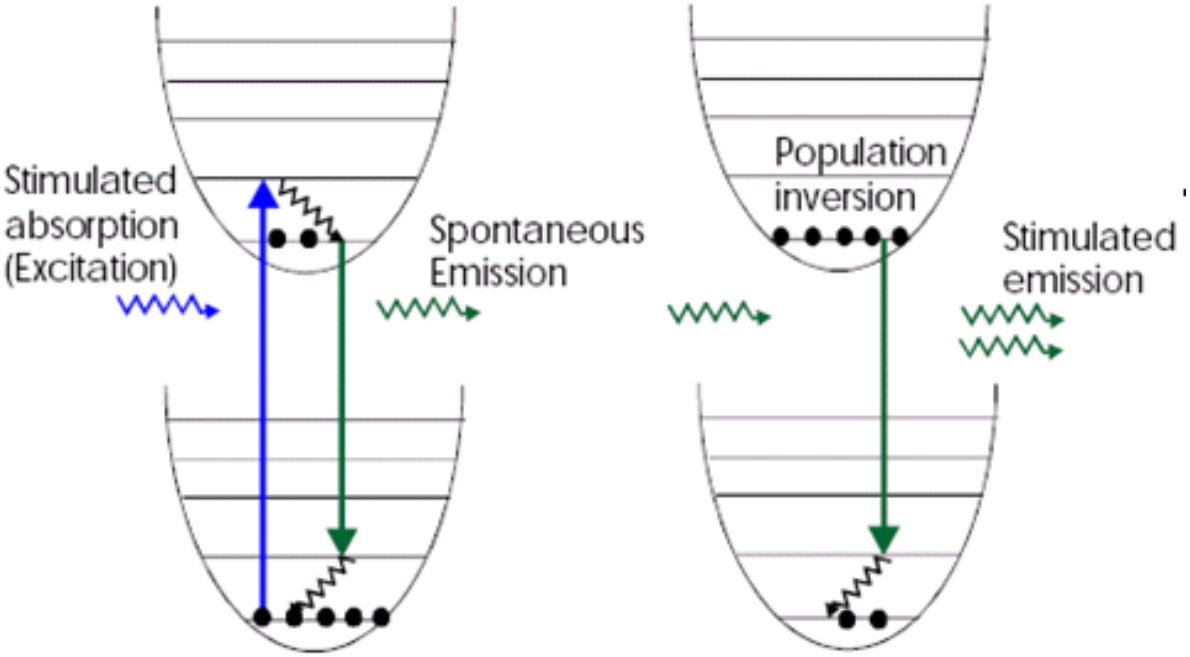

Stimulation emission is the opposite of (stimulated) absorption
Stimulated emission is a “photon copier.”
The emitted photon has identical properties as the “stimulating” photon:
same color, direction, polarization: Indistinguishable

What does all these have to do with laser?

What is good about laser? What we want from a light source that a lamp is not?

(1) Monochromatic
(2) High spectral radiance
(3) Low divergence
(4) Unique polarization
(5) Long coherence length

How do we achieve this? If we can “copy” a photon many times. Then we have IT … laser, Nobel prize, ….

We need two things: (1) amplification, (2) population inversion

Basic Idea of A Laser

Put a lasing medium in "population inversion" between two mirrors. An avalanche, amplification, process occurs as a spontaneous emitted photon bounce back and forth between the two mirrors to "copy" more of itself.

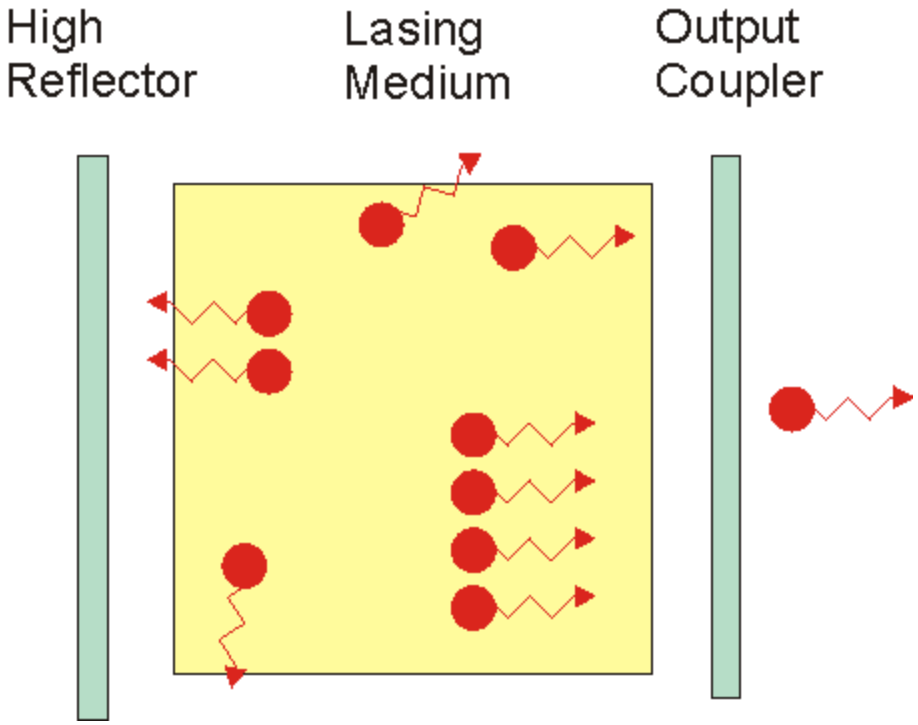

Uni-directionality comes from the fact that only photons going between the two mirrors are amplified.

Population inversion is needed so that the probability of stimulated emission is much greater than absorption to sustained the avalanche process

A Better Understanding of How Light Interaction with Molecules Is Needed to Know How to Create Population Inversion

Einstein studied these three processes: stimulated absorption, Stimulated emission, and spontaneous emission

Let N_i, N_j be the population of molecules in the ground and excited states

Let I be the energy density of light

$$\frac{dN_j}{dt} = -B_{ji} N_j I - A_{ji} N_j + B_{ij} N_i I$$

At steady state, the ground and excited states population is constant:

$$B_{ij} N_i I = B_{ji} N_j I + A_{ji} N_j \qquad \frac{N_j}{N_i} = \frac{B_{ij} I}{B_{ji} I + A_{ji}}$$

The relative populations of the states not only can be determined by kinetic consideration but also by thermodynamics

We also know from statistical mechanics that the populations of two states in thermal equilibrium is described by Boltzmann statistics

$$N_{i,j} = N_0 e^{-\frac{E_{i,j}}{kT}}$$

where E is the energy of states i and j, k is the Boltzmann's constant and T is the absolute temperature

$$\frac{N_j}{N_i} = e^{-\frac{(E_j - E_i)}{kT}} = e^{-\frac{\Delta E}{kT}}$$

Einstein B Coefficients

Combining kinetics and thermodynamics:

$$\rho = \frac{\frac{A_{ji}}{B_{ji}}}{\frac{B_{ij}}{B_{ji}} e^{\frac{\Delta E}{kT}} - 1}$$

What happens when temperature approach infinity?

We expect light density also grows to infinity
(driving all the molecules instantly to the excited state).

$$\rho \to \infty \quad as \quad T \to \infty \quad requires \quad B_{ij} = B_{ji} = B$$

"Einstein B coefficient"

The rate constants of stimulated absorption and emission are equal

$$\rho = \frac{\frac{A}{B}}{e^{\frac{\Delta E}{kT}} - 1}$$

Population inversion is not possible in a 2-state system

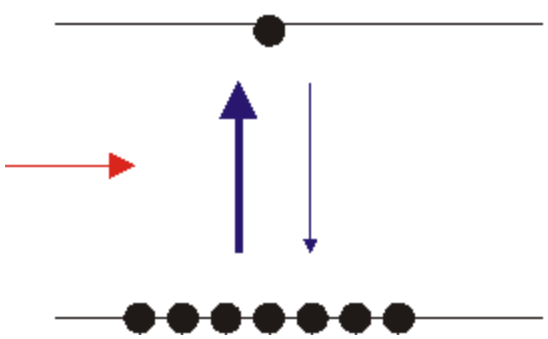

Low Light

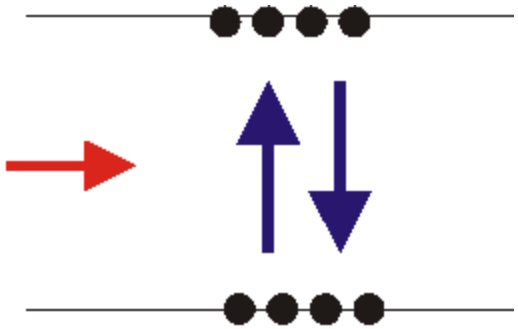

High Light

As excited state becomes well populated, the excitation and de-excitation probability becomes equal because the Einstein coefficients for up and down are equal

Population inversion is possible in a 3-state system

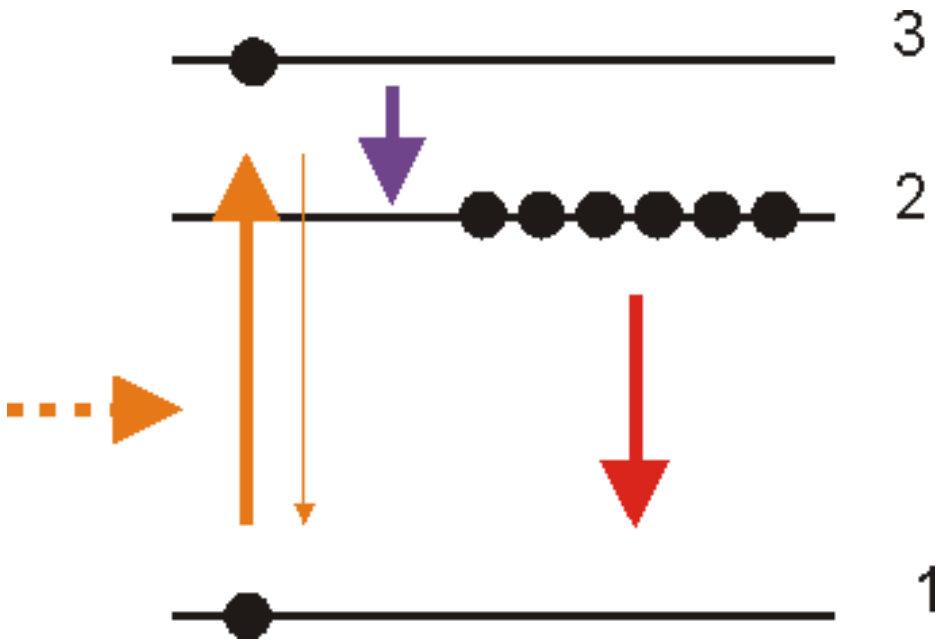

Population inversion can be created if:

(1) Spontaneous decay rate to from state 3 to state 2 is the fastest
(2) Stimulated excitation rate from state 1 to state 3 is faster or comparable to the decay rate from state 2 to state 1
(3) Population inversion is created between state 1 and 2
(4) Increasing “pump” power (orange) do not cause stimulated emission from state 2

A typical microscopy experiment

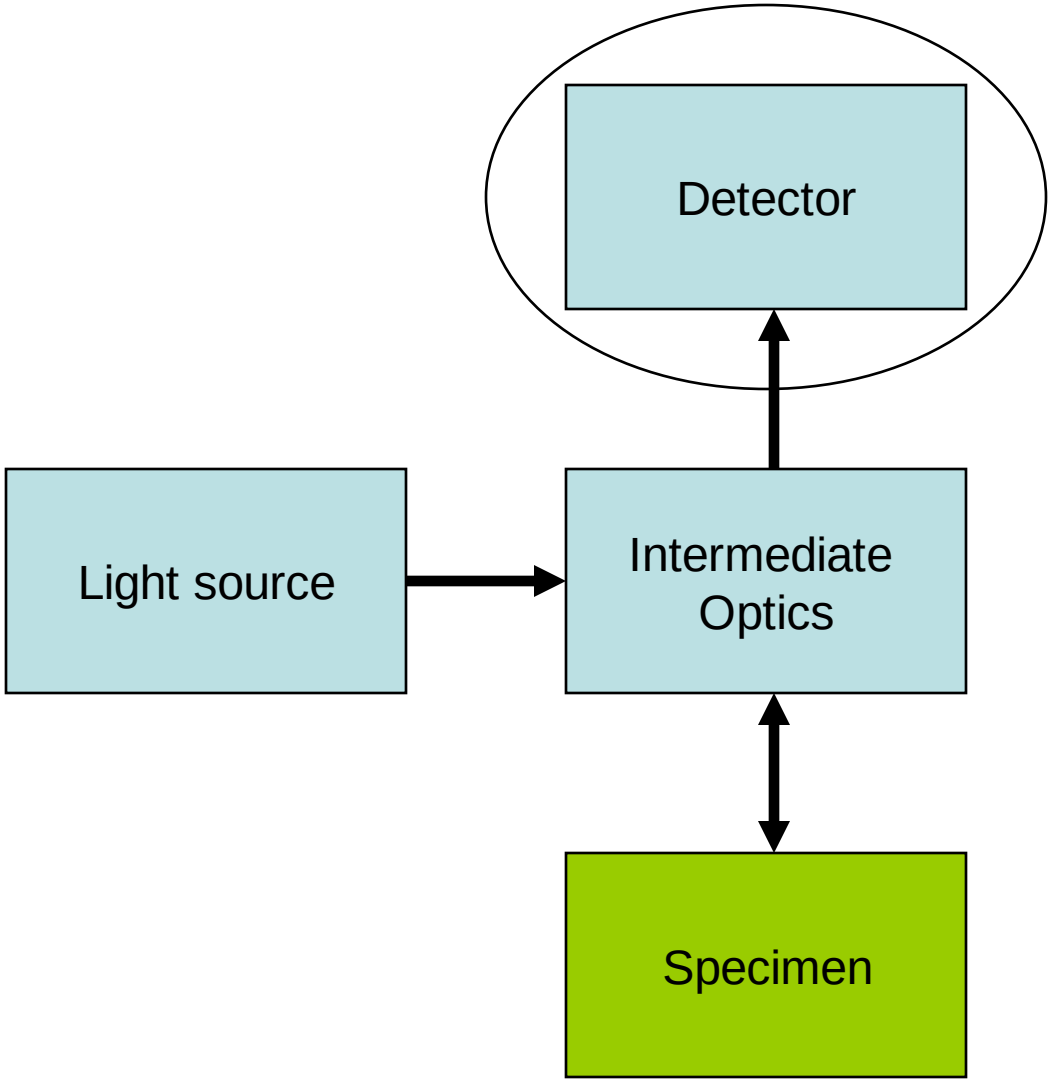

Noise Sources of A Detector

1. Photon Shot Noise – Counting statistics of the signal photons

2. Dark Current Noise – Counting statistics of spontaneous electron generated in the device

3. Johnson Noise – Thermally induced current in the transimpedence amplifier

Optical Shot Noise

Photon arrival at detector are statistically independent, "uncorrelated", events

What do we meant by uncorrelated?

$$\lim_{T\to\infty}\frac{1}{T}\int_{-T/2}^{T/2}(n(t+\tau)-\bar{n})(n(t)-\bar{n}))^{*}=<\Delta n(t+\tau)\Delta n^{*}(t)>=0 \quad \tau\neq 0$$

(* denotes complex conjugate)

Although the mean number of photons arriving per unit time, λ, is constant on average, at each measurement time interval, the number of detected photons can vary.

The statistical fluctuation of these un-correlated random events are characterized by Poisson statistics.

Poisson Statistics

If the mean number of photon detected is $\bar{n}$, the probability of observing n photons in time interval t is:

$$P(n \mid \bar{n}) = e^{-n} \frac{\bar{n}^n}{n!}$$

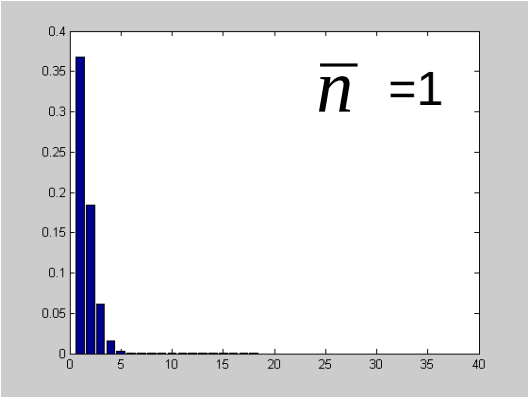

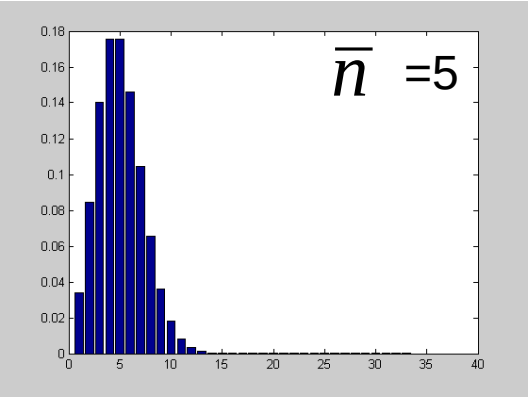

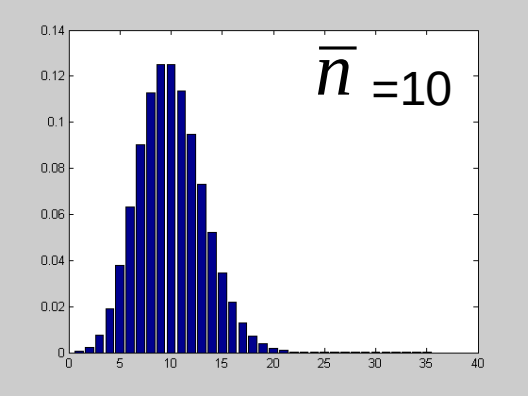

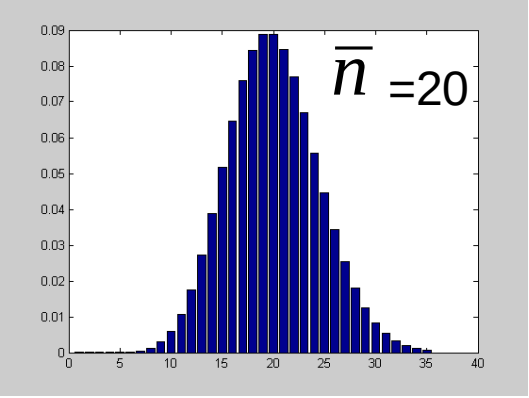

Mean:

$$\bar{n} = \frac{1}{M} \sum_{i}^{M} n_i$$

Variance:

$$\sigma_n^2 = \frac{1}{M} \sum_{i}^{M} (n_i - \bar{n})^2$$

$$\bar{n} = \sigma_n^2$$

Spectrum of Possion Noise I

$$\Delta\tilde{I}(f) = \int_{-\infty}^{\infty} \Delta I(t) e^{-i2\pi ft}\, dt \quad \text{where} \quad \Delta I(t) = q\Delta f\,(n(t) - \bar{n})$$

Assume photon number is Poisson distributed

Power spectral density: $\tilde{P}(f) = R\Delta f \Delta\tilde{I}^{*}(f)\Delta\tilde{I}(f)$

Noise power: $\tilde{N}(f, \Delta f) = \tilde{P}(f)\Delta f$

The power spectral density can be evaluated in a slightly round about way by considering the autocorrelation function:

Autocorrelation function: $g(\tau) = R\Delta f \int_{-\infty}^{\infty} \Delta I(t+\tau)\Delta I(t)^{*} dt$

Because the event of Poisson process is completely independent of each other

$$g(\tau) = R\sigma_I^2 \delta(\tau)/\Delta f$$

Spectrum of Poisson Noise II

$\delta(\tau)$ is the Dirac-Delta function with the following properties:

It has the unit of frequency

$$\delta(0) = \infty;\ \delta(t) = 0 \ \ for\ t \neq 0$$

$$\int \delta(t)dt = 1;\ \int f(t)\delta(t-\tau)dt = f(\tau)$$

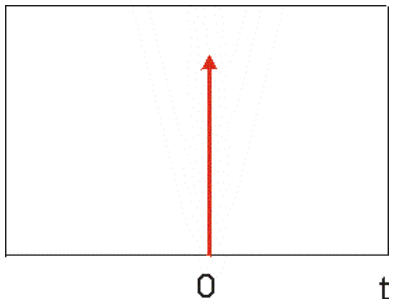

From Poisson process: $\sigma_I^2 = 2\alpha q \Delta f < I >$

Factor of 2 account for positive and negative frequency bands

The autocorelation function of Poisson noise is:

$$g(\tau) = 2R\alpha q < I > \delta(\tau)$$

Spectrum of Poisson Noise III

Wiener-Khintchine Theorem: $\tilde{P}(f) = \int_{-\infty}^{\infty} g(\tau) e^{-i2\pi f\tau} d\tau$

Let's why Wiener-Khintchine theorem is true:

$$\int_{-\infty}^{\infty} g(\tau) e^{-i2\pi f\tau} d\tau = R\Delta f \int_{-\infty}^{\infty} [\int_{-\infty}^{\infty} \Delta I(t+\tau)\Delta I(t) dt] e^{-i2\pi f\tau} d\tau$$

$$= R\Delta f \int_{-\infty}^{\infty} [\int_{-\infty}^{\infty} \Delta I(t+\tau) e^{-i2\pi f\tau} d\tau] \Delta I(t) dt$$

$$= R\Delta f \int_{-\infty}^{\infty} [\int_{-\infty}^{\infty} \Delta I(\tau') e^{-i2\pi f\tau'} d\tau'] e^{+i2\pi ft} \Delta I(t) dt$$

$$\tau' = t + \tau,\ d\tau' = d\tau$$

$$= R\Delta f [\int_{-\infty}^{\infty} \Delta I(\tau') e^{-i2\pi f\tau'} d\tau'][\int_{-\infty}^{\infty} \Delta I(t) e^{+i2\pi ft} dt]$$

$$= R\Delta f \tilde{\Delta I}(f) \tilde{\Delta I}(f)^*$$

Fourier transform of the autocorrelation function is the power spectral density

Spectrum of Possion Noise IV

$$\tilde{P}(f) = \int_{-\infty}^{\infty} 2R\alpha q < I > \delta(\tau) e^{-i2\pi f\tau} df = 2R\alpha q < I >$$

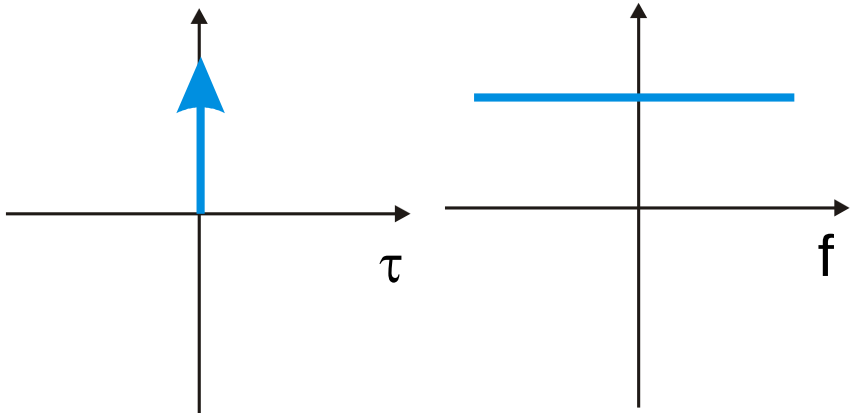

Poisson noise has a “white” spectrum

Noise in a given spectral band:

$$\tilde{N}(f, \Delta f) = 2R\alpha q < I > \Delta f$$

Photon Shot Noise

The origin of the photon shot noise comes from the Poisson statistics of the incoming photons itself

The shot noise power is:

$$\tilde{N}_s(f,\Delta f) = 2R\alpha q < I > \Delta f$$

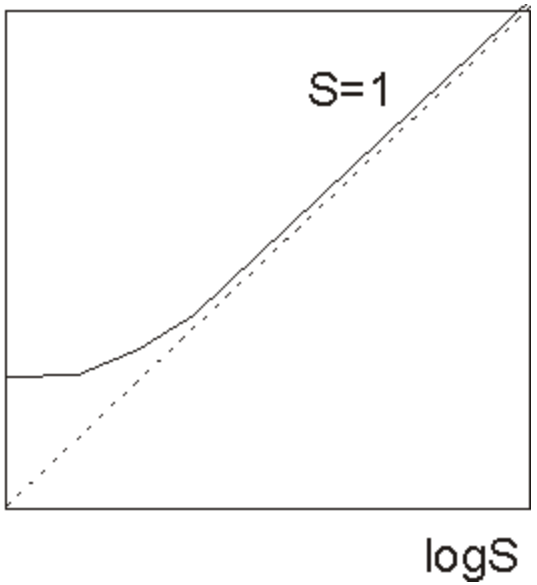

The signal power is: $S =< I >^2 R$

$$SNR = \frac{< I >}{2\alpha q\Delta f} = \frac{\alpha q\bar{n}/\Delta t}{2\alpha q\Delta f} = \frac{2\alpha q\bar{n}\Delta f}{2\alpha q\Delta f} = \bar{n}$$

Used sampling theorem: $1/\Delta t = 2\Delta f$

A detector is consider to be “ideal” if it is dominated by just shot noise.

Dark Current Noise

The ideal photoelectric or photovoltic device does not produces current (electrons) in the absence of light. However, thermal effect results in some probability of spontaneous production of free electrons. This effect is measured by the dark current amplitude of the device: $< I_d >$

The average dark current is constant at constant temperature, but the electron generated fluctuate in time according to Poisson statistic similar to the fluctuation of the signal photons.

From our discussion of photon shot noise, we have immediately

$$\tilde{N}_d(f, \Delta f) = 2R\alpha q < I_d > \Delta f$$

Johnson Noise

Johnson noise originates from the temperature dependent fluctuation in the load resistance R of the transimpedance detection circuit.

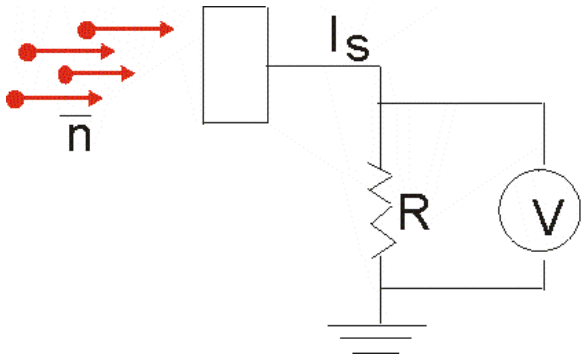

Consider a simple dimensional analysis argument:

Thermal energy: kT

Thermal power: $kT\Delta f$

Power of Johnson noise current I_J : $I_J^2 R$

$$I_J = \sqrt{\frac{kT\Delta f}{R}}$$

$$\tilde{N}_J(f, \Delta f) = kT\Delta f$$

Characterizing Photodetectors

1. Quantum Efficiency: The probability of generating of a photoelectron from an incident photon

2. Internal Amplification: The amplification ratio for converting a photoelectron into an output current

3. Dynamic Range: What is the largest and the lowest signal that can be measured linearly

4. Response Speed: The time difference and spread between an incoming photon and the output current burst

5. Geometric form factor: Size and shape of the active area and the detector

6. Noise: Discussed extensively already

Photomultiplier tube (PMT)

The PMT are characterized by two important parameters

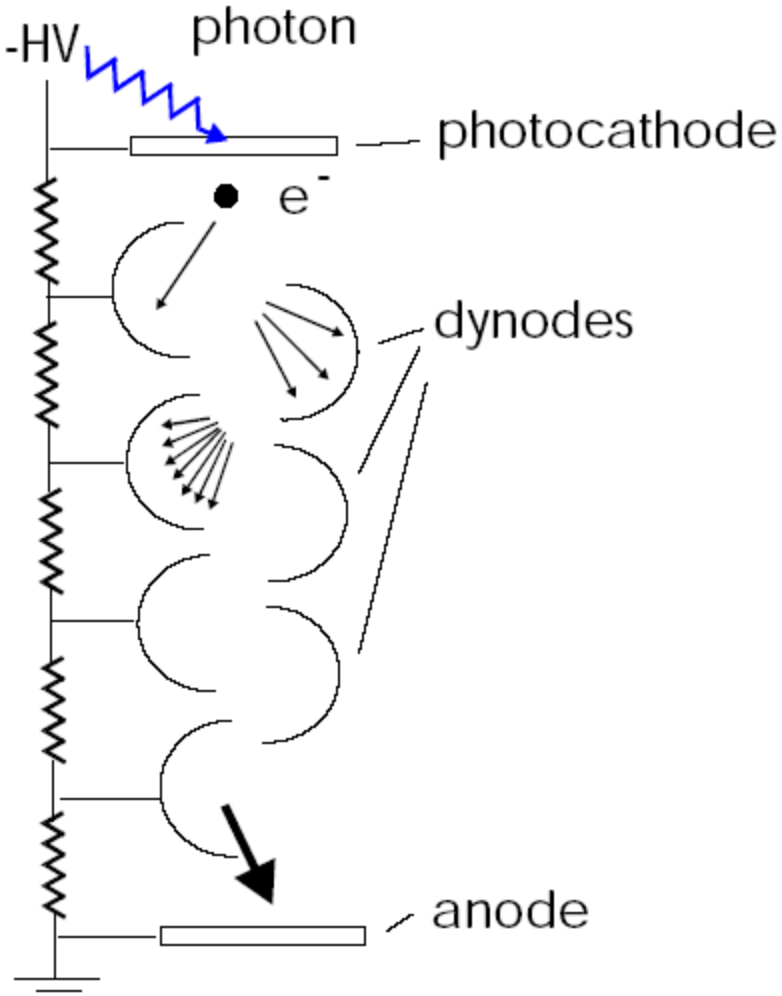

Cathode sensitivity, *S* (A/W): 0.06 A/W

Gain, α: 10^7 to 10^8

We can relate current measured at the anode to the number of incident photons, *n*, arriving within a time interval Δt

$$I = S \cdot \alpha \cdot E_\gamma \cdot n / \Delta t$$

E_γ is photon energy

For green (500 nm wavelength) photons:

$$E_\gamma = \frac{hc}{\lambda} = \frac{6.6\times10^{-34}\,Js \cdot 3\times10^{8}\,m/s}{5\times10^{-7}\,m} = 4\times10^{-19}\,J$$

Sensitivity of PMT Cathode as a Function of Material

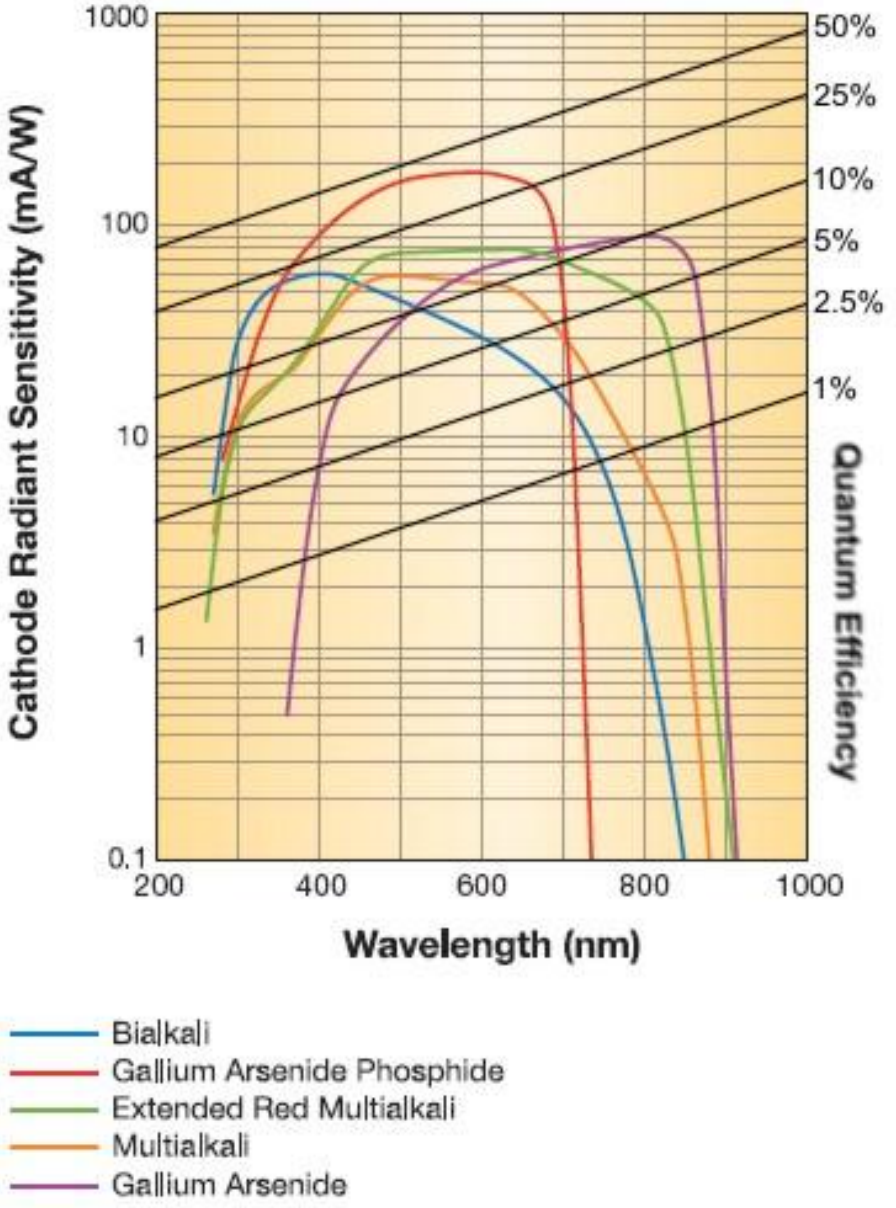

Photodiodes

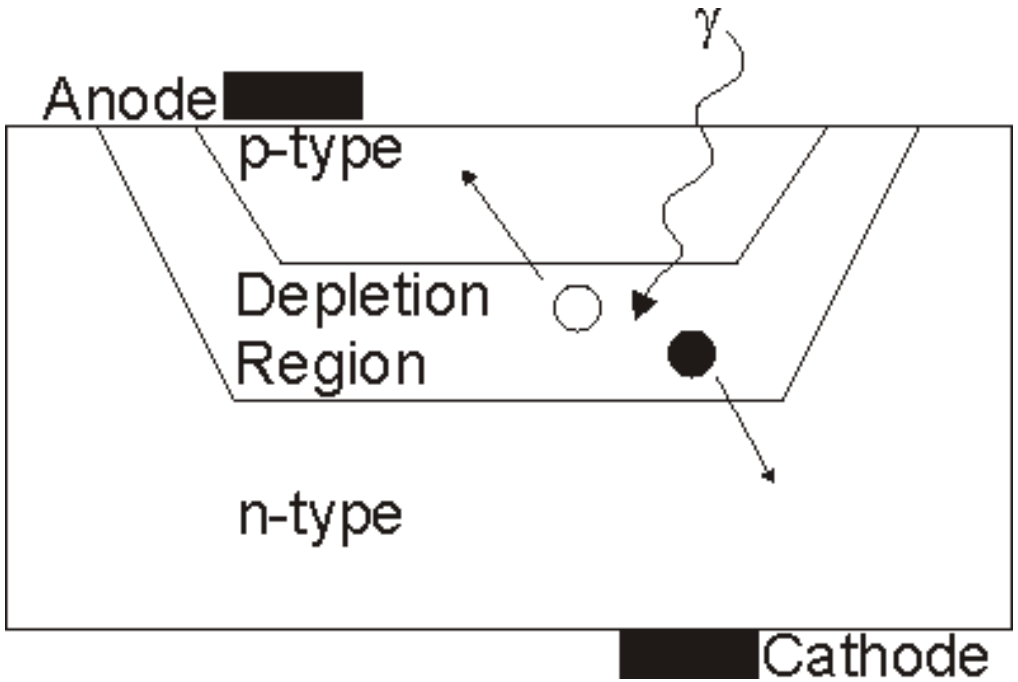

Biasing can increase device temporal Response speed

Recall:

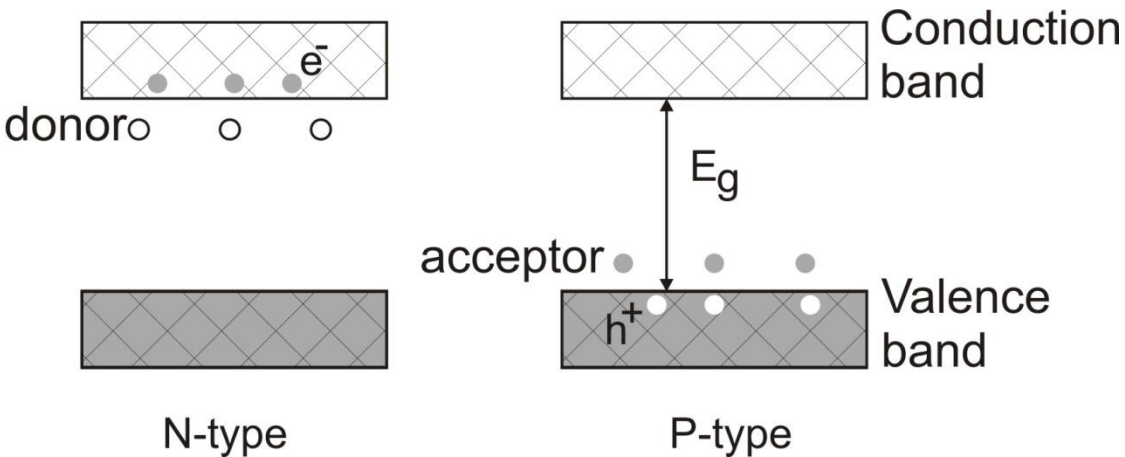

Charge Coupled Device (CCD) Cameras

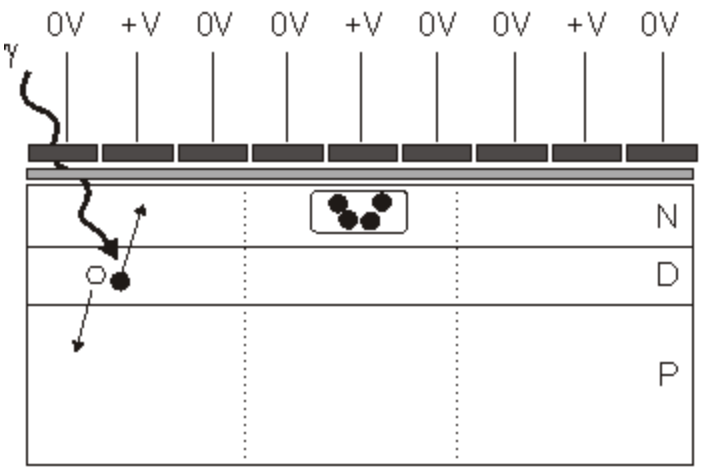

Front Illuminated

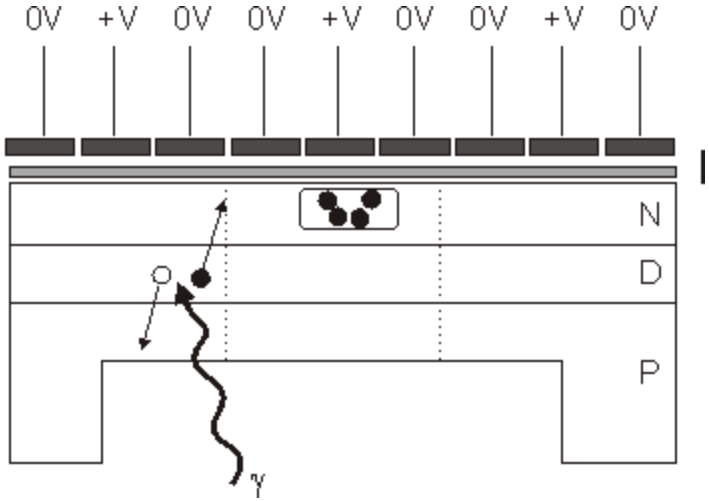

Back (thinned) Illuminated

Readout Sequence Principle of CCD

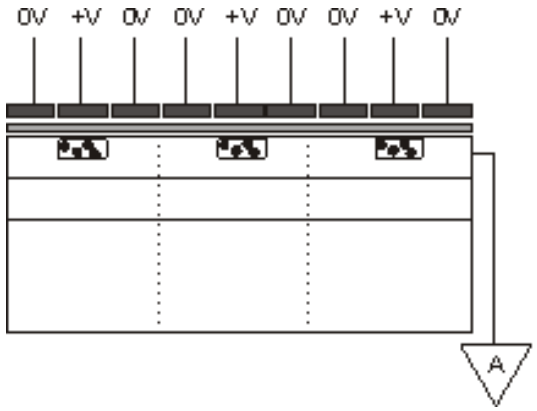

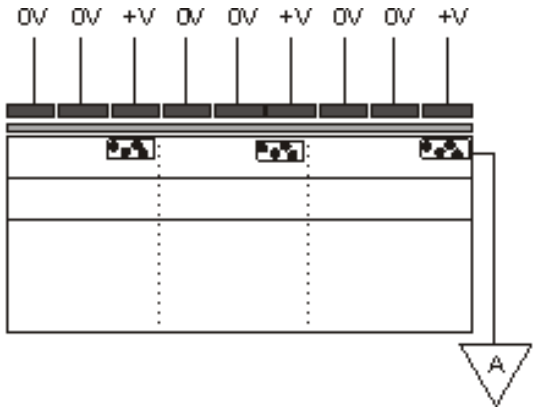

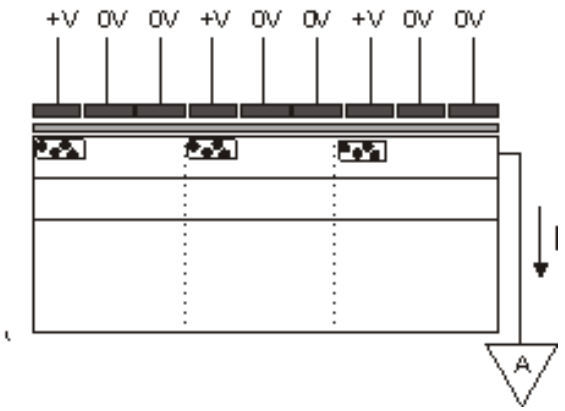

A typical microscopy experiment

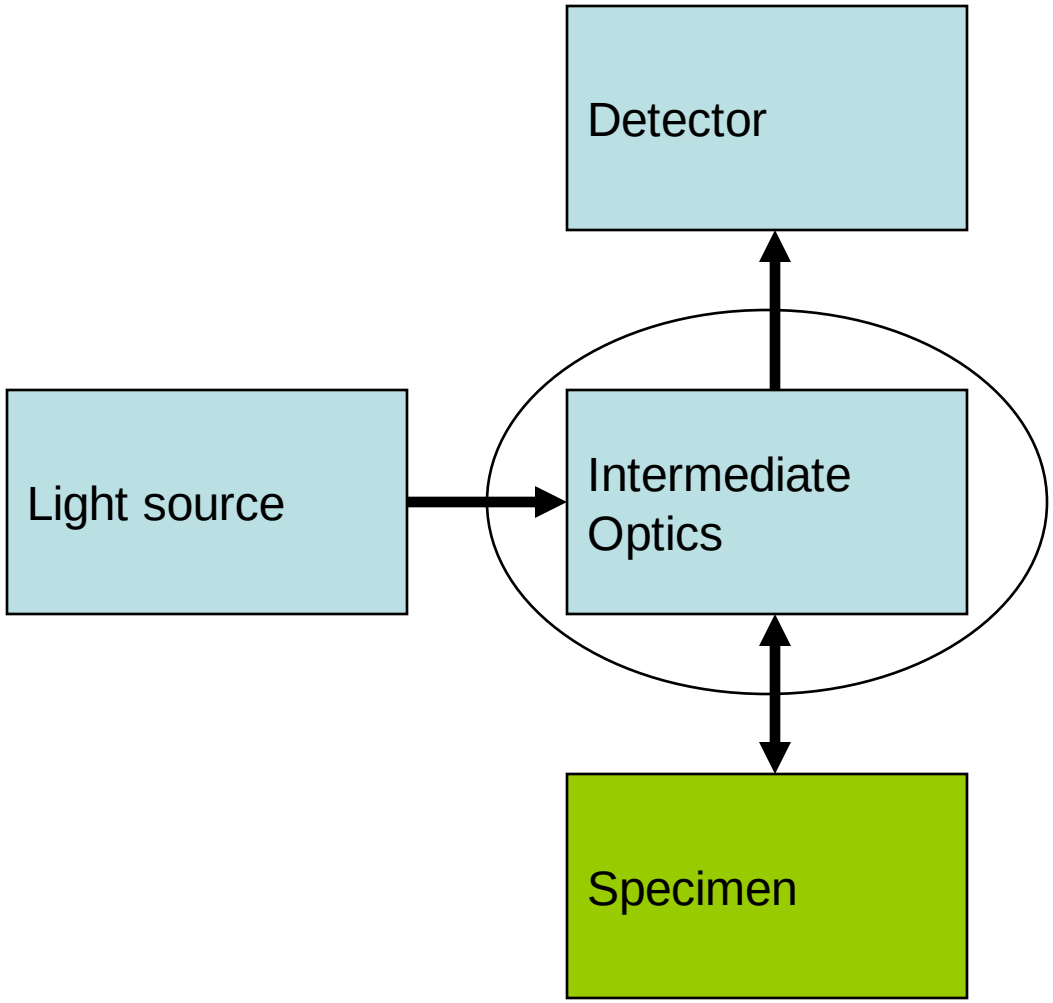

Wave and Particlel Nature of Light

Wave Nature of Light -- Huygen

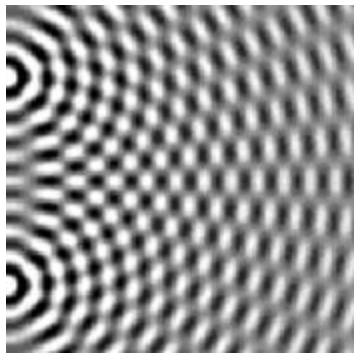

Particle Nature of Light -- Newton

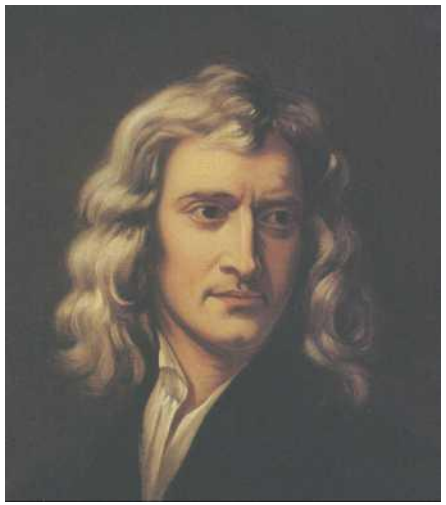

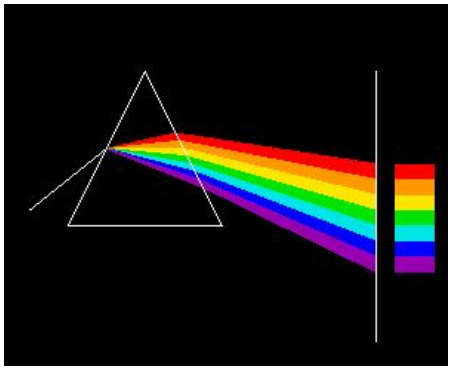

Physical Optics – Wave nature of light

Maxwell and His Equations

$$\nabla \cdot \vec{E} = 4\pi\rho$$

$$\nabla \cdot \vec{B} = 0$$

$$\nabla \times \vec{E} + \frac{1}{c}\frac{\partial \vec{B}}{\partial t} = 0$$

$$\nabla \times \vec{B} - \frac{1}{c}\frac{\partial \vec{E}}{\partial t} = \frac{4\pi}{c}\vec{J}$$

Wave Equations

$$\nabla^2 \vec{E} - \frac{1}{c^2}\frac{\partial^2 \vec{E}}{\partial t^2} = 0$$

$$\nabla^2 \vec{B} - \frac{1}{c^2}\frac{\partial^2 \vec{B}}{\partial t^2} = 0$$

Plane Wave Solution

$$\vec{E}(x,t) = \vec{E}_0 \cos(kx - \omega t)$$

$$k = \frac{2\pi}{\lambda} \quad \omega = 2\pi f \quad ck = \omega$$

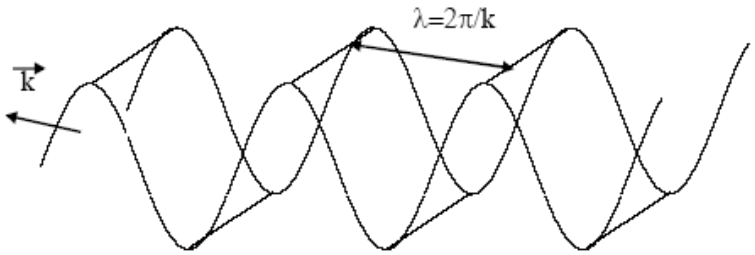

Plane wave propagates like a “ray” of light

Reflection and Refraction of Light at Boundary

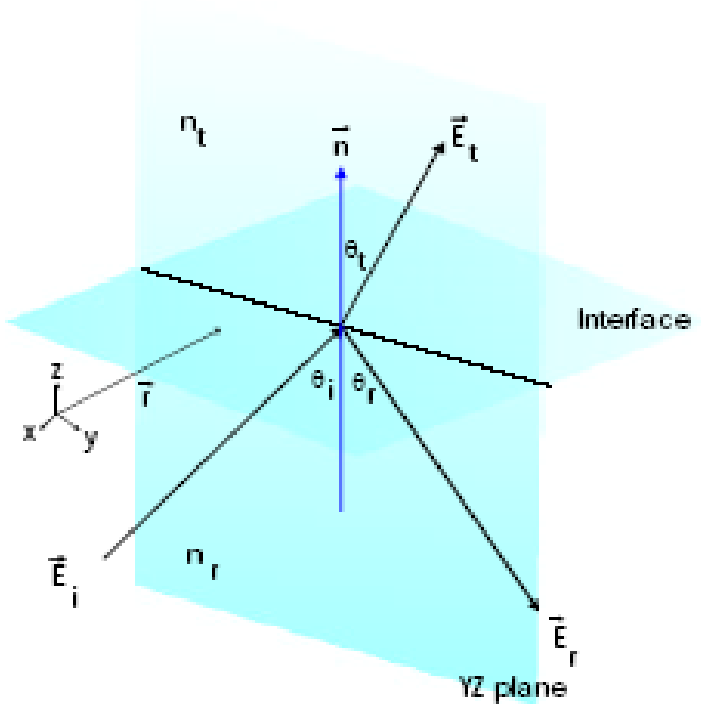

Reflection

$$\sin\theta_i = \sin\theta_r$$

Refraction (Snell's Law)

$$n_i \sin\theta_i = n_t \sin\theta_t$$

Simple Ray Tracing I

Ray Tracing is just based on the application of Snell's law to a curved (spherical) surface. We will focus on 4 simple rules of ray tracing.

Rays pass through the focal point becomes parallel to the optical axis.
Rays parallel to the optical axis are deflected through the focal point.

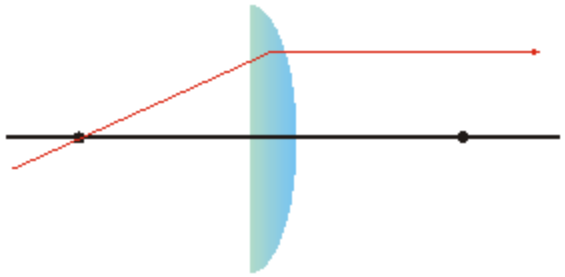

(1)

Rays originated from the focal point emerge parallel to the optical axis

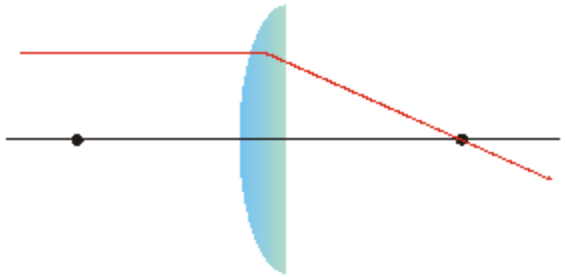

(2)

Rays parallel to the optical axis converges to the focal point

Simple Ray Tracing II

Rays originate from the focal plane becomes collimated.
Collimated rays converges at the focal plane.

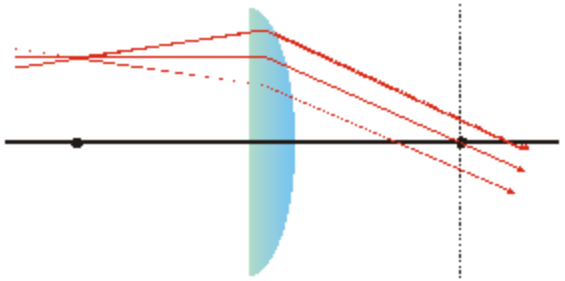

(3)

Rays originated from the plane emerge collimated

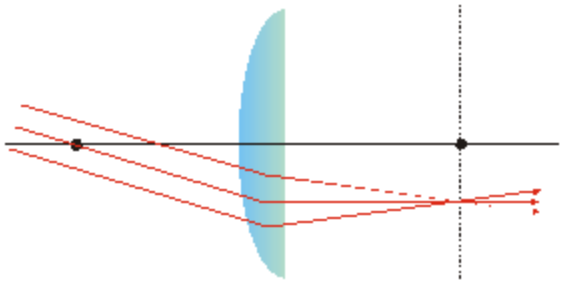

(4)

Collimated rays emerge focus at The focal plane

Optical elements I: Lens

We have been using lens throughout this lecture, it may be useful to pause for a moment to describe what are the typical terminology associated with lens.

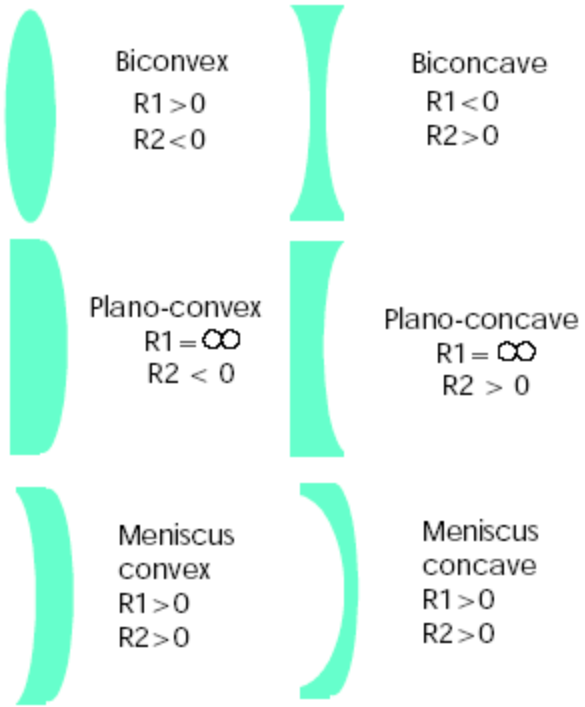

Optical element II: mirrors, prism, apertures

These are common optical elements that is mostly self explanatory and I will not spend much time on these.

Mirrors: Mirrors has similar terminology as lens but only has one surfave.

Prisms: Prisms has a number of applications such as dispersing different color of light and directing light and image.

Apertures & Stops: As discussed before, aperture and stops serves to define optical path and to minimize aberration effect by eliminating non-paraxial rays.

Optical Microscopy I

Detection path of an optical microscope. Note that at the detector, the magnification is the ratio of the focal length of the objective and the tube lens.

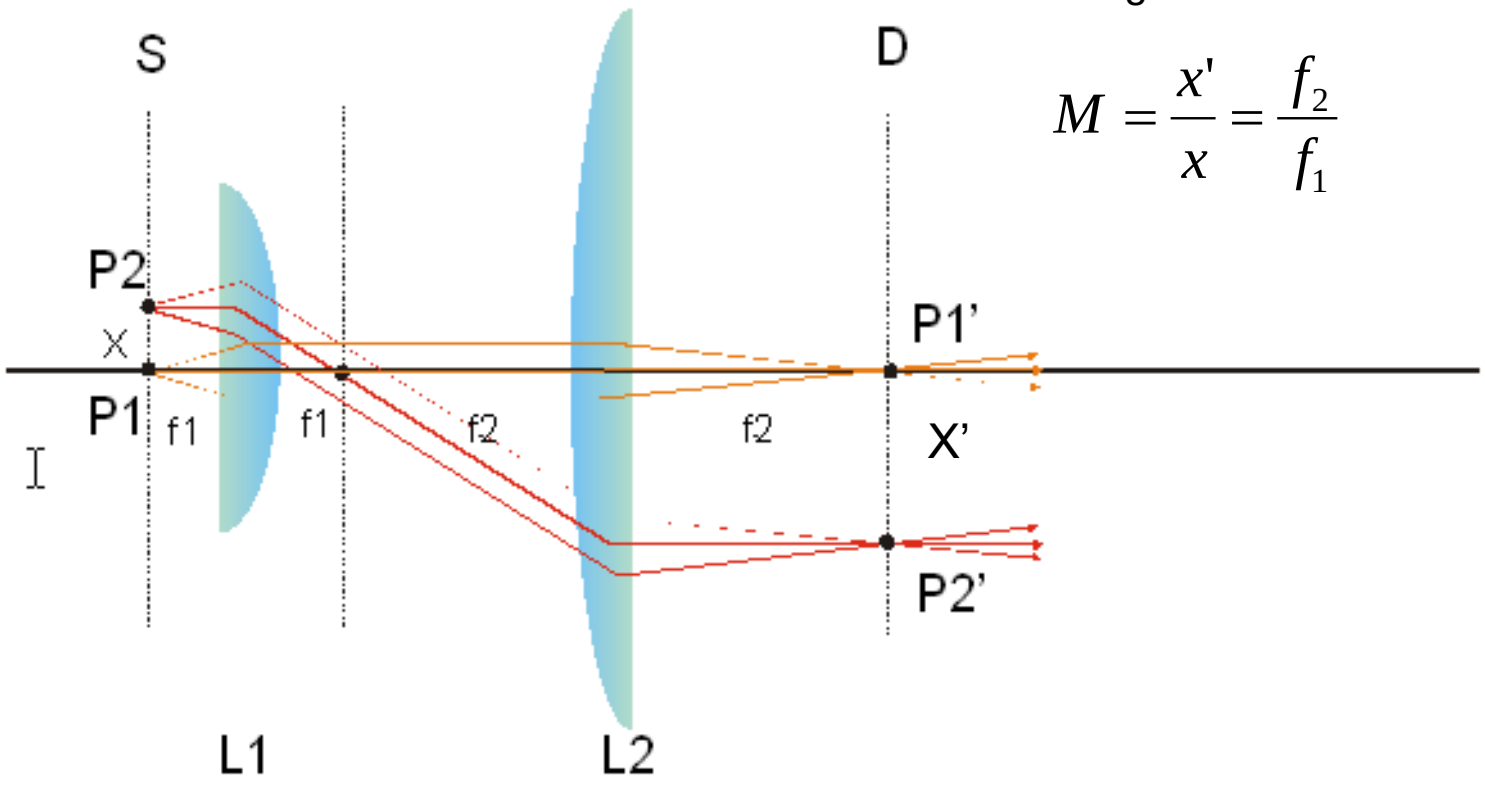

Magnification

$$M = \frac{x'}{x} = \frac{f_2}{f_1}$$

Optical Microscopy III

Kohler illumination ensure that the structure of the light source (such as the filament of lamp) is not imaged at the specimen.

Trans-illumination

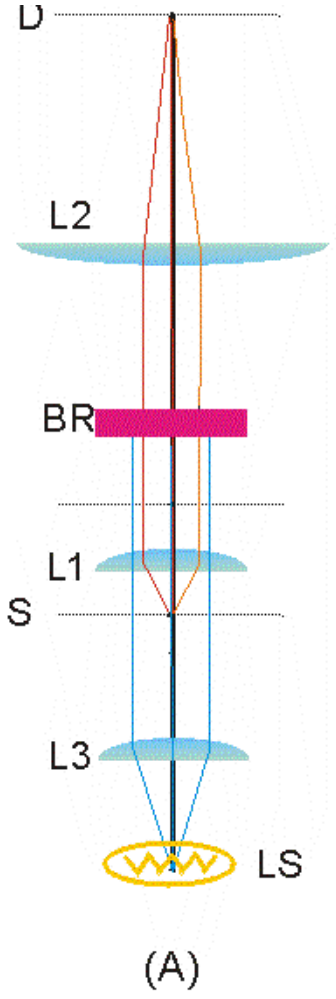

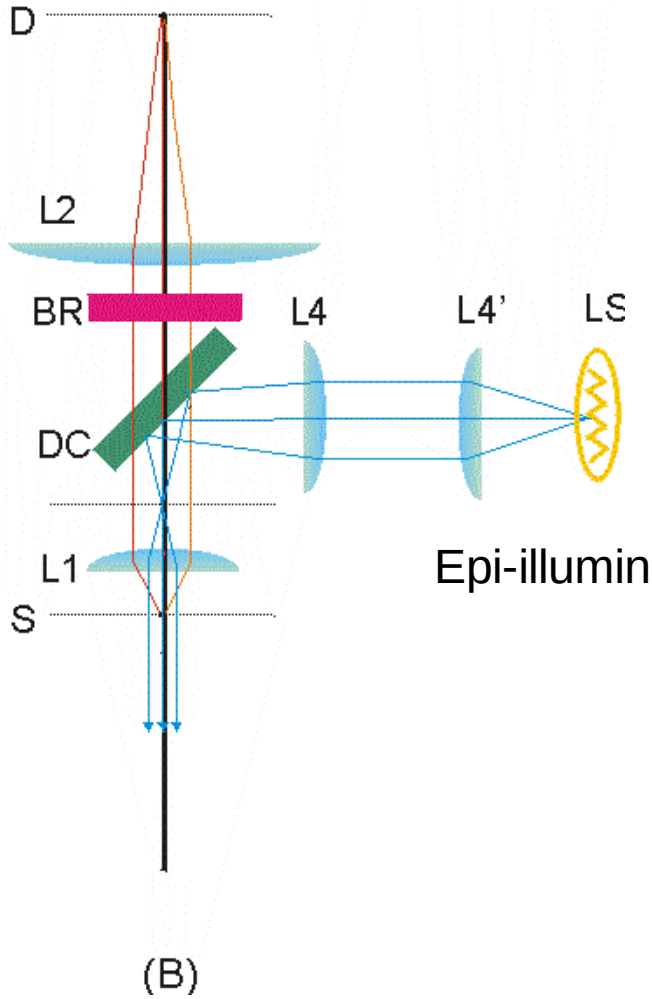

Epi-illumination

Microscopic contrast and resolution

Two of the most important and difficult to quantify aspects of an optical microscope are its ability to generate contrast and it ability to resolve fine structures

What is contrast? Contrast refers to an "intensity" difference between a specimen of interest and its background.

Optically contrast is defined as the visibility:

$$V = \frac{I_{\max} - I_{\min}}{I_{\max} + I_{\min}}$$

What is resolution? Resolution defines how fine we can see … how far apart two objects have to be for them to be distinguishable.

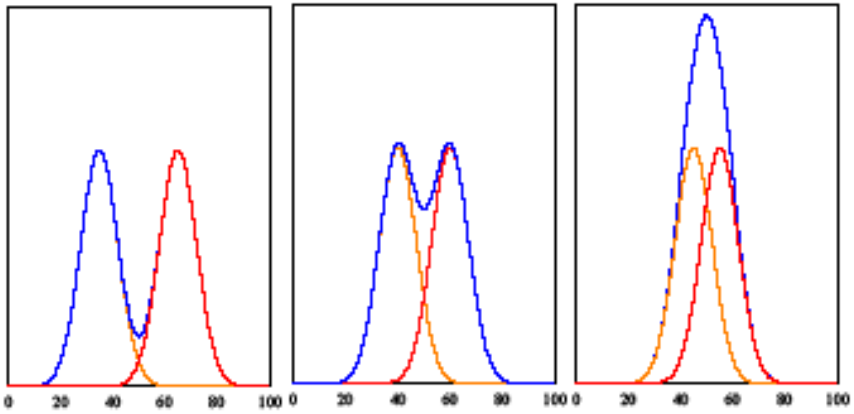

Rayleigh's Criterion:

Two objects are distinguishable if their centers are separation by further than their full width at half maximum

Huygens-Fresnel Principle

Diffraction

Diffraction can be considered as a more advanced treatment of interference effect. The basic physics of the two phenomena are identical. While we have treated interference as light originating from point sources (like the double slit experiment), diffraction considers interference of light from finite size objects such as an aperture.

Diffraction effect can be easily seen when light is restricted into dimensions that are comparable to its wavelength. For coherent light source, like a laser, diffraction effects can be readily observed. An example is sending laser light through a narrow sli

The treatment of diffraction effects started in the 1700s-1800s wi the introduction of the Huygens-Fresnel Principle.

Huygens-Fresnel Principle: Every unobstructed points of a wave front are a source of secondary spherical wave. The optical field far away can be determined by the interference of the secondary waves.

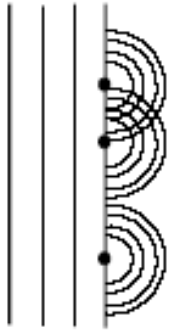

The Huygen's principle can be derived directly from the wave equation assuming the electric field can be treated as scalar quantities. It is quite a bit of work and I will not go through it here.

Spherical Wave Solution

$$\tilde{E}(r,t) = \tilde{E}_o \frac{\sin(k_r r - \omega t)}{r} \quad \text{and} \quad ck_r = \omega$$

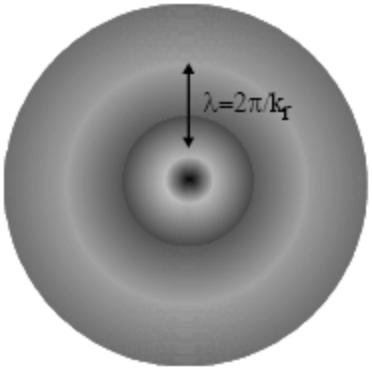

Interference

Consider combining two plane waves:

$$\vec{E}_1(\vec{r},t) = \vec{E}_{01}\cos(\vec{k}_1\cdot\vec{r}-\omega t)$$

$$\vec{E}_2(\vec{r},t) = \vec{E}_{02}\cos(\vec{k}_2\cdot\vec{r}-\omega t)$$

$$\left|\vec{k}_1\right| = \left|\vec{k}_2\right| = k$$

The combined field is

$$\vec{E}(\vec{r},t) = \vec{E}_{01}\cos(\vec{k}_1\cdot\vec{r}-\omega t) + \vec{E}_{02}\cos(\vec{k}_2\cdot\vec{r}-\omega t)$$

The brightness or intensity is the "mean square" of the field

$$I = \frac{1}{T}\int_0^T \vec{E}(\vec{r},t)\cdot\vec{E}^*(\vec{r},t)dt \equiv \left\langle E^2 \right\rangle$$

$$= \frac{E_{01}^2}{2} + \frac{E_{02}^2}{2} + 2\sqrt{\frac{E_{01}^2}{2}\frac{E_{02}^2}{2}}\cos[(\vec{k}_1-\vec{k}_2)\cdot\vec{r}]$$

$$= I_1 + I_2 + 2\sqrt{I_1 I_2}\cos\delta$$

δ is a phase factor measuring the path length difference of the two beams at $\vec{r}$ multiplied by k

Diffraction I

Single slit diffraction is a result of the interference of light due to its wave nature

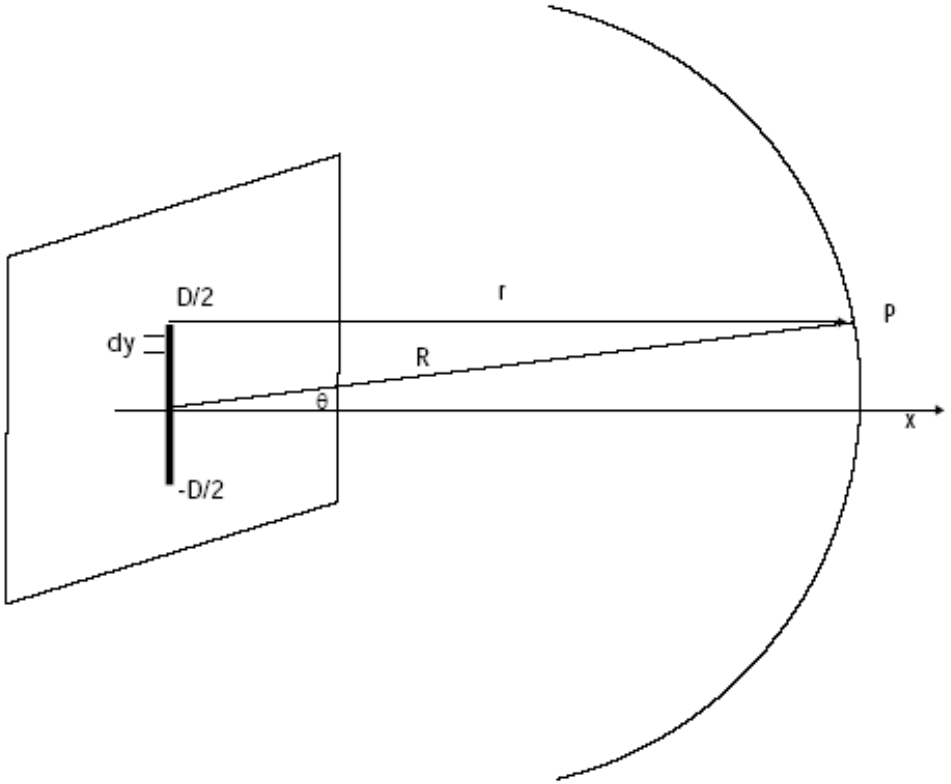

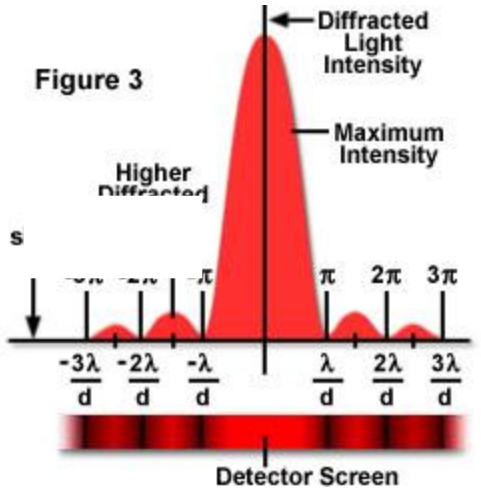

Diffraction II

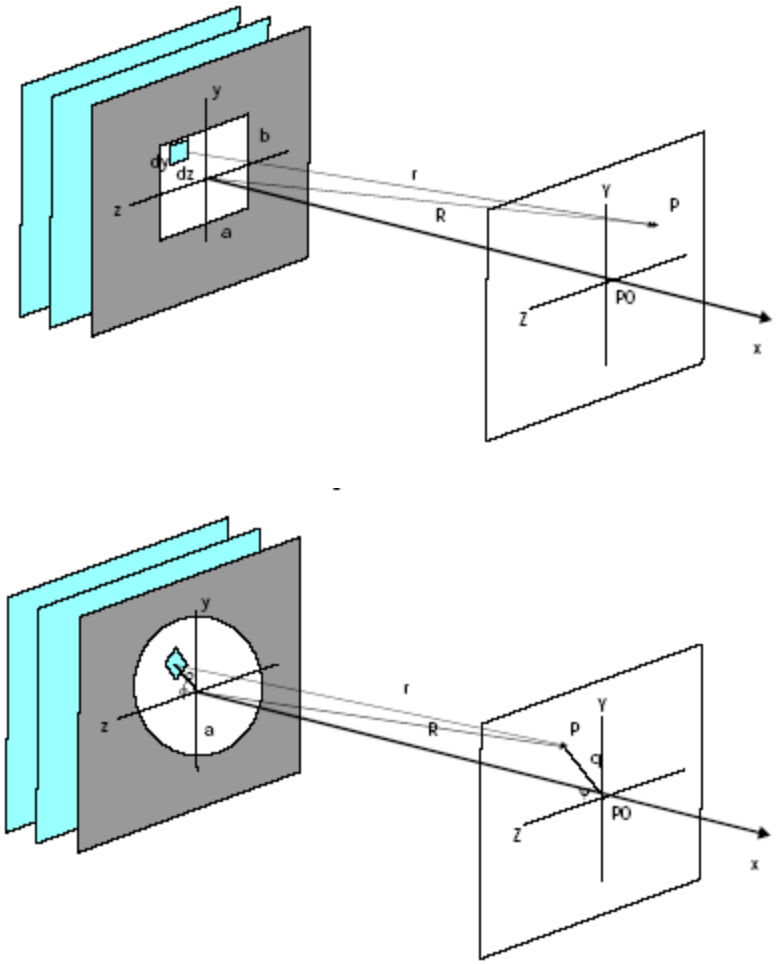

$$I(\theta) = I(0)[\frac{2J_1(ka\sin\theta)}{ka\sin\theta}]^2$$

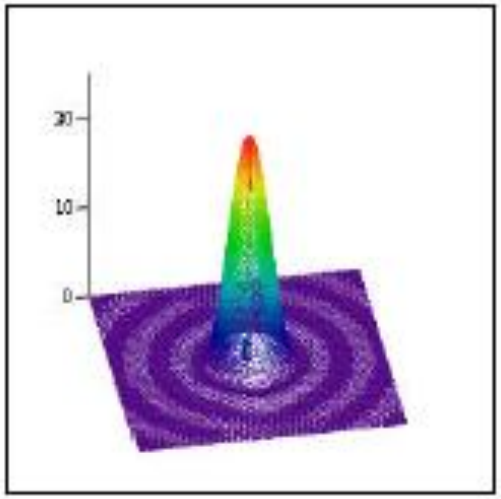

Microscopy imaging can be consider as the diffraction from a circular aperture with a lens for focusing – diffraction results in “broadening” of the focal point.

Interference

Consider combining two plane waves:

$$\vec{E}_1(\vec{r},t) = \vec{E}_{01}\cos(\vec{k}_1\cdot\vec{r}-\omega t)$$

$$\vec{E}_2(\vec{r},t) = \vec{E}_{02}\cos(\vec{k}_2\cdot\vec{r}-\omega t)$$

$$\left|\vec{k}_1\right| = \left|\vec{k}_2\right| = k$$

The combined field is

$$\vec{E}(\vec{r},t) = \vec{E}_{01}\cos(\vec{k}_1\cdot\vec{r}-\omega t) + \vec{E}_{02}\cos(\vec{k}_2\cdot\vec{r}-\omega t)$$

The brightness or intensity is the "mean square" of the field

$$I = \frac{1}{T}\int_0^T \vec{E}(\vec{r},t)\cdot\vec{E}^*(\vec{r},t)dt \equiv \left\langle E^2 \right\rangle$$

$$= \frac{E_{01}^2}{2} + \frac{E_{02}^2}{2} + 2\sqrt{\frac{E_{01}^2}{2}\frac{E_{02}^2}{2}}\cos[(\vec{k}_1-\vec{k}_2)\cdot\vec{r}]$$

$$= I_1 + I_2 + 2\sqrt{I_1 I_2}\cos\delta$$

δ is a phase factor measuring the path length difference of the two beams at $\vec{r}$ multiplied by k

Fourier Optics I

Recall the interference of two plane waves

$$\vec{E}_1(\vec{r},t) = \vec{E}\cos(\vec{k}_1.\vec{r} + \omega t)$$
$$\vec{E}_2(\vec{r},t) = \vec{E}\cos(\vec{k}_2.\vec{r} + \omega t)$$

$$I(\vec{r},t) = 2I + 2I\cos(\vec{k}_1.\vec{r} - \vec{k}_2.\vec{r})$$

In the case where the waves incident symmetrically and looking at the intensity along the y axis

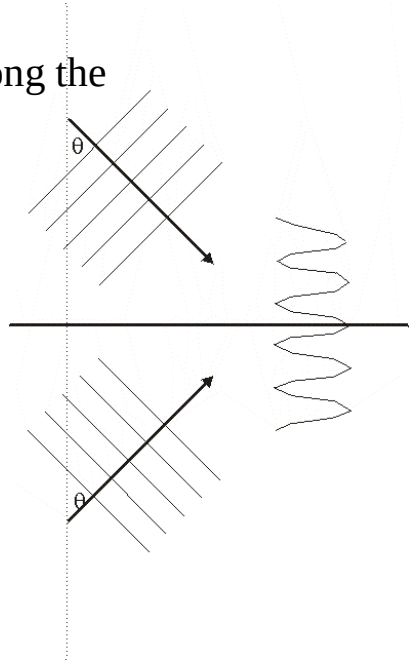

$$\vec{k}_1 = k\sin\theta\hat{x} + k\cos\theta\hat{y}$$
$$\vec{k}_2 = k\sin\theta\hat{x} - k\cos\theta\hat{y}$$
$$\vec{r} = y\hat{y}$$

The intensity has a simple distribution depend on angle θ:

$$I(\vec{r},t) = 2I(1 + \cos(2k\cos\theta y))$$

Note that when angle is zero degree (light wave counter propagating), the highest frequency oscillation is observed at spatial frequency: $2k = 2\pi(\frac{2}{\lambda})$. When the waves are parallel, angle is 90 degree, the spatial frequency is zero (constant intensity light).

Fourier Optics II

Consider two point source at the focal plane of a lens, the light rays become collimated plane waves after the lens and interference is observed.

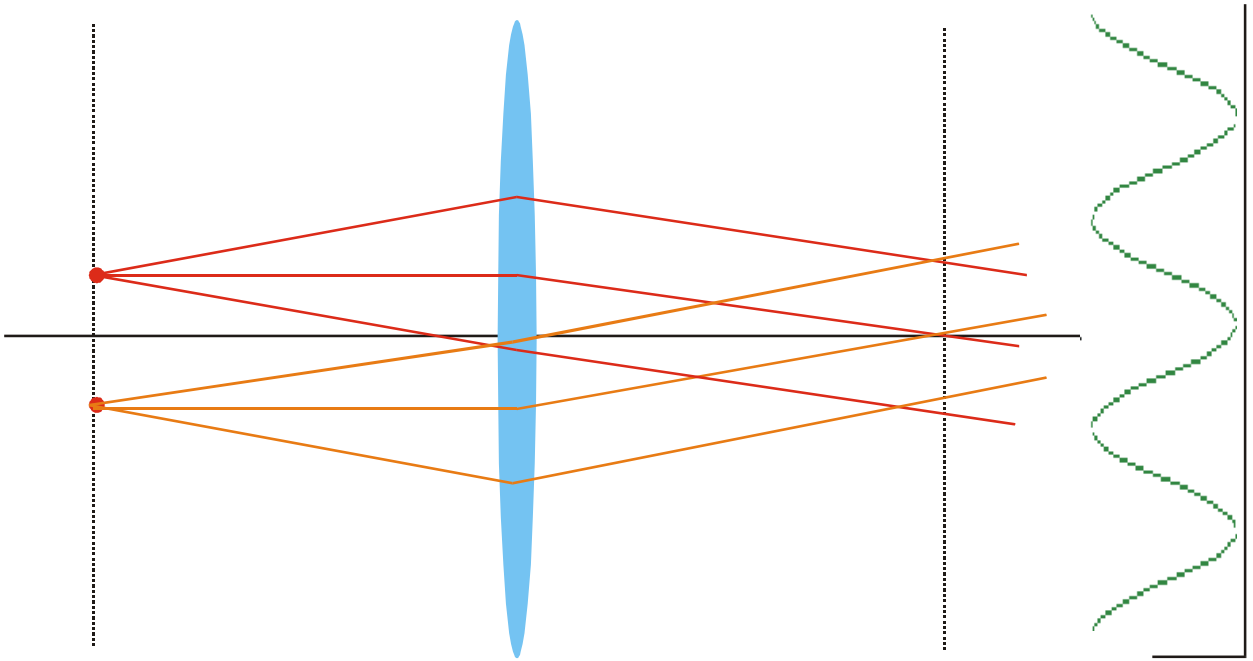

Fourier Optics III

What happen when the two sources coincide? Only parallel plane waves are generated.

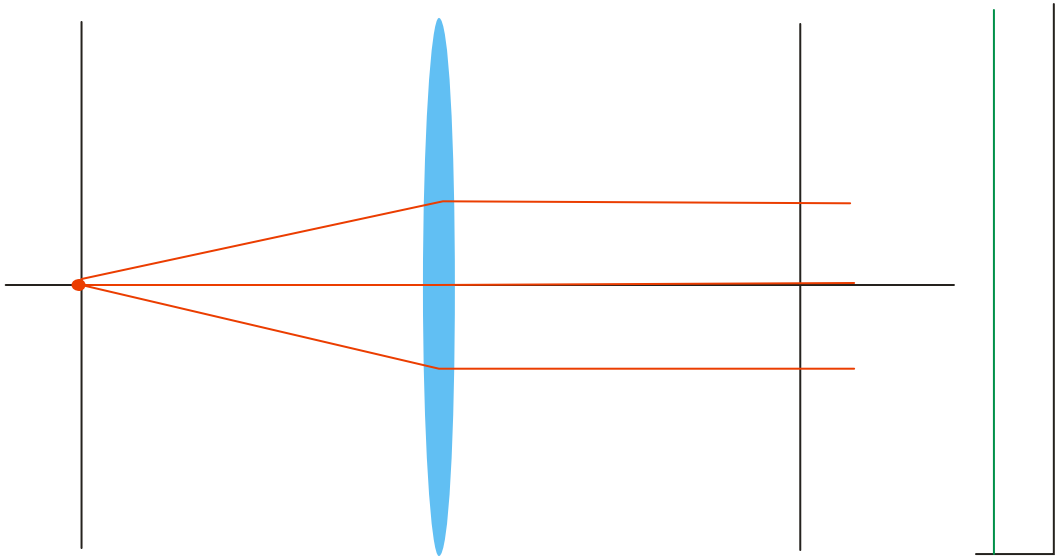

Fourier Optics IV

What happen if the point sources are made further apart?

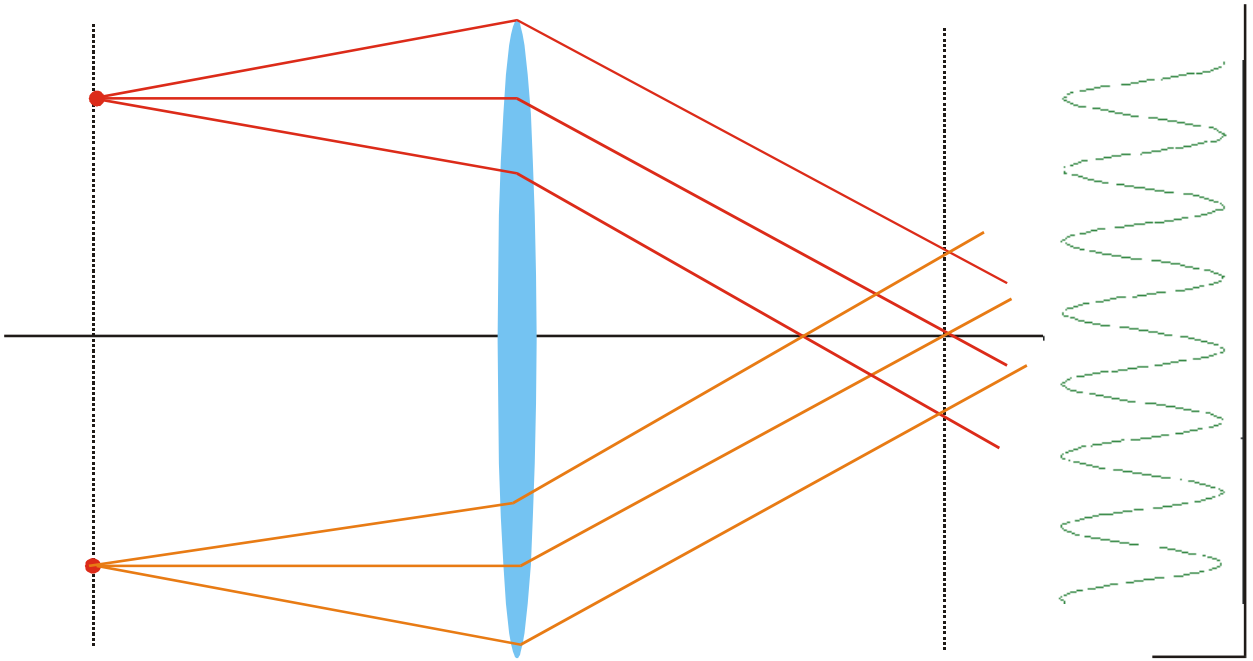

Resolution viewed from Fourier Optics

Light emission from any object in the specimen plane can be Decomposed into its Fourier components. Which Fourier component will pass the finite aperture of the objective lens? Low frequencies!

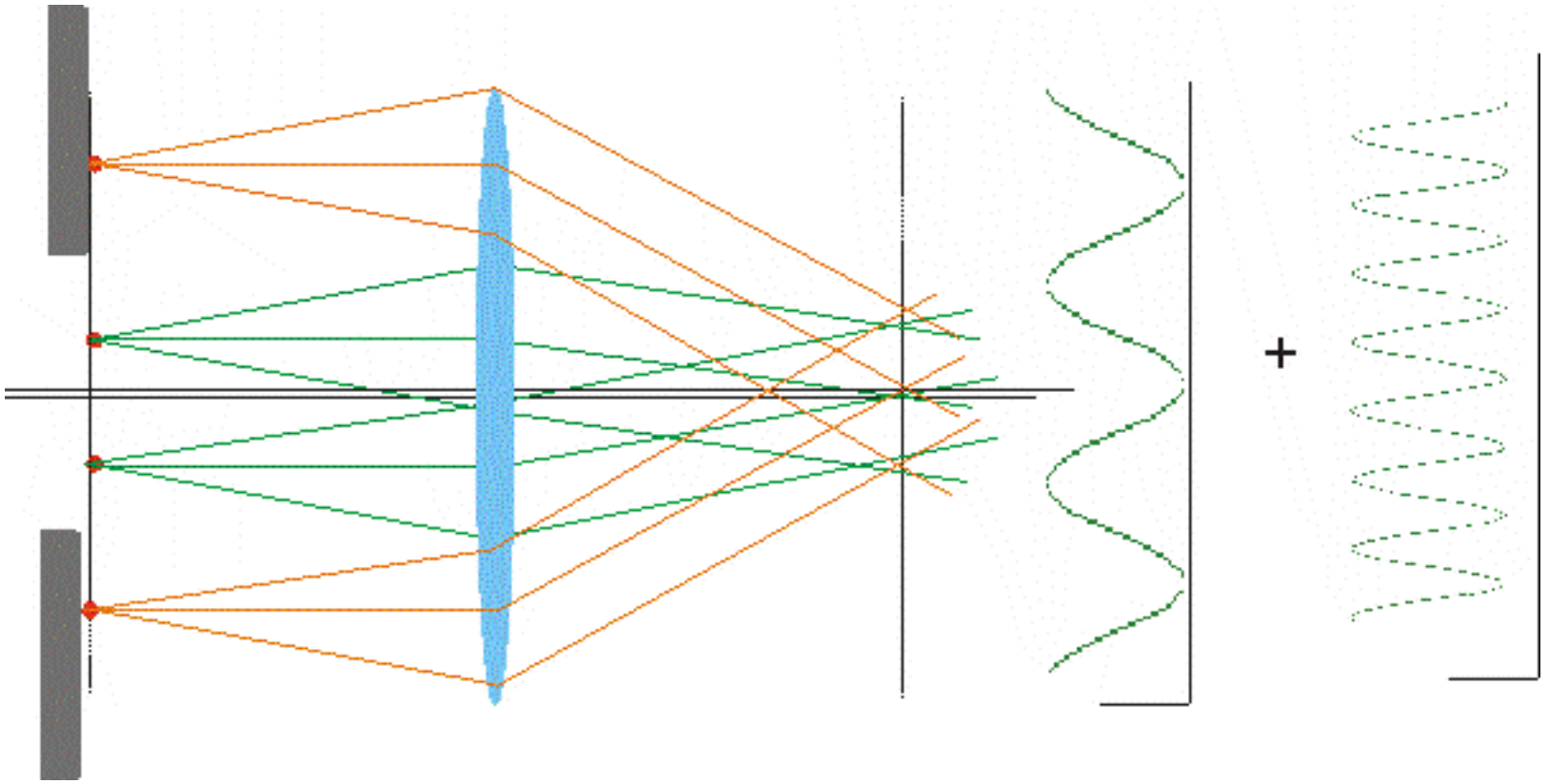

Resolution viewed from Fourier Optics II

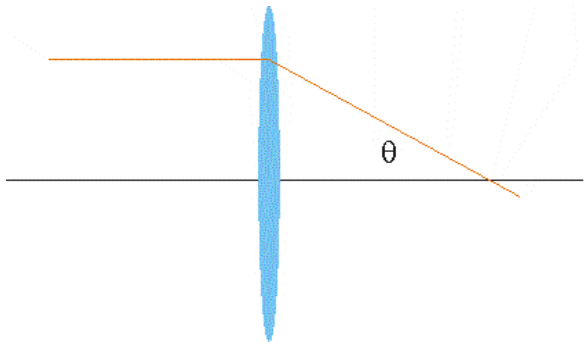

$$NA = n\sin(\theta)$$

What is the maximum frequency that can be pass? Consider the case of a very large lens (numerical aperture, NA approach one). The waves will approach counter propagating and the maximum frequency is:

$$k_{\max} = 2\pi(\frac{2}{\lambda})$$

Note that maximum spatial frequency is a function of wavelength. Shorter wavelength implies higher frequency (resolution) imaging.

At a given wavelength, we should expect a resolution of about $\frac{\lambda}{2}$

Resolution viewed from Fourier Optics III

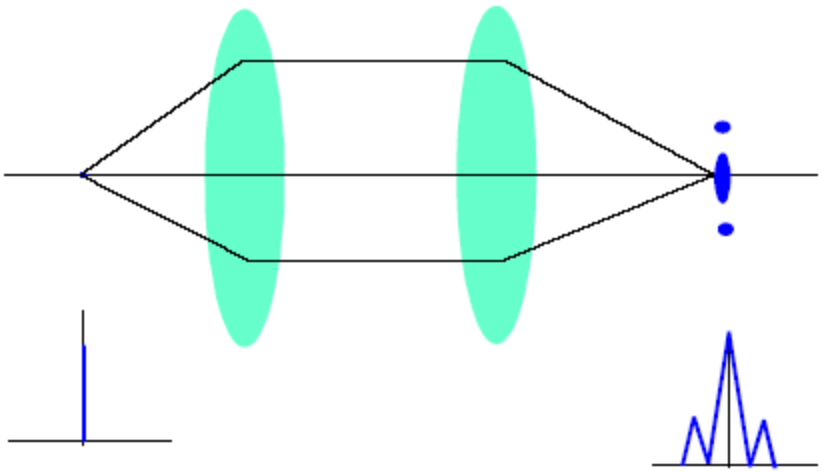

Point Spread function

More quantitative analysis shows that:

$$I(\theta) = I(0)[\frac{2J_1(ka\sin\theta)}{ka\sin\theta}]^2$$

$$J_1(ka\sin\theta) = J_1(\frac{2\pi}{\lambda} a \frac{r}{f}) = J_1(\frac{2\pi}{\lambda} \frac{a}{f} r) = J_1(\frac{2\pi}{\lambda} NAr)$$

$$J_1(x) = 0 \quad at \quad x = 3.83 \quad \Rightarrow \quad r_{\min} = \frac{0.6\lambda}{NA}$$

Resolution viewed from Fourier Optics VI

$$OTF(k) = \mathsf{F}(PSF(r))$$

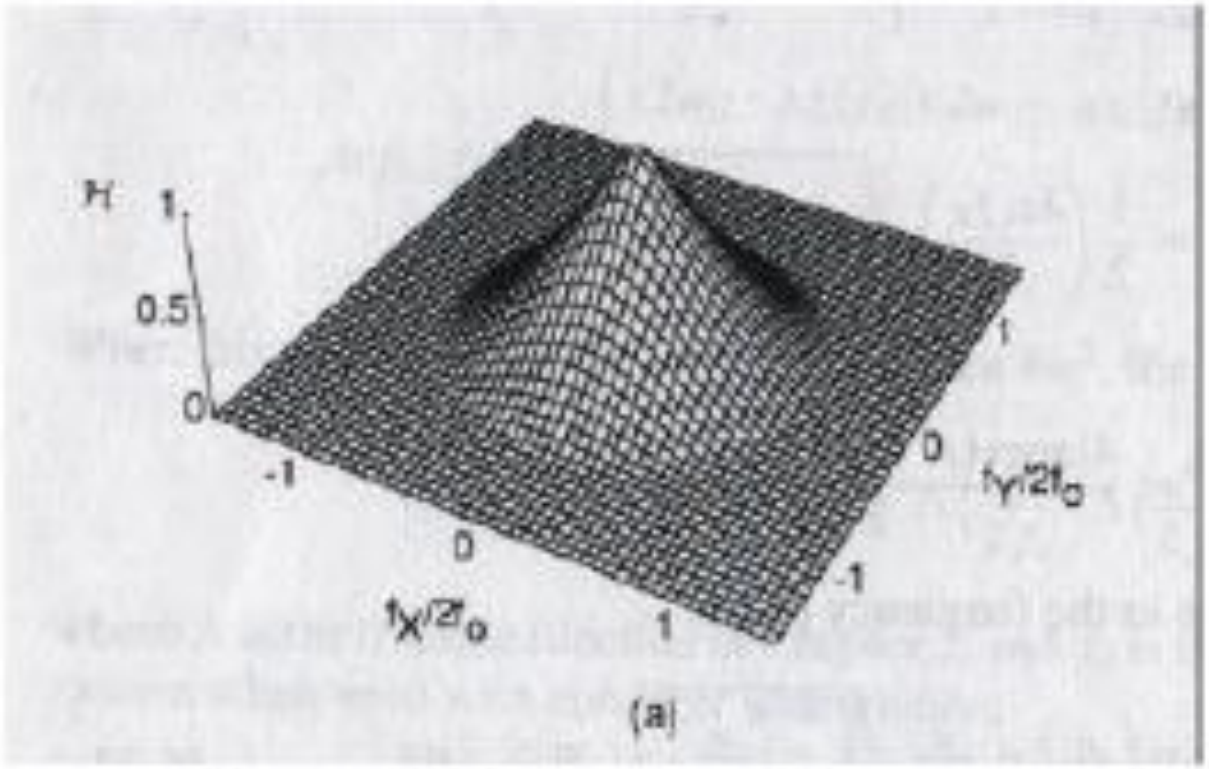

Microscope Configurations

Trans

Epi

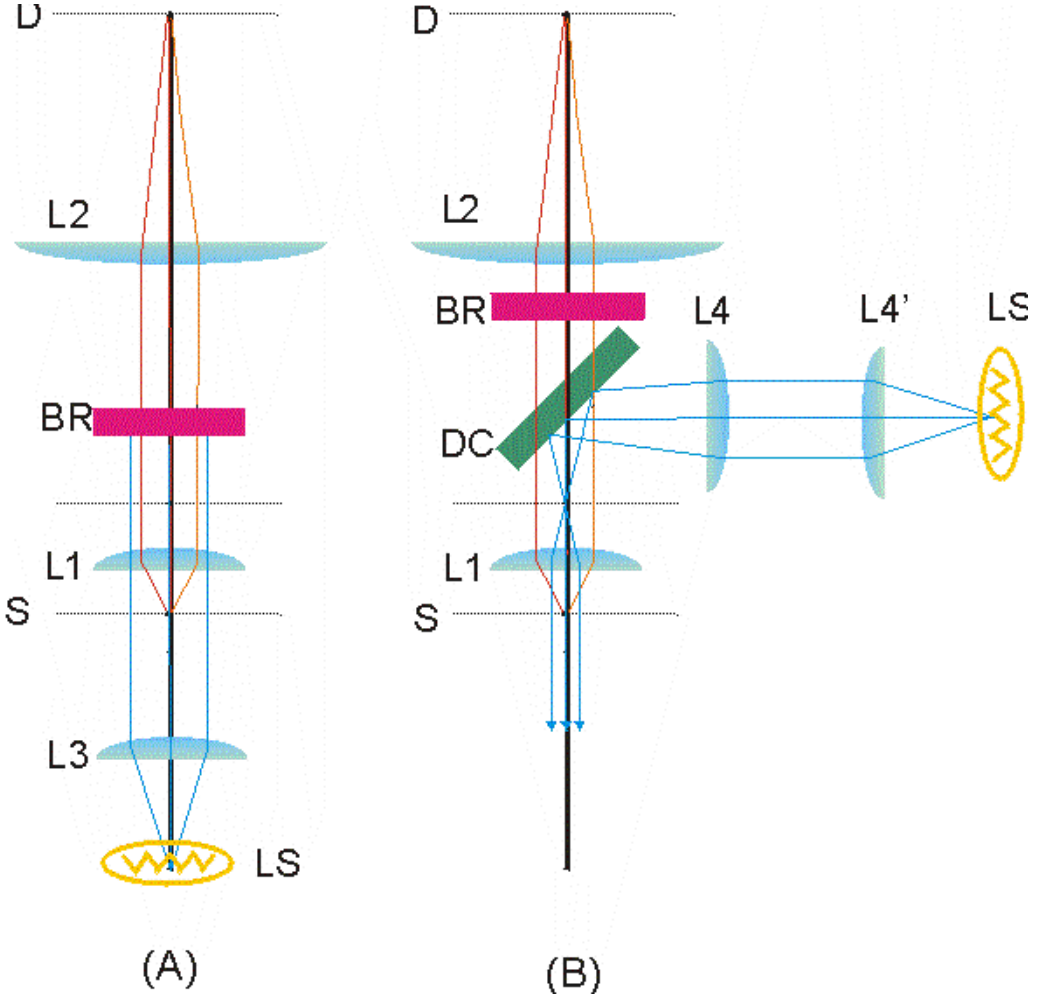

Fluorescence is fundamentally a quantum phenomena

Light ray can be thought of as a stream of photons each having energy:

$$E = h\upsilon = h\frac{c}{\lambda}$$

Light-Molecule Interaction

Polyatomic molecules

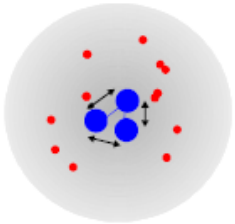

Simple orbitals

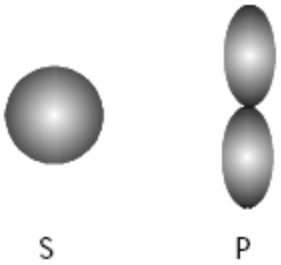

Jablonski Diagram

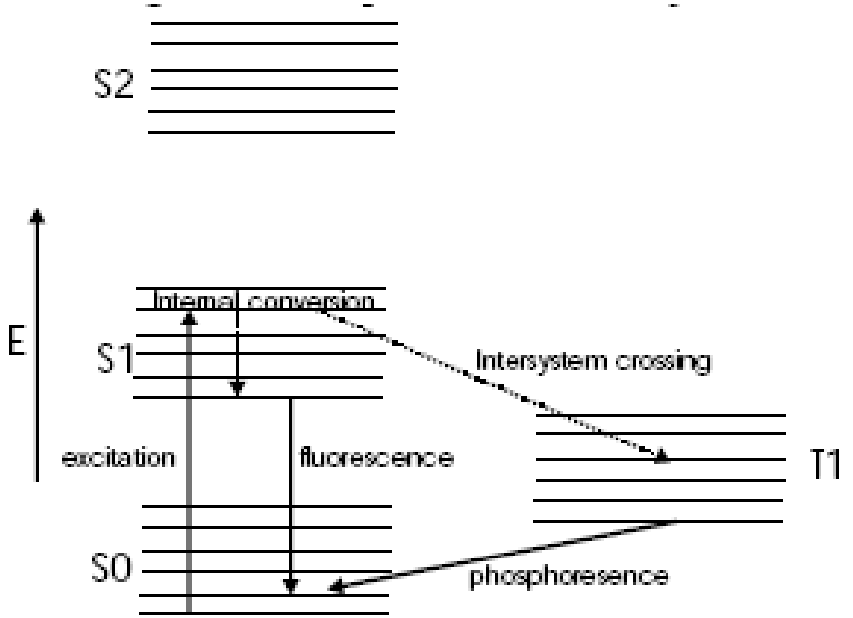

Jablonski Diagram

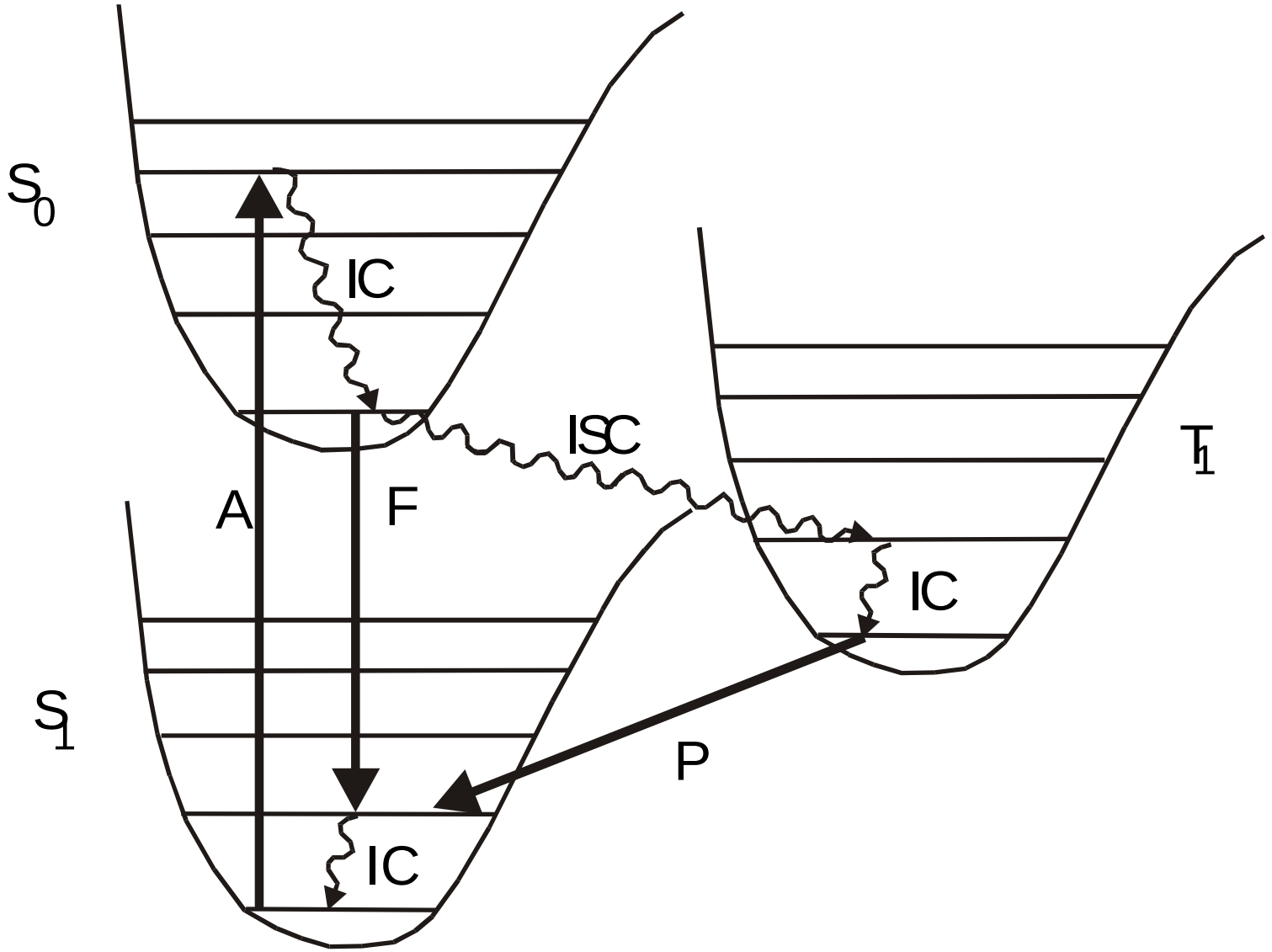

Basic properties of fluorescence

Stokes' shift. This refers to the observation that fluorescence (phosphorescence) always occur at a longer wavelength (lower photon energy) as compared with the excitation process. This fact is immediately obvious from the Jablonski diagram. Fluorescence (phosphorescence) does not emit from the excited vibrational level originally reached during the excitation process but occur in a lower energy state due to internal conversion and intersystem cross.

Invariance of emission with excitation: In general, emission spectrum is roughly (with some exceptions) independent of excitation wavelength. This fact is a direct result of internal conversion will put the molecule to the bottom of S1 independent of excitation process.

(4) Lifetime and quantum yield

Fluorescence molecule does not have to relax by emitting a photon (radiative decay) but they can also relax by thermal process without emitting a photon (non-radiative decay). The quality of a fluorophore is clearly related to the rates of these two decay modes.

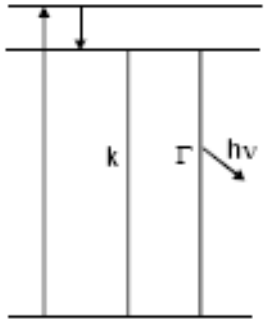

In this simplified Jablonski diagram, the radiative decay is denoted by Γ and the non-radiative decay is denoted by k.

The residence time of the molecule in the excited state (S1), lifetime, is affected by both radiative and non-radiative rates. In particular,

$$\tau = \frac{1}{\Gamma + k}$$

In the absence of non-radiative decay processes, the lifetime measured is called the intrinsic lifetime of the fluorophore.

$$\tau_0 = \frac{1}{\Gamma}$$

The "efficiency" of the fluorophore, the quantum efficiency, is defined as:

$$Q = \frac{\Gamma}{\Gamma + k} = \frac{\tau}{\tau_0}$$

Basic Fluorescence Measurement

Intensity measurement:

This is the most basic measurement. It is not very diagnostic and it mainly reflects the presence or absence of fluorophore and their concentration. Note that quantitative intensity measurement is very hard as many factors affect the excited state of the fluorophore and will modify its intensity especially in biological systems.

Spectral measurement:

Spectral measurement is quite diagnostic. Most fluorophores has a fairly unique spectral pattern. Spectral measurement allows the experimenter to determine what fluorophores are present. In microscopy setting, the interaction of microscopic structures can be studied if they can be labeled with different color fluorophores. Equally important, many fluorophores changes color (excited state vibrational level shifts) as a function of biochemical environment. This allow a sensitive monitoring of intracellular or tissue biochemical state. The calcium probe described earlier is a good example. Another example is this membrane probe Laurdan which changes color as a function of the fluidity of the membrane.

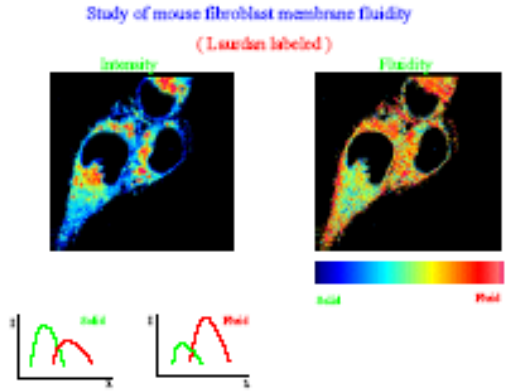

Emission spectra is defined as measuring emission intensity as a function of wavelength at a given excitation wavelength. Excitation spectra is defined as the measurement of emission intensity at a given emission wavelength as a function of excitation wavelength.

Polarization and Isotropy

Polarization is also another useful property of fluorescence. All fluorescence molecules have a preferential direction of excitation (excitation dipole) and emission (emission dipole). Note that the excitation and emission dipoles do not have to coincide in general. The probability of exciting a molecule depends on the relative orientation of the molecular excitation dipole and the polarization of light. Let θ be the angle between the light polarization and the molecule excitation dipole. The probability of excitation is: $P \propto \cos^2\theta$. This is similar to what we see for the transmission of a polarizer. One can also see that exciting molecules with polarized light selects a sub-population of molecule that are oriented close the polarization of light.

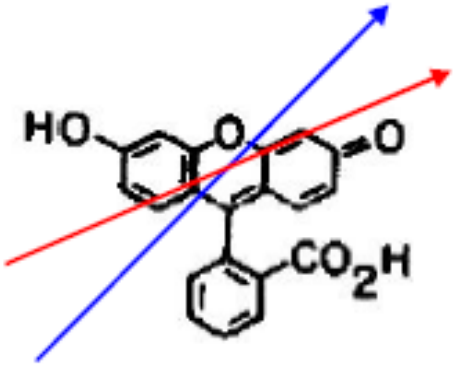

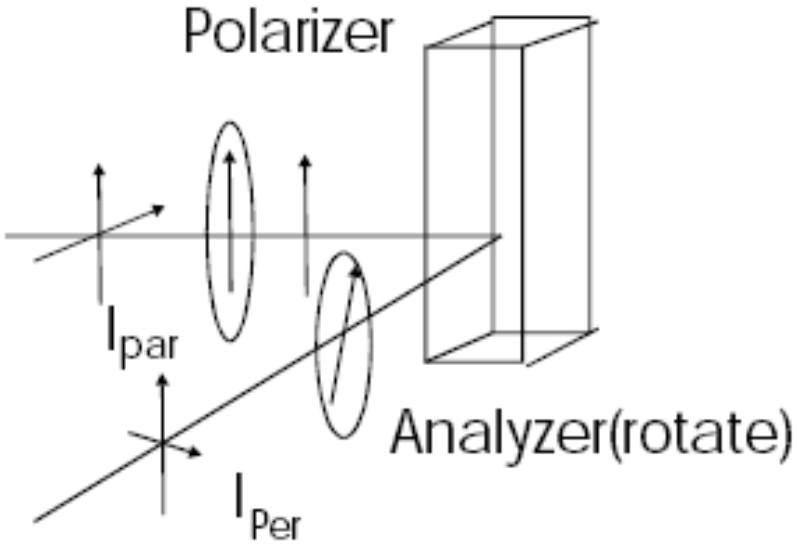

The measurement of polarization of aqueous specimen is typically performed using the above geometry. Excitation light is first polarized. The emission light is analyzed for its polarization parallel and perpendicular to the excitation direction.

The result is expressed in terms of polarization, P, or anisotropy, r:

$$P = \frac{I_{par} - I_{per}}{I_{par} + I_{per}}, \quad r = \frac{I_{par} - I_{per}}{I_{par} + 2I_{per}}$$

Note that the steady state polarization is high with rotation diffusion rate slow compared with its lifetime but its polarization is low if diffusion is fast compared with its lifetime. This is very useful for measuring the binding of small ligand to large molecules or surfaces. Polarization is also often used to measure the mean orientation of molecules.

Fluorescent Probes

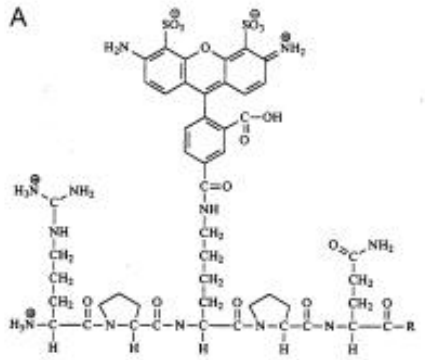

Molecular Probes, Oregon

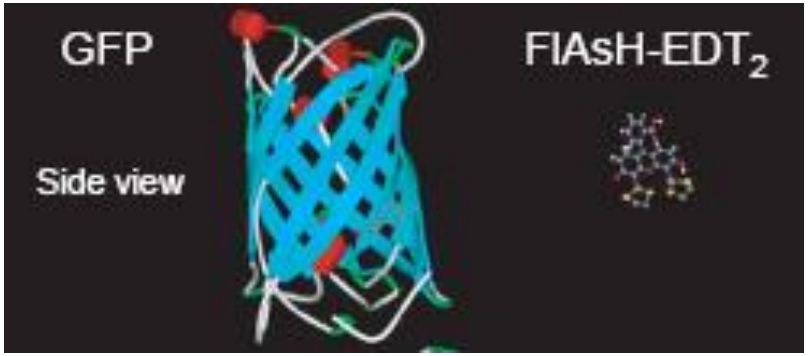

Hoffmann et al, Nat. Meth, 2005

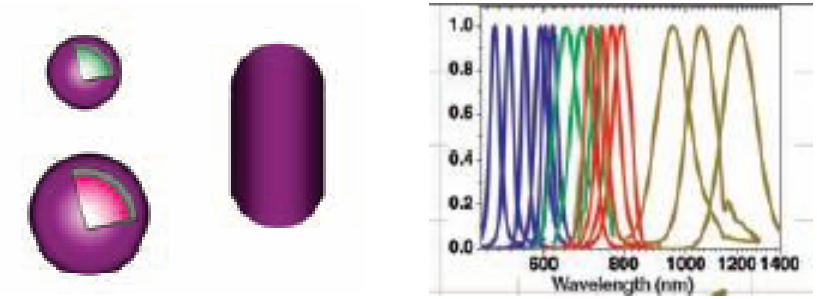

Michalet et al, Science, 2005

Strengths of Fluorescence Microscopy

(1) New contrast enhancement mechanism

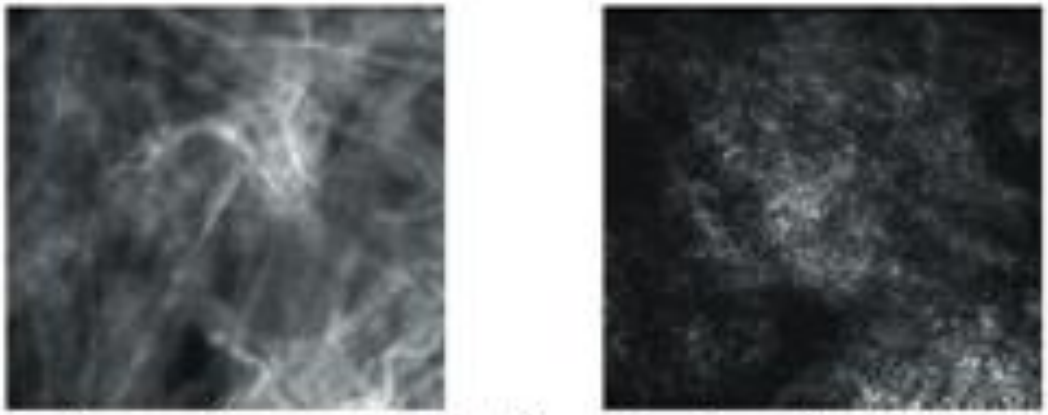

Imaging collagen/elastin fibers in dermis. Fluorescence image (left), scattered light image (right)

Strengths of Fluorescence Microscopy

(2) Specificity – individual structural components can be tagged based on their biochemical difference

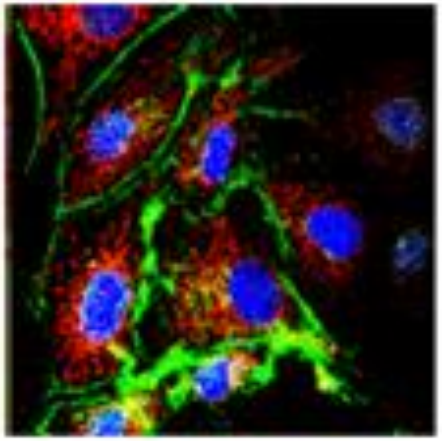

Nuclei (blue) is label with DAPI, Actin (green) is label with Bodipy phallodin, mitochondria (red) is label with MitoTracker.

Strengths of Fluorescence Microscopy

(3) Molecular Sensitivity

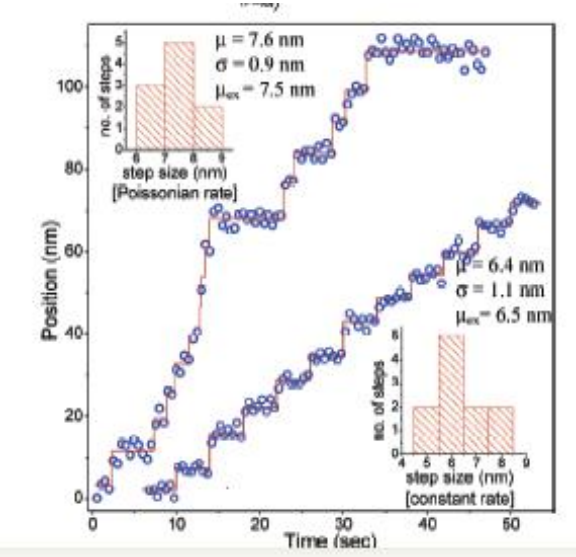

Yildiz, Acc. Chem. Res., 2005

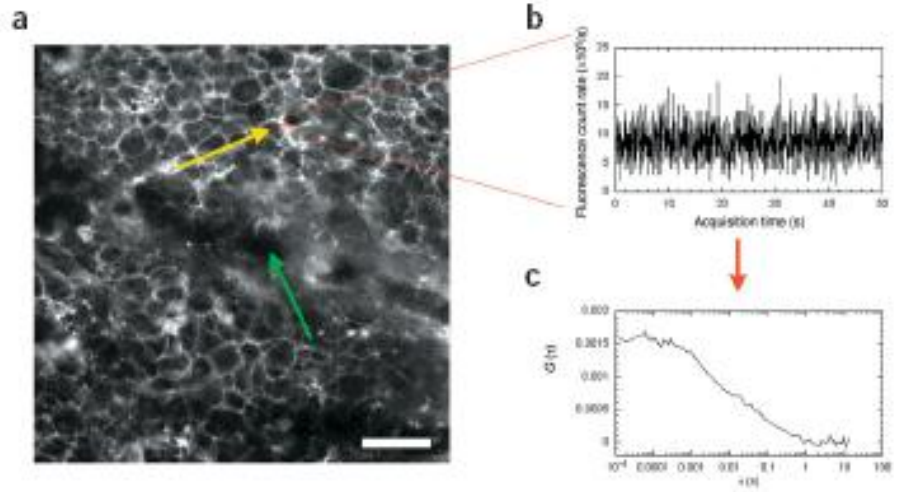

Alexandrakis, Nat. Med., 2004

Strengths of Fluorescence Microscopy

(4) Image biochemical reactions/ Monitor microenvironmental changes

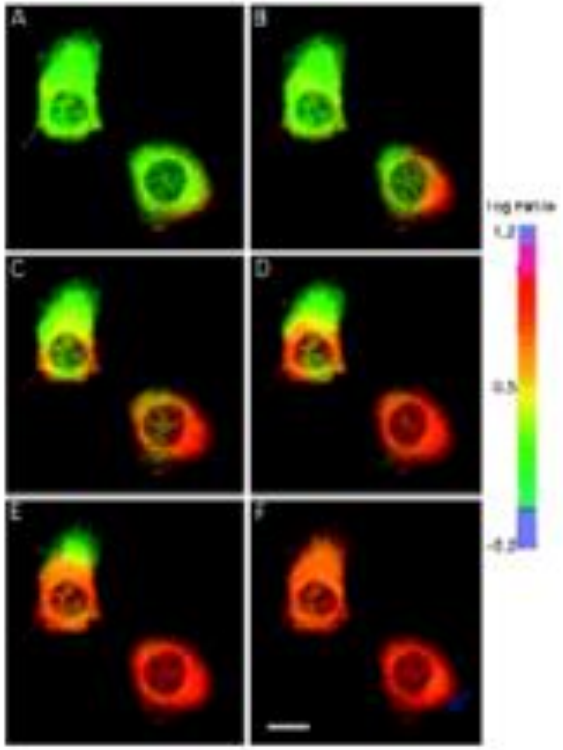

Fan et al. Biophys. J., 1999
Calcium wave in HeLa cells

Strengths of Fluorescence Microscopy

(5) Monitors genetic expression

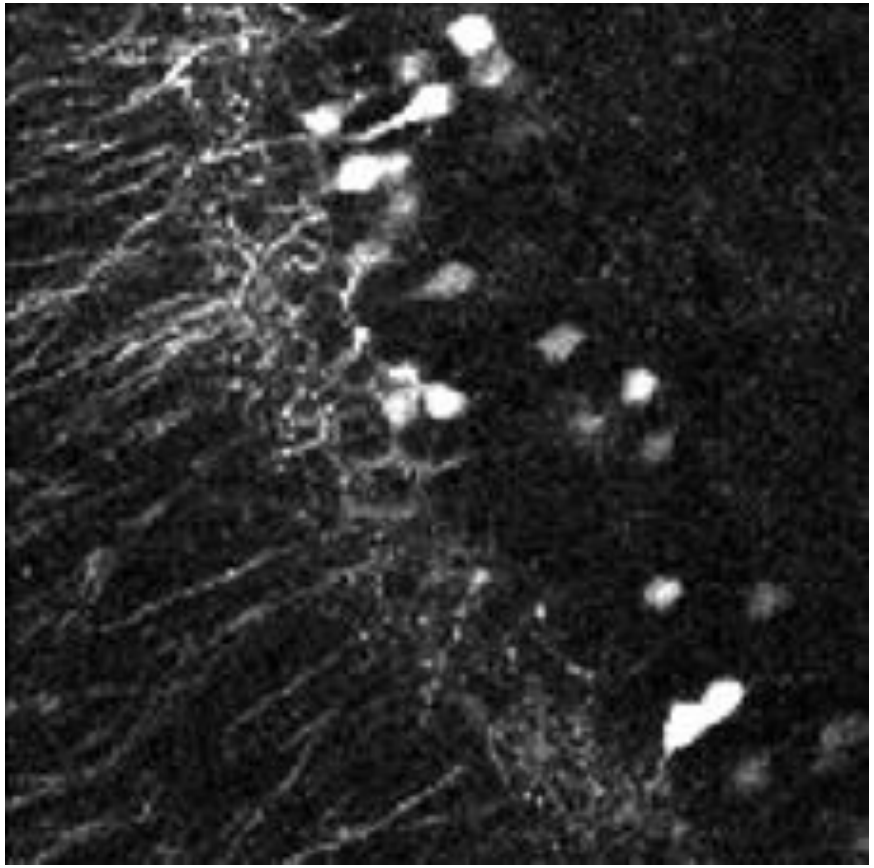

The Need For 3D Resolved Imaging

Biological systems are inherently 3D!

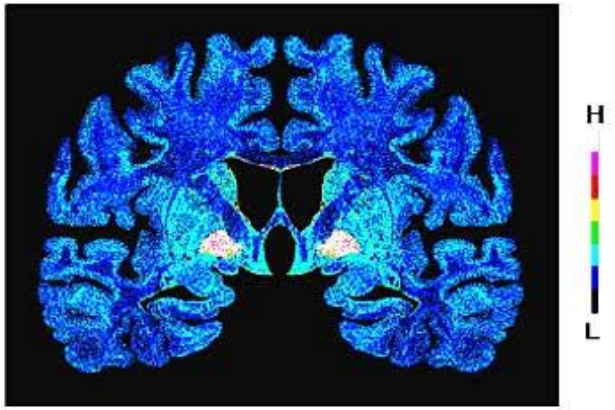

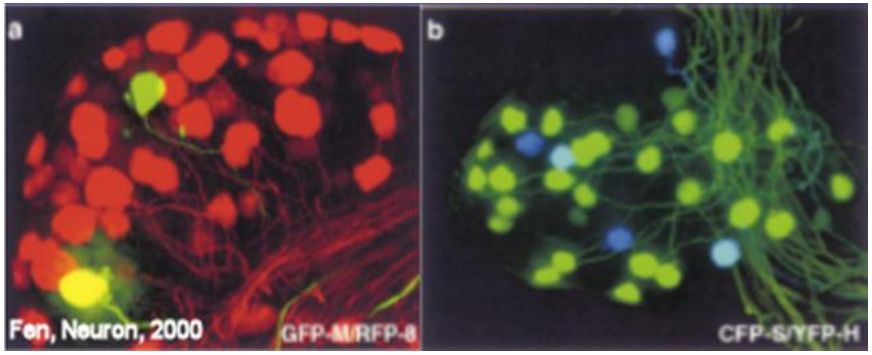

Biological processes also occur on multiple length scale

Histopathology

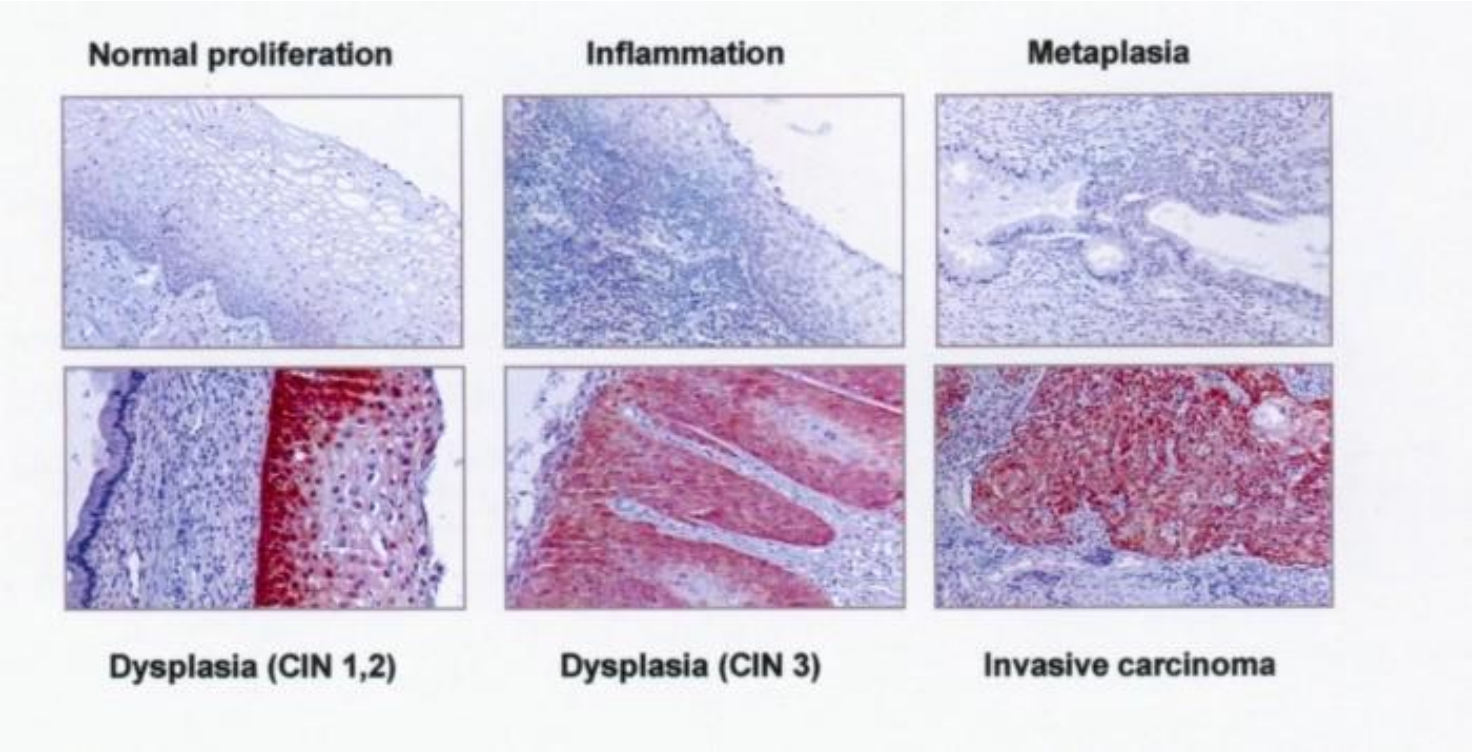

Solution: mechanical sectioning of specimen

Comment: (1) Clinical standard (2) Simple technology
(3) Sectioning artifacts (4) Not in vivo

Total Internal Reflection Microscopy

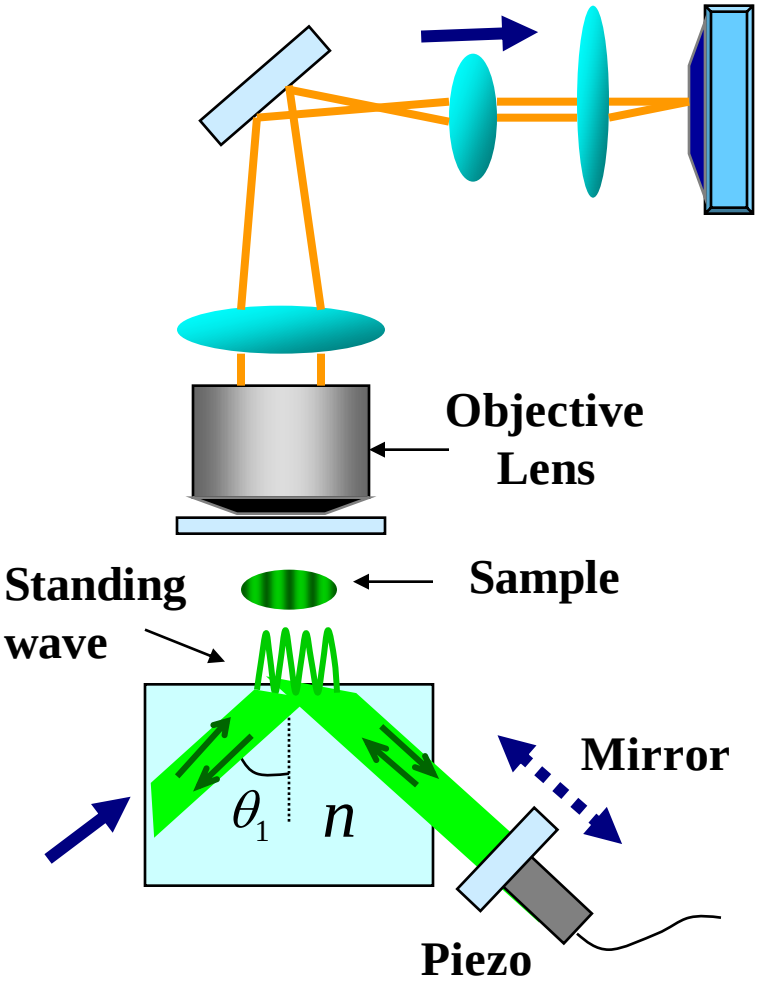

Solution: Evanescence wave at interfaces

Comments: (1) only basal surface structure (2) high z resolution, 50 nm

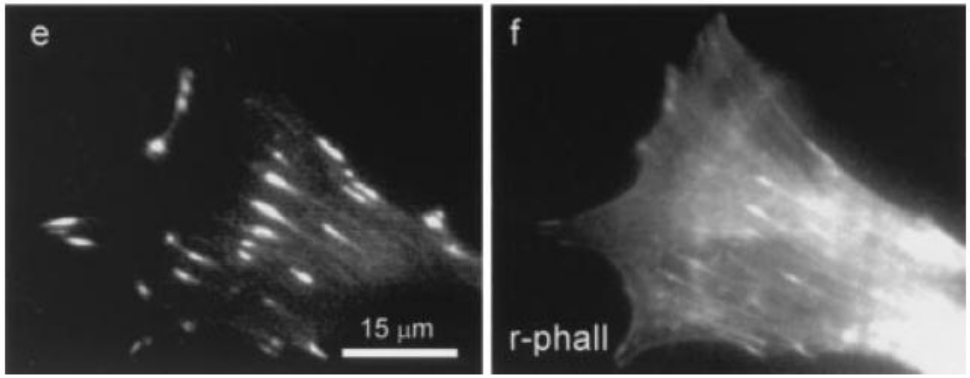

TIRF Wide Field

Sund & Alexrod, Biophys J 2000

True 3D Microscopy

Confocal Microscopy: Minsky, US Patent, 1961

Two-Photon Microscopy: Sheppard et al., IEEE J of QE, 1977
Denk et al., Science, 1990

The Invention of Confocal Microscopy

Confocal microscopy is invented by Prof. Melvin Minsky of MIT in about 1950s.

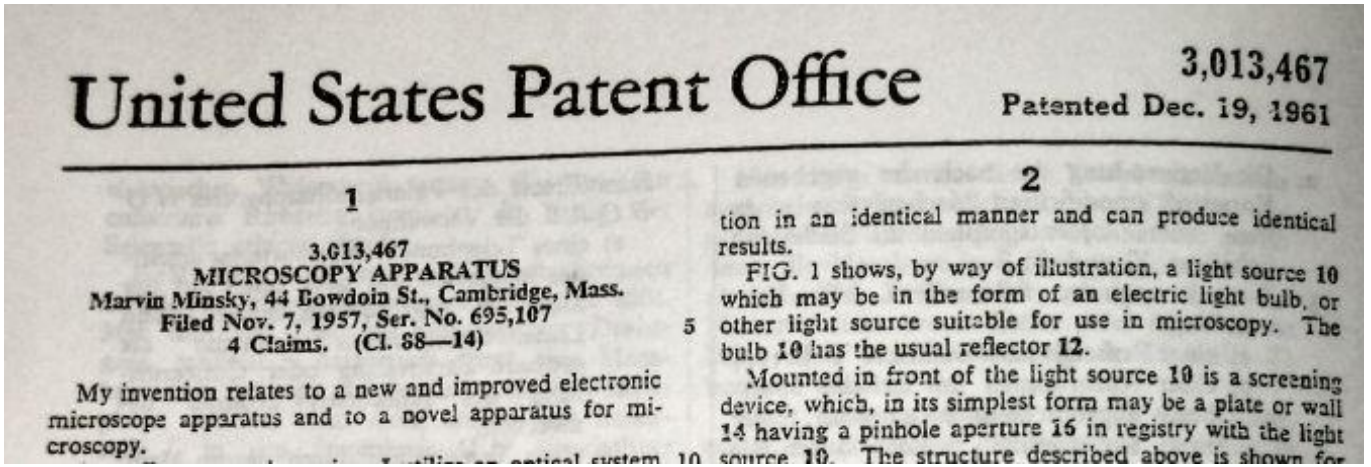

United States Patent Office

3,013,467
Patented Dec. 19, 1961

1

3,013,467
MICROSCOPY APPARATUS
Marvin Minsky, 44 Bowdoin St., Cambridge, Mass.
Filed Nov. 7, 1957, Ser. No. 695,107
4 Claims. (Cl. 88—14)

My invention relates to a new and improved electronic microscope apparatus and to a novel apparatus for microscopy.

2

tion in an identical manner and can produce identical results.

FIG. 1 shows, by way of illustration, a light source 10 which may be in the form of an electric light bulb, or other light source suitable for use in microscopy. The bulb 10 has the usual reflector 12.

Mounted in front of the light source 10 is a screening device, which, in its simplest form may be a plate or wall 14 having a pinhole aperture 16 in registry with the light source 10. The structure described above is shown for

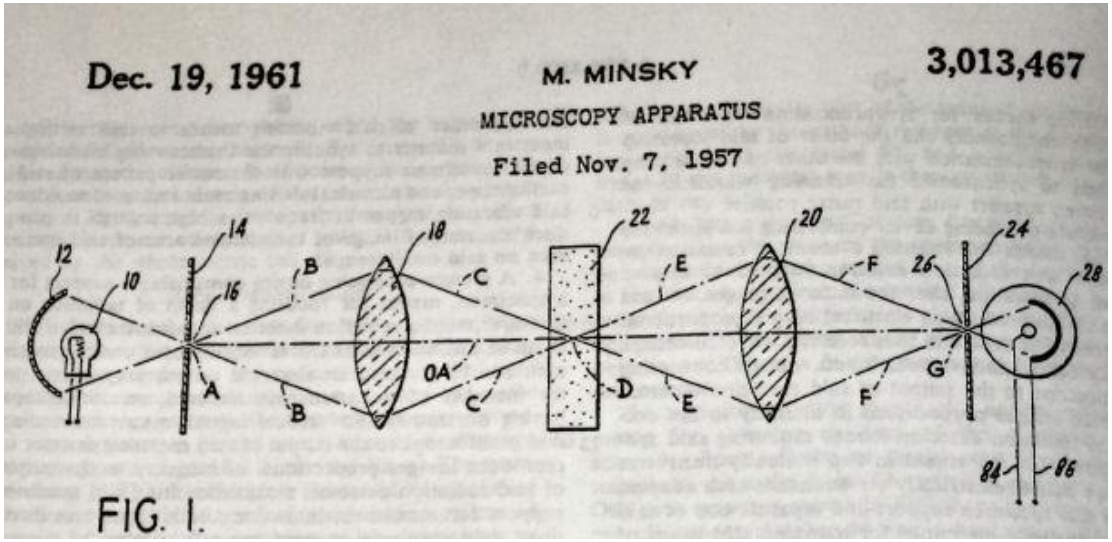

FIG. 1.

Principle of Confocal Microscopy

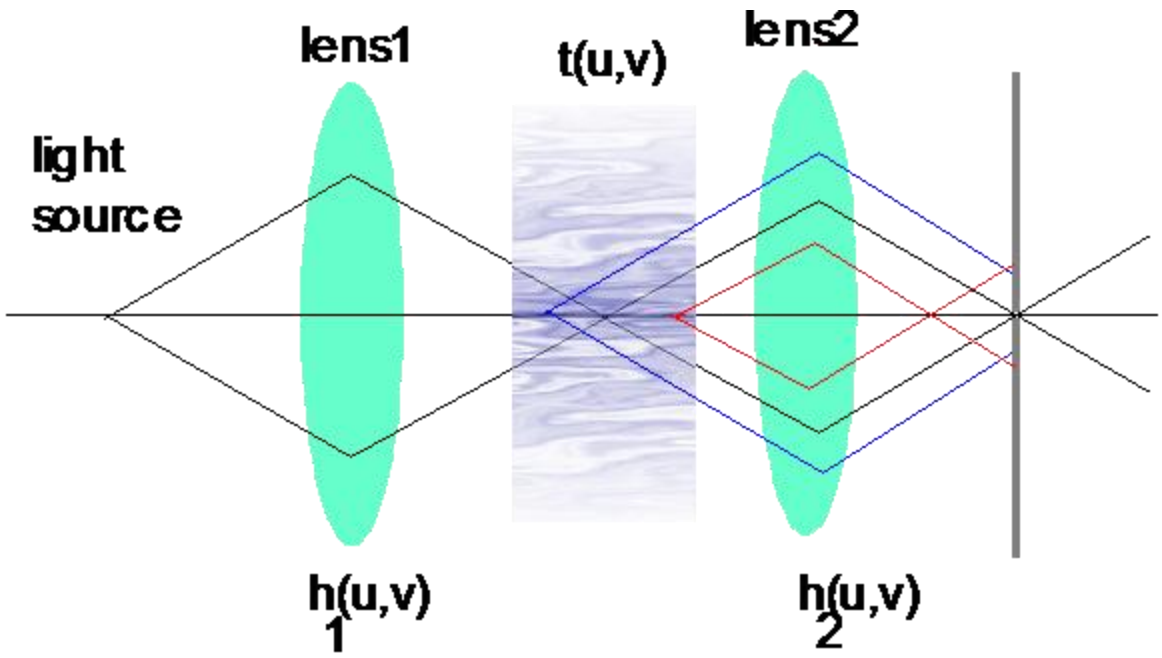

Point Spread Function of Confocal Microscopy

Lateral Dimension: Airy function

$$PSF_{confocal}(kr) \propto [\frac{2J_1(kr)}{kr}]^4$$

k is the wave number

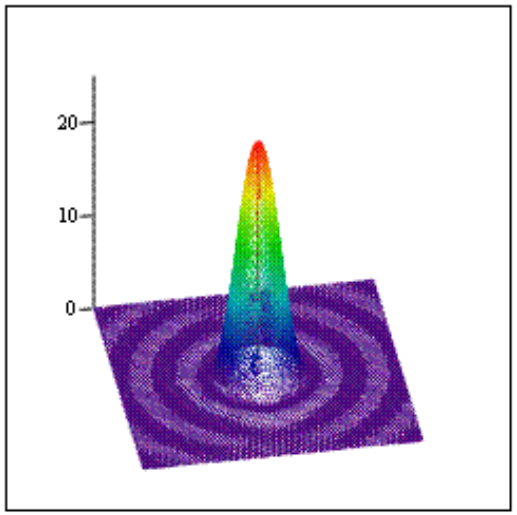

g

Axial Dimension : Sinz function

$$PSF_{confocal}(kz) \propto [\frac{\sin(kz)}{(kz)}]^4$$

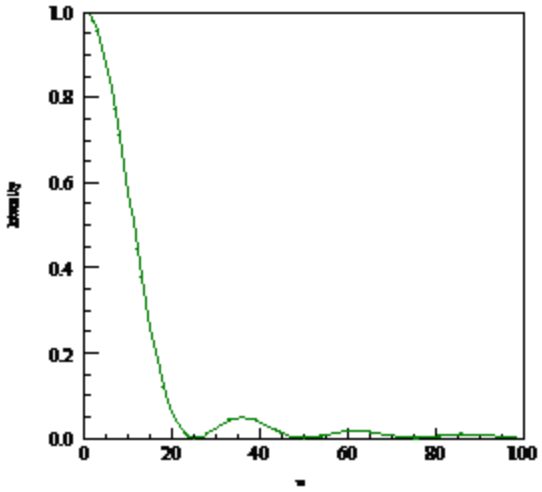

Resolution:

Lateral $\propto NA$

Axial $\propto NA^2$

Depth discrimination

For a uniform specimen, we can ask how much fluorescence is generated at each z-section above and below the focal plane
assuming that negligible amount of light is absorbed throughout.

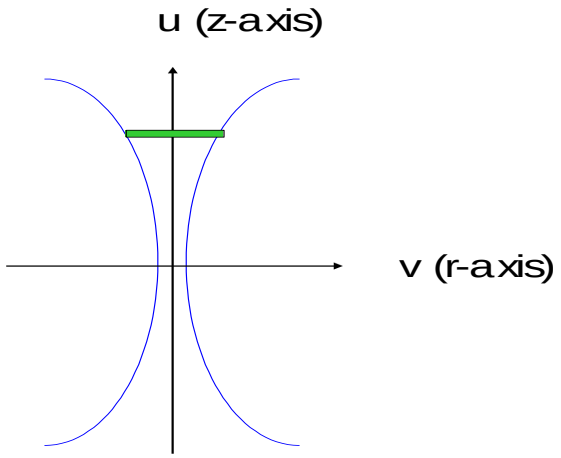

$$F_{z-\sec}(u) \equiv 2\pi \int_0^\infty F(u,v) v dv$$

Depth discrimination

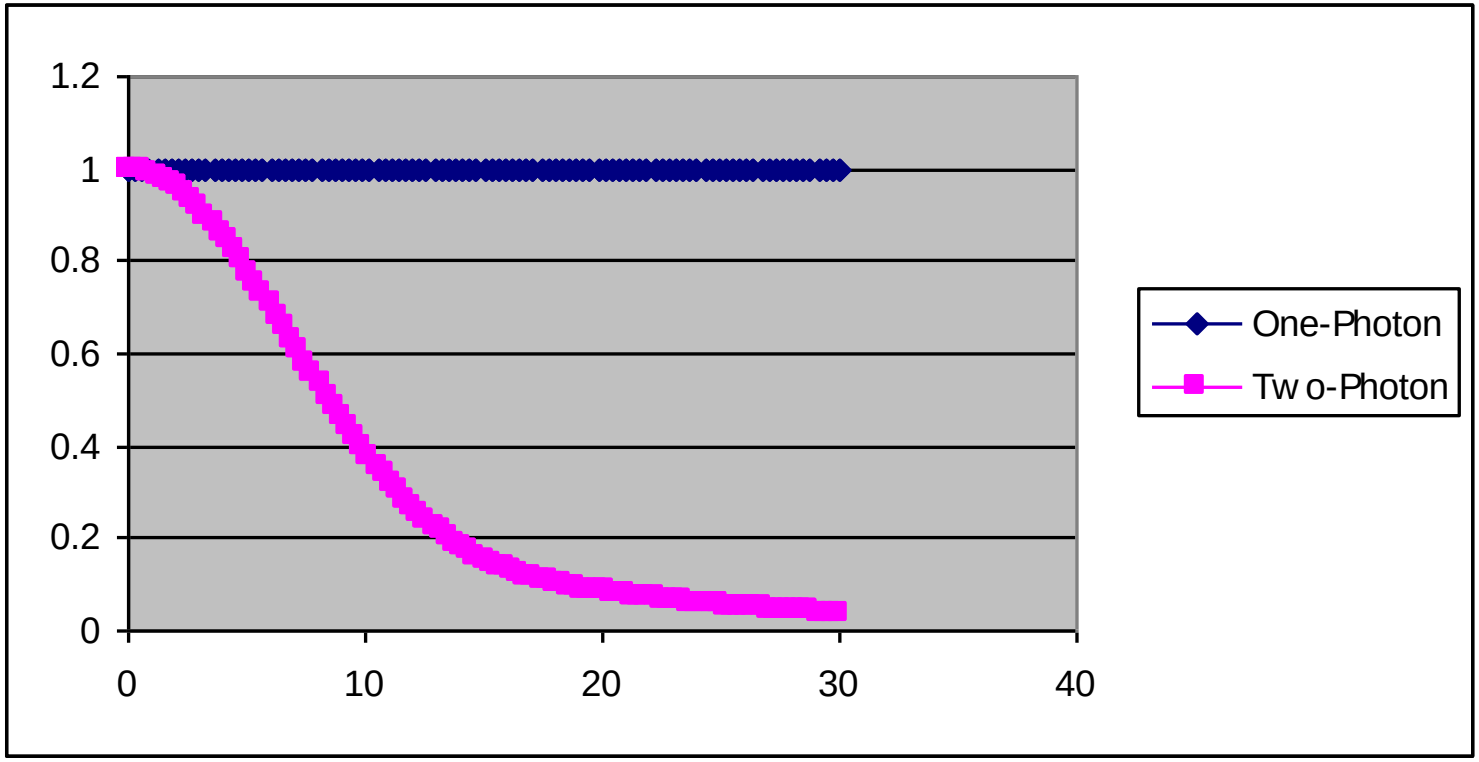

Early Demonstration of Confocal Microscopy in Biological Imaging

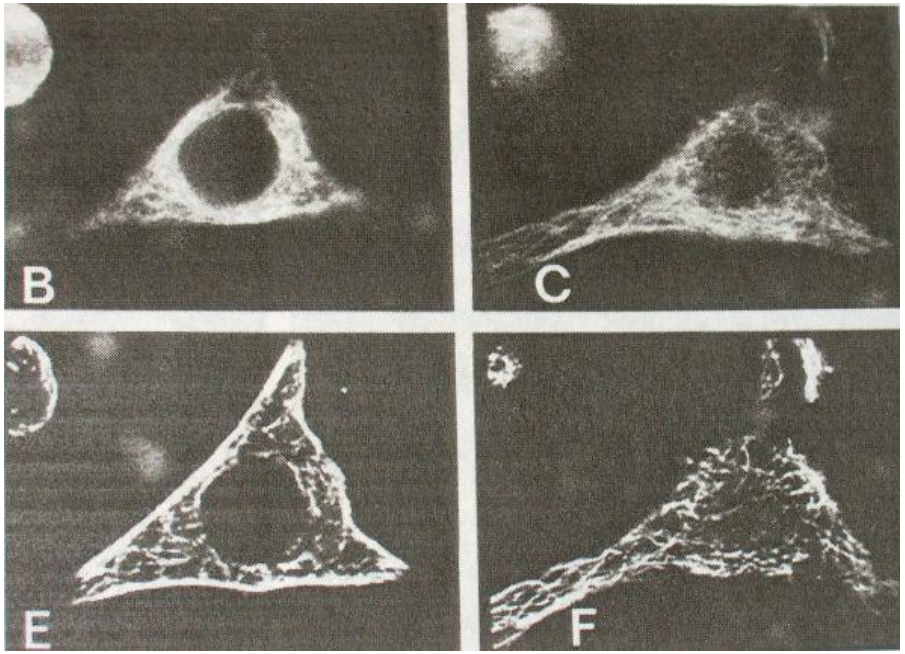

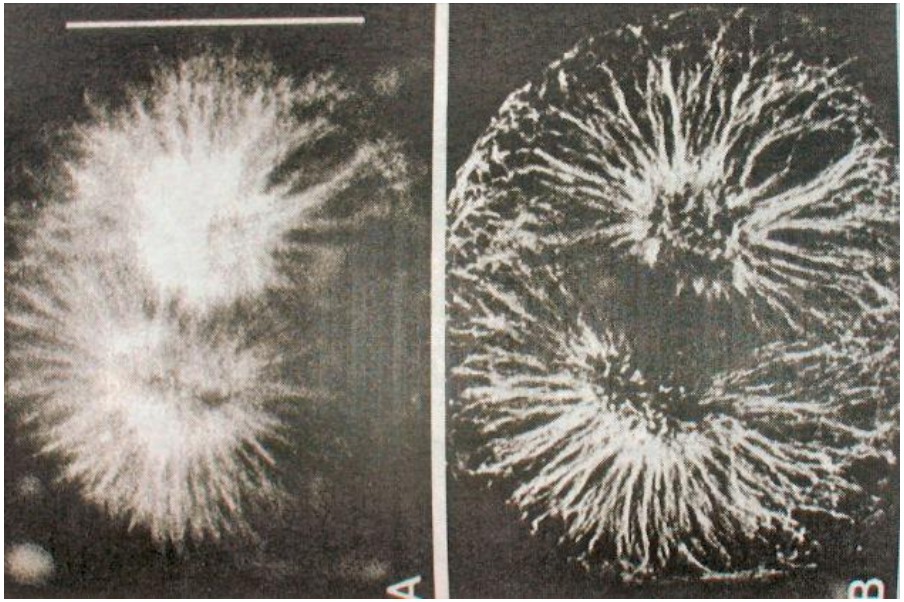

White et al., JCB 1987

Some Recent Application of Confocal Tissue Imaging

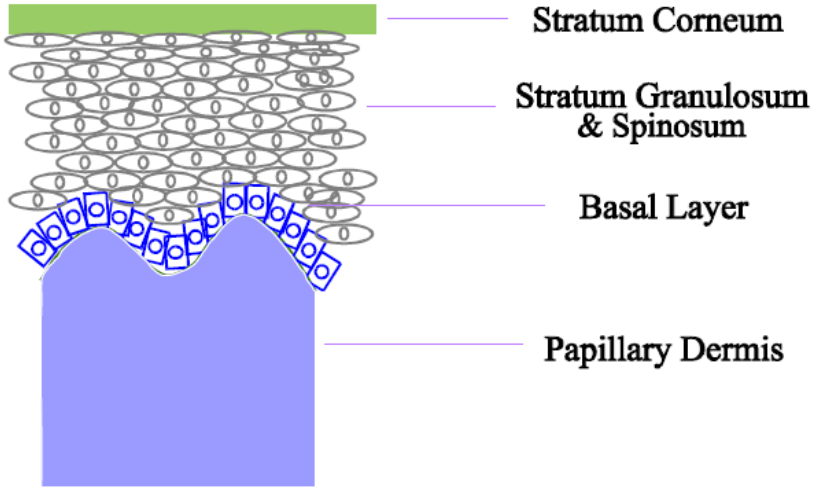

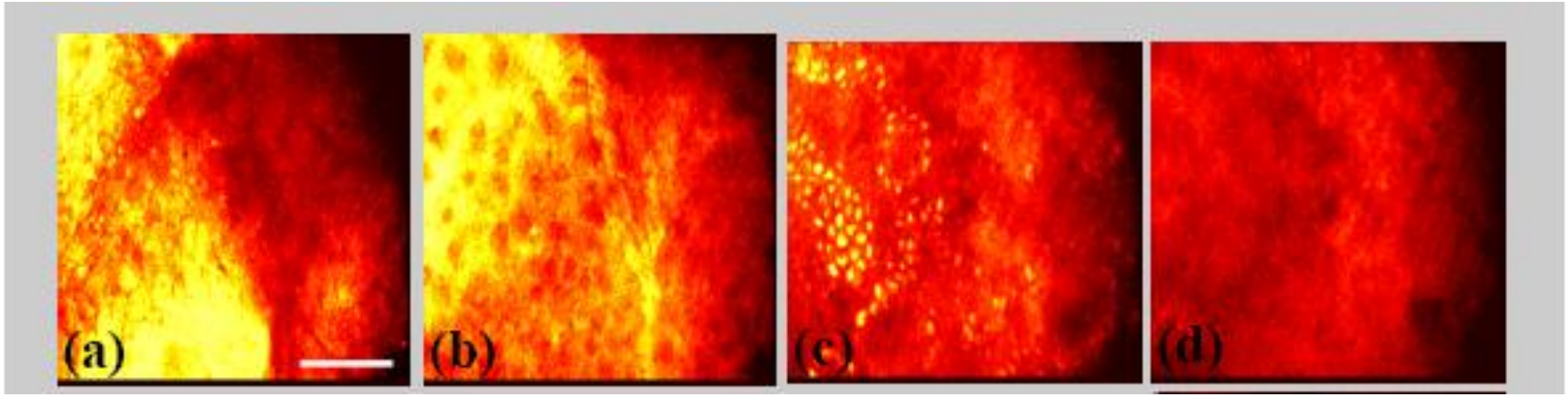

Confocal Tissue Imaging

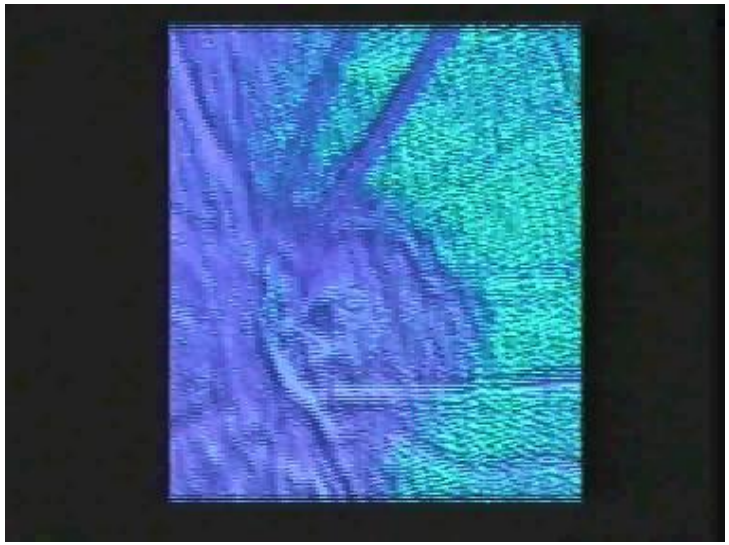

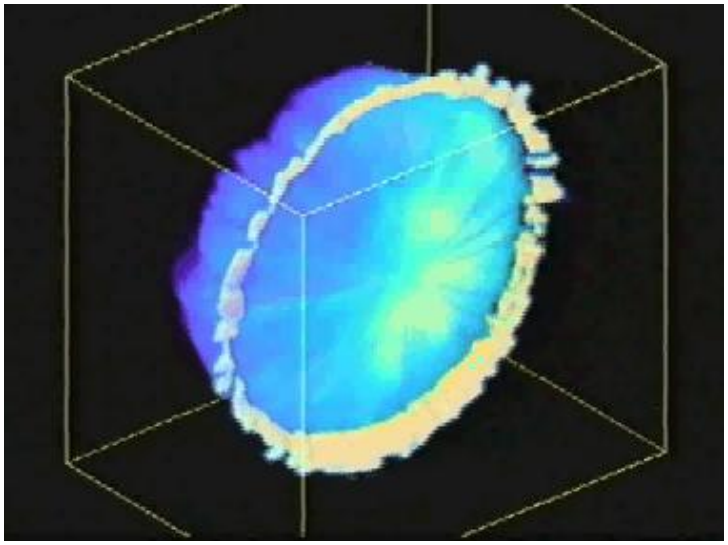

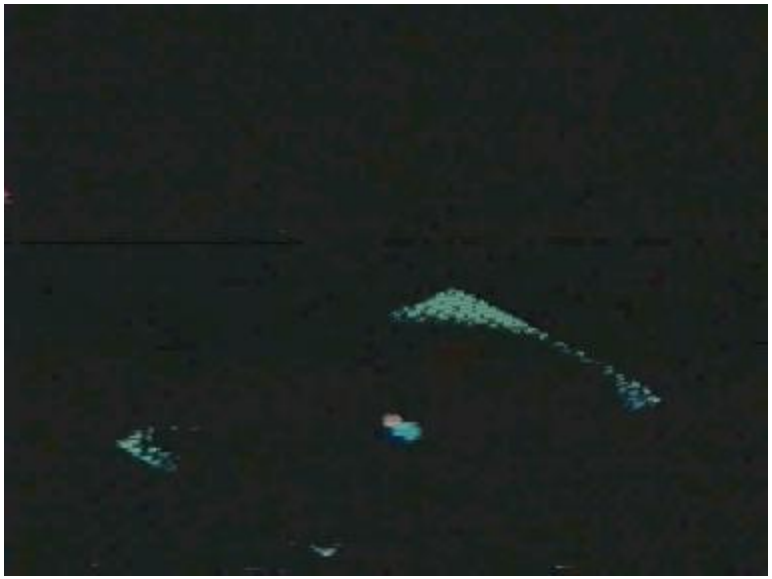

Masters, Opt Lett, 1999

Effect of index matching and excitation saturation

There are two additional subtle effects that users of confocal microscope should be aware of.

Index matching

While microscope objectives are aberration corrected for specimen right on top of the cover slip, their performance often degrade significantly as one looks deeper into a specimen especially when imaging depth approach 50-100 μm. This effect is much more significant for oil immersion objectives looking into aqueous biological specimens (Visser, 1992). This aberration is in large part due to index mismatch and can be greatly minimized by using water immersion lens for thick specimen.

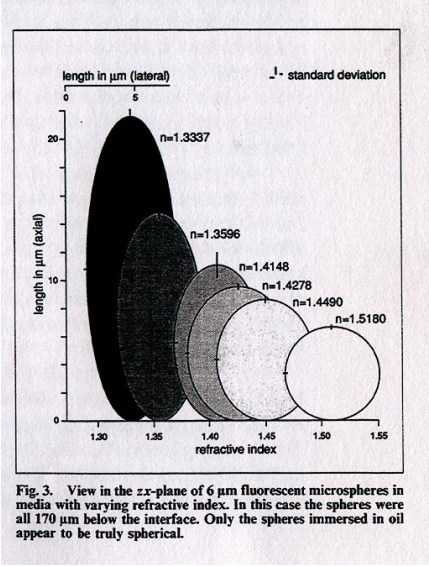

Fig. 3. View in the zx-plane of 6 μm fluorescent microspheres in media with varying refractive index. In this case the spheres were all 170 μm below the interface. Only the spheres immersed in oil appear to be truly spherical.

Tandem Scanning Confocal Microscope

Utilizes a Nipkow Disk

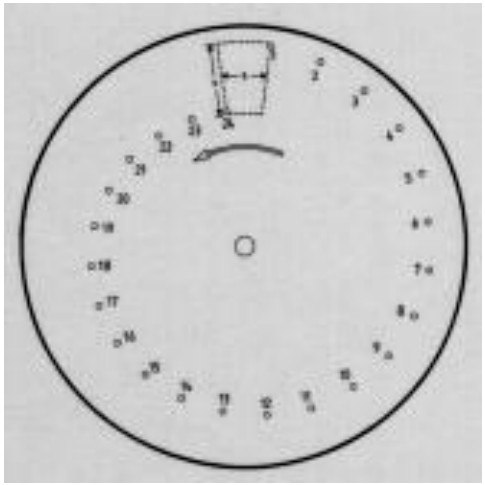

Holes organize in an Archimedes spiral

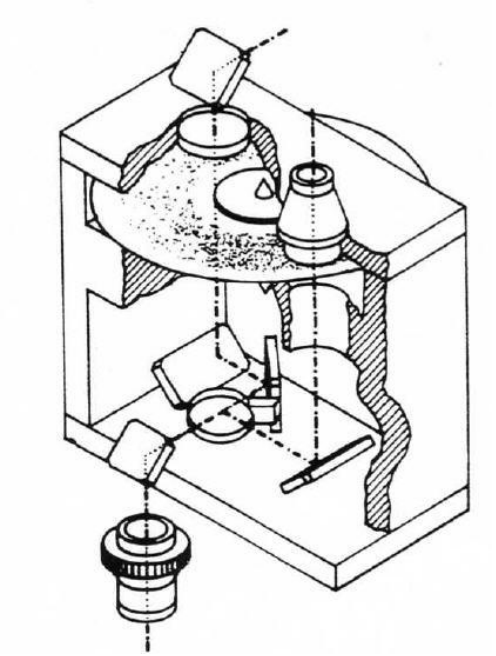

Petran's System

A Model Tandem Confocal Microscope Utilizing Yokogawa Scan Head

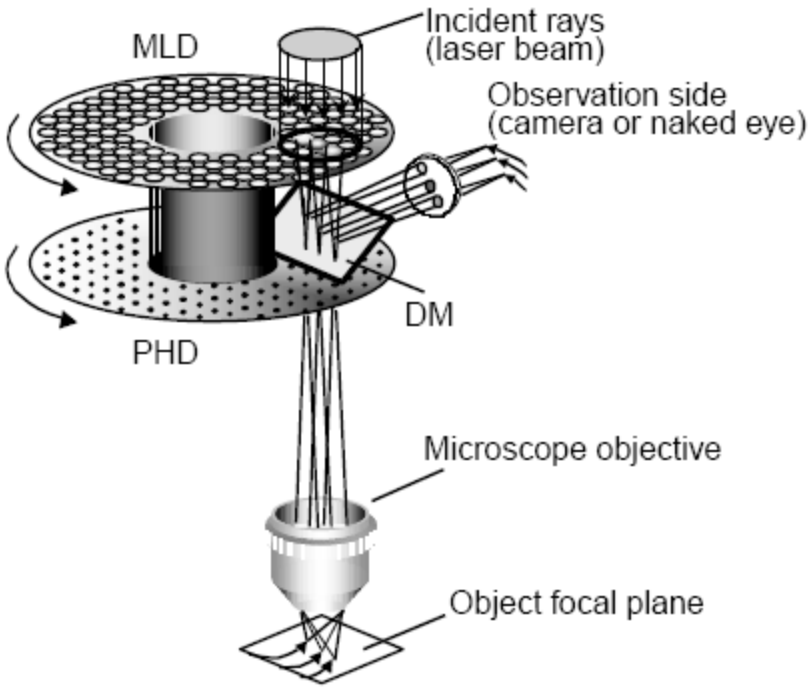

Eliminate light throughput
Issue by spinning both
a plate of lenslets and
nother plate of pinholes

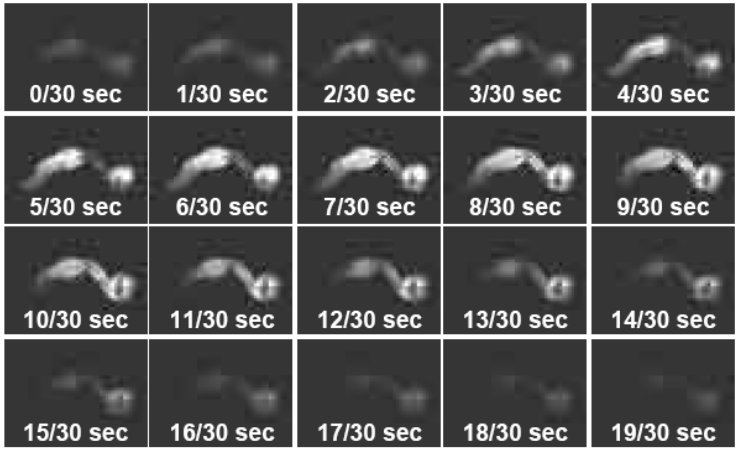

C. Elegans

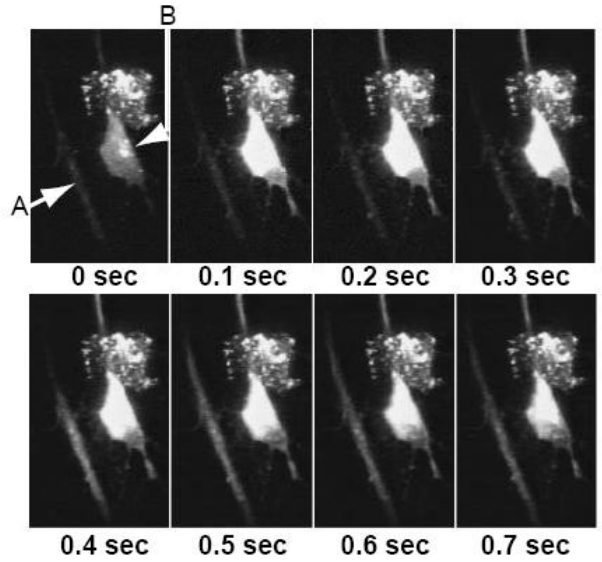

Calcium events in nerve fiber

Basic Ideas of two-photon excitation

Two-photon excitation is similar to the one-photon process except the use of two lower energy (infrared) photons.

The difference between the two can be seen in these movies:

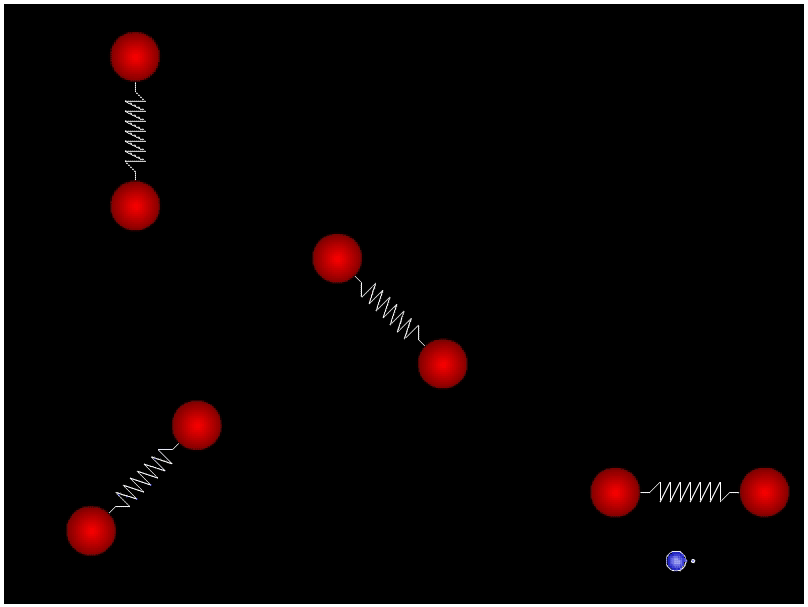

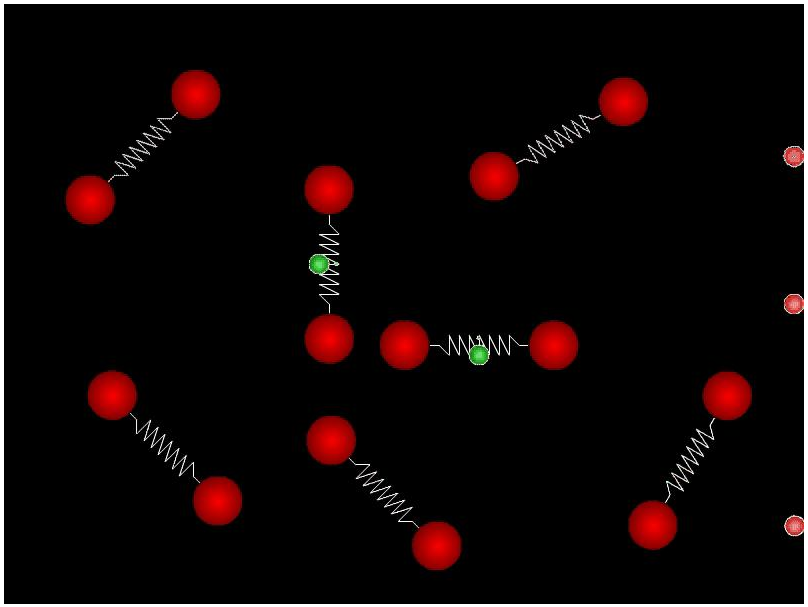

An abbreviated history of two-photon microscopy

(1930) Maria Goeppert-Mayer predicted the existence of two-photon effect

(1961) Franken et al. demonstrated second harmonic generation in ruby

(1961) Kaiser et al. showed two-photon fluorescence in a solid state material

(1964) Singh and Bradley reports three-photon fluorescence

(1970s-1980s) Two-photon effect has been used in biological spectroscopy by researchers such as Birge, Fredrich, and McCain

(1970s-1980s) Microanalysis based on non-linear 2nd harmonic generation was developed by researchers such as Freund and Hellwarth

(1976-80s) A number of researchers such as Sheppard, Kompfner, Gannaway and Wilson suggested the possibility of incorporating non-linear excitation \into scanning microscopy

(1989) Denk, Webb and coworkers definitively demonstrated two-photon scanning microscopy and a number of its unique properties such as the triggering of localized chemical reaction

Two-Photon Excitation Microscopy

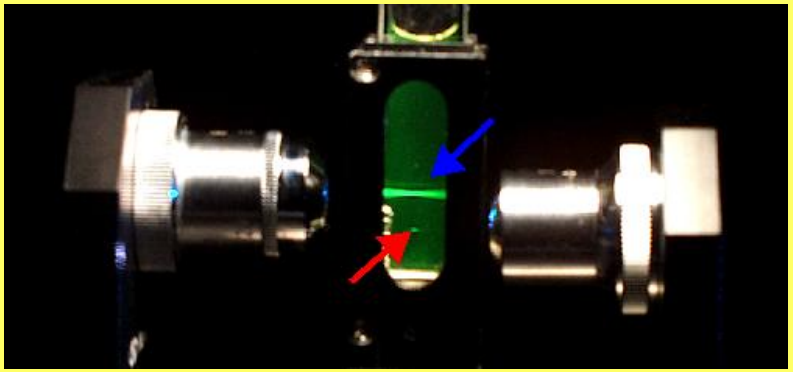

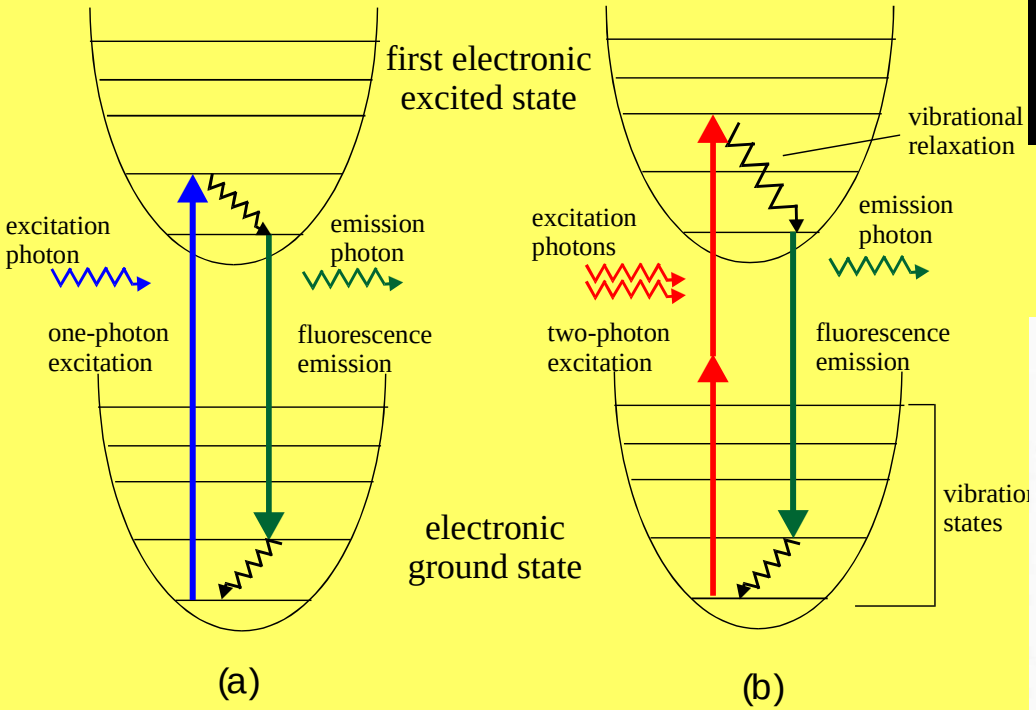

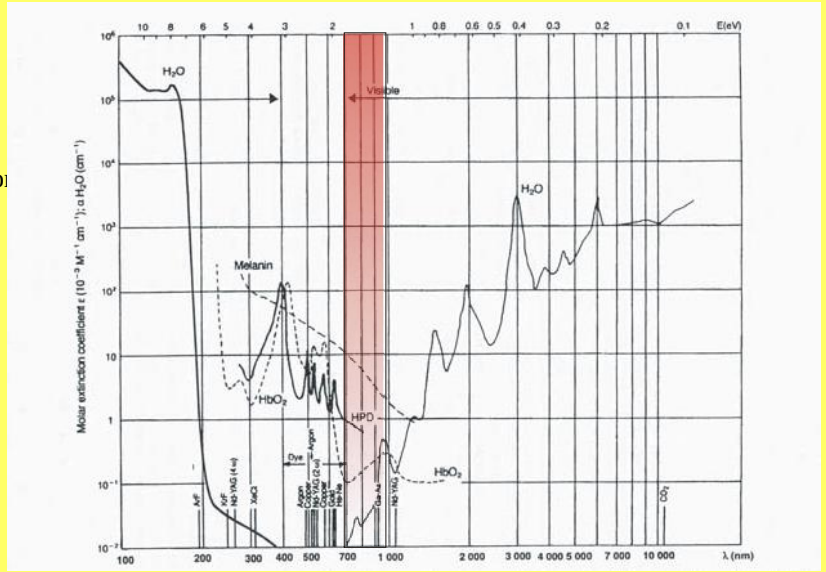

A comparison of two-photon and confocal microscopes

(1) Confocal microscopes have better resolution than two-photon microscopes without confocal detection.

(2) Two-photon microscope results in less photodamage in biological specimens. The seminal work by the White group in U. Wisconsin on the development of *c. elegans* and hamsters provides some of the best demonstration. After embryos have been continuously imaged for over hours, live specimens are born after implantation.

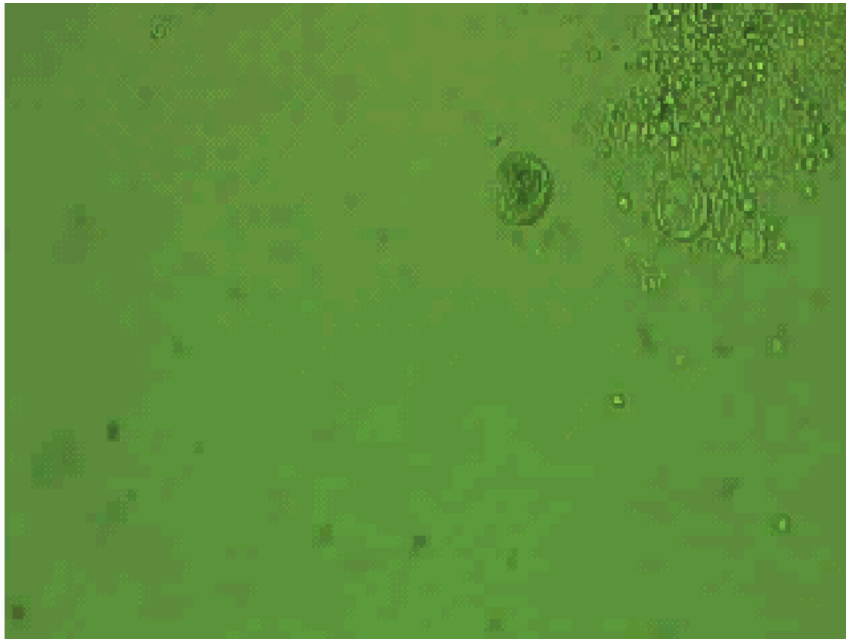

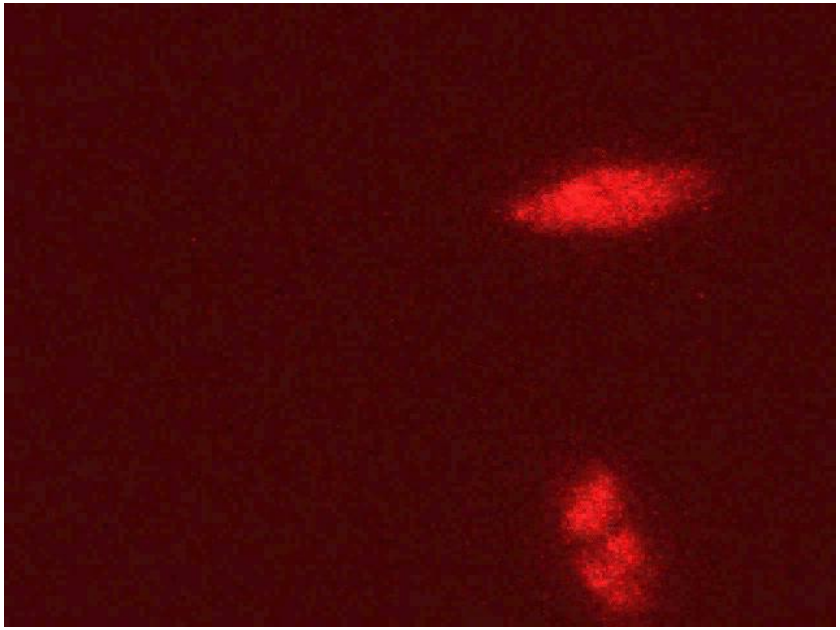

(3) Two-photon microscope provides better penetration into highly scattering tissue specimen. Infrared light has lower absorption and lower scattering in turbid media.

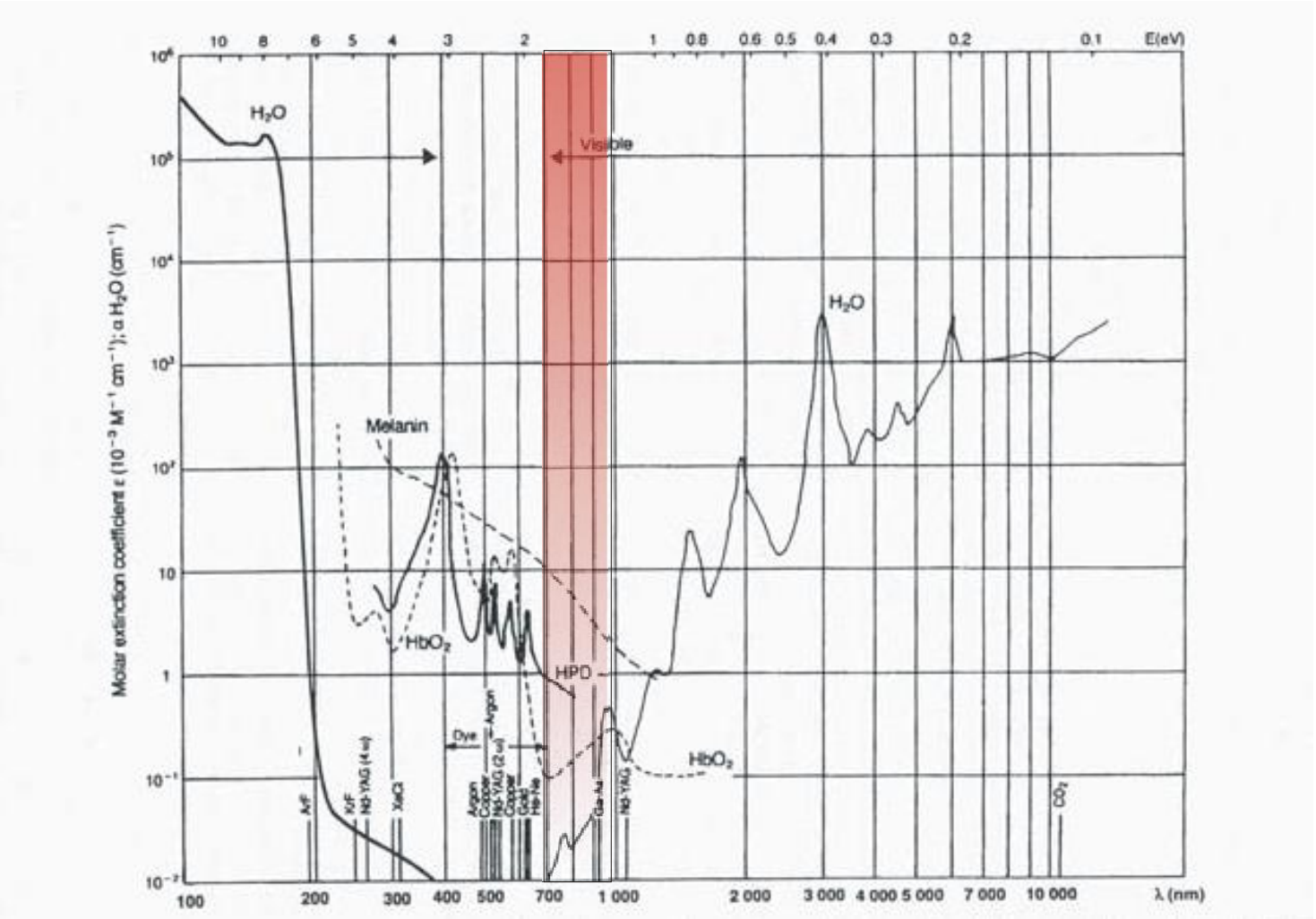

Two-photon excitation cross section

Since two-photon absorption is a second-order process involving the almost simultaneous interaction of two photons with one fluorophore, this process has a small cross-section, δ, on the order of 10^{-50} cm^4s (defined as 1 GM, Goppert-Mayer).

The instantaneous intensity of the fluorescence signal:

$F(t)$ (photons/sec/molecule)

The incident photon flux:

$I(t)$ (photon/sec/m^2)

One-photon excitation fluorescence:

$F^{1P}(t) \approx \sigma I(t)$ where σ is the one-photon cross section with unit of cm^2:

Two-photon excitation fluorescence:

$$F^{2P}(t) \approx \delta I(t)^2$$

$$F^{2P}(t) \approx \delta P(t)^2 \left(\frac{(NA)^2}{2\hbar c \lambda} \right)^2$$

$P(t)$ is the laser instantaneous power

λ is the wavelength of light

NA is the numerical aperture of the focusing objective

$\hbar$ and c are Planck's constant and the speed of light

Comparing CW and pulse laser excitation efficiency

*For CW laser, T is an arbitrary time interval

*For pulse laser, T is the inverse of the pulse repetition rate, f_P

$$T = \frac{1}{f_P}$$

For CW lasers, where

$P(t) = P_0$ the average power

$$F_{cw}^{2P} = \delta P_0^2 \left(\frac{(NA)^2}{2\hbar c \lambda} \right)^2$$

For pulsed lasers with pulse width, τ , repetition rate, f_P

and averaged power, P_0 , and assuming the following pulse profile:

$$P(t) = \frac{P_0}{f_P \tau} \quad \text{for} \quad 0 < t < \tau$$

$$P(t) = 0 \quad \text{for} \quad \tau < t < \frac{1}{f_P}$$

$$F_p^{2P} = \delta \frac{P_0^2}{f_P^2 \tau^2} \left(\frac{(NA)^2}{2\hbar c \lambda} \right)^2 \frac{1}{T} \int_0^\tau dt = \delta \frac{P_0^2}{f_P \tau} \left(\frac{(NA)^2}{2\hbar c \lambda} \right)^2$$

For CW and pulse lasers to have equivalent excitation efficiency, the average power of the CW laser has to be higher by a factor of $\frac{1}{\sqrt{\tau f_P}}$

Calculation of Two-Photon Emission Rate

Assumptions:

Laser parameter: wavelength λ: 780 nm, repetition rate f_P: 80 MHz
pulse width τ: 100 fs
Probe parameter: two-photon cross section δ: 40 GM = 40×10^{-50} cm^4s
Microscope parameter: numerical aperture NA = 1.0
Fundamental constants: speed of light c: 3×10^8m/s, Planck's constant $\hbar$: 1.05×10^{-34} Js

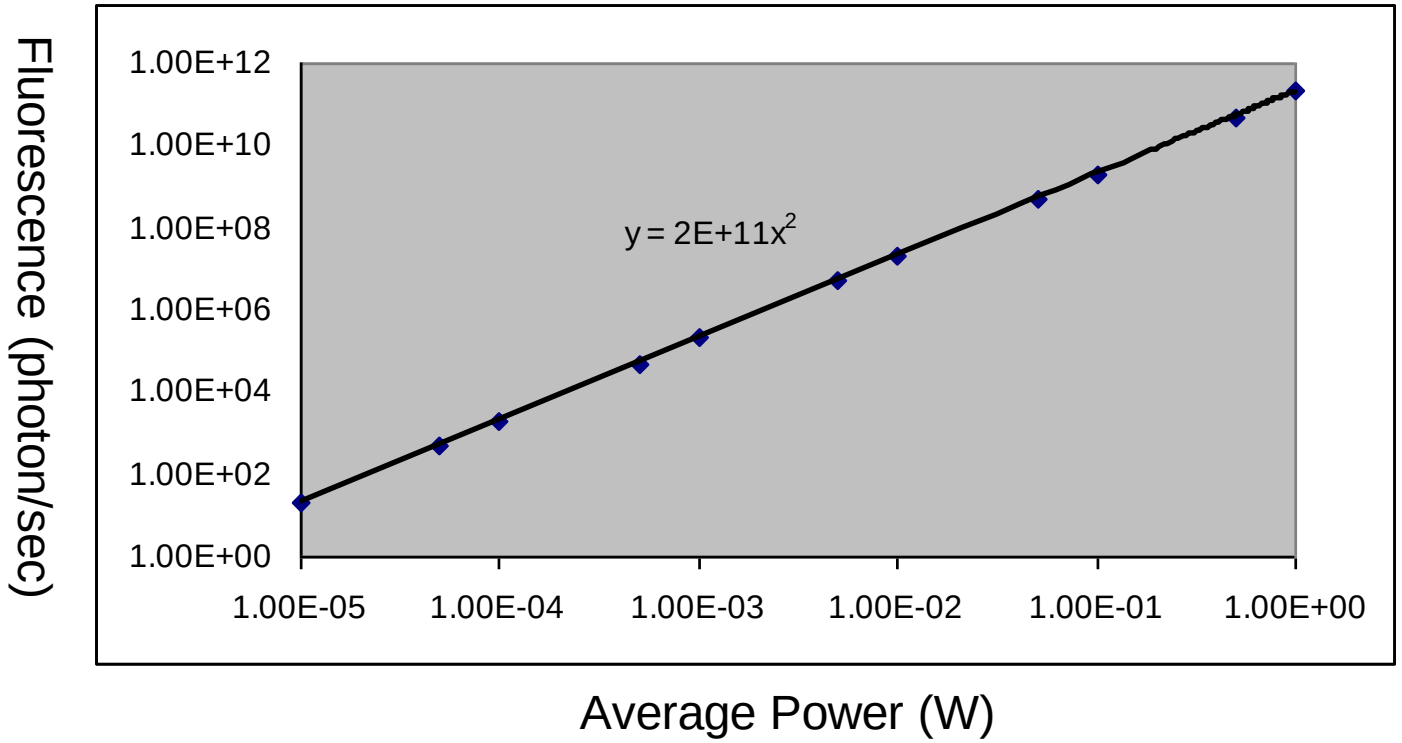

Saturation Effect

We can also calculate the number of photon pairs absorbed per laser pulse per molecule

$$n_P^{2P} = \delta \frac{P_0^2}{f_P^2 \tau} \left(\frac{(NA)^2}{2\hbar c \lambda} \right)^2$$

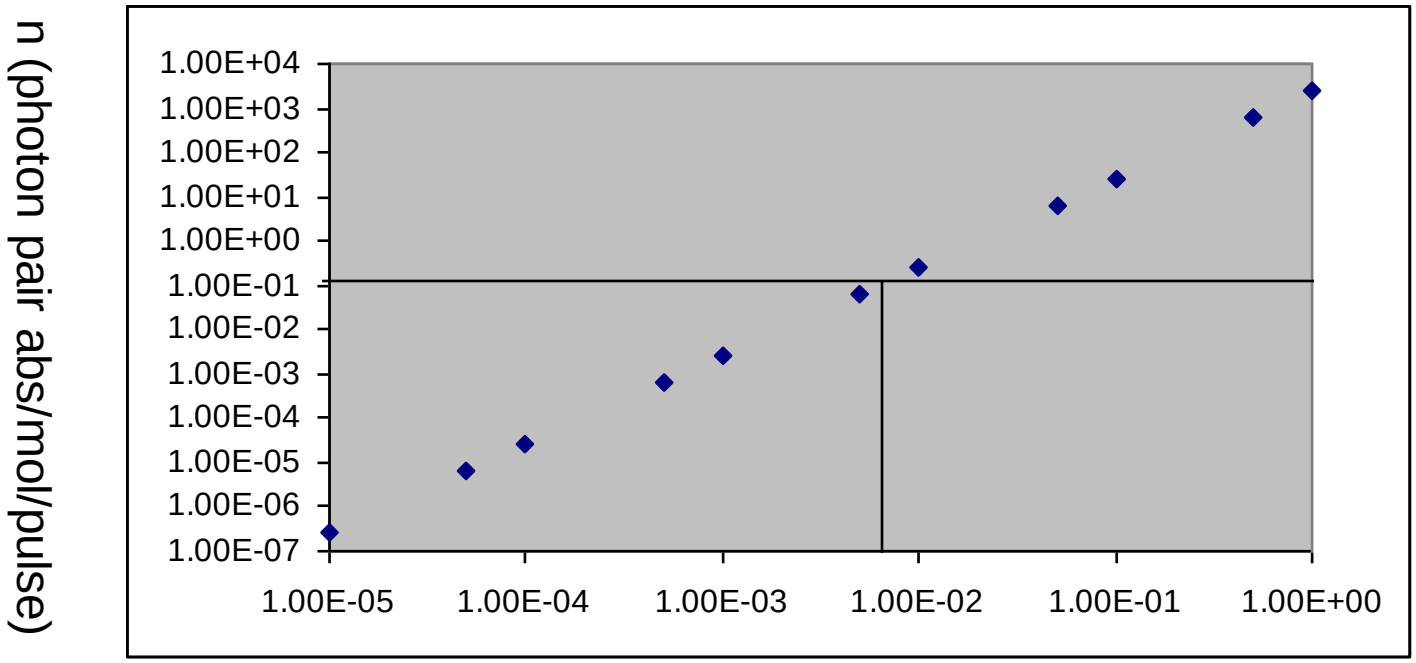

We should not be saturated otherwise PSF will broaden

The design of a two-photon microscope

Two-photon microscope design is actually significantly simpler than that of confocal microscope and has much in common.

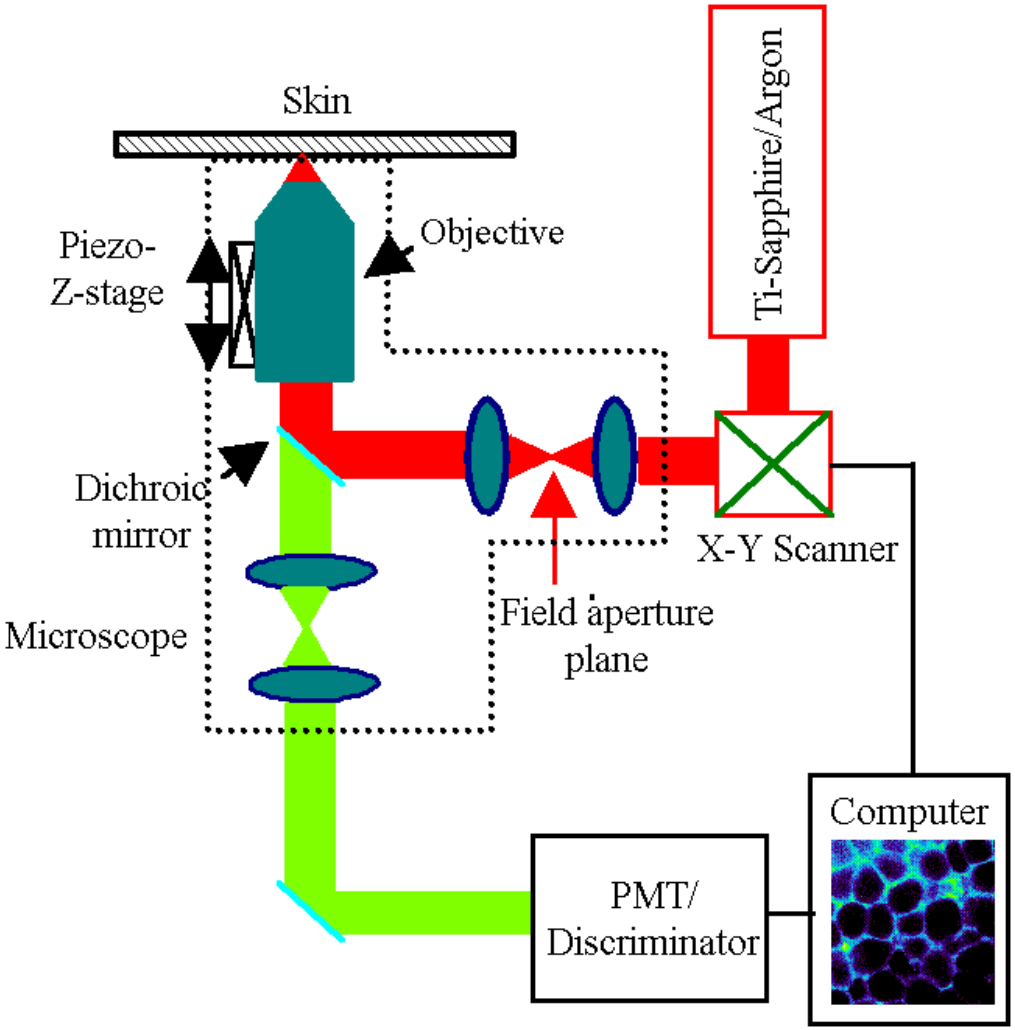

A 3D Reconstructed Movie Of Skin Structures From A Mouse Ear Tissue Punch

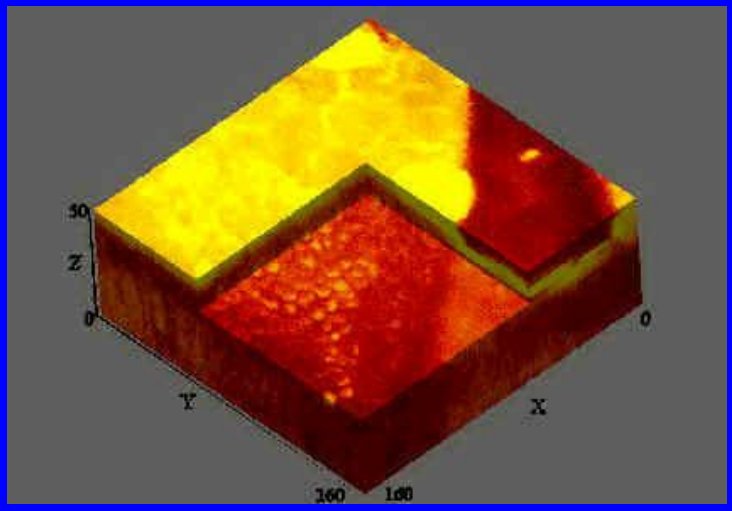

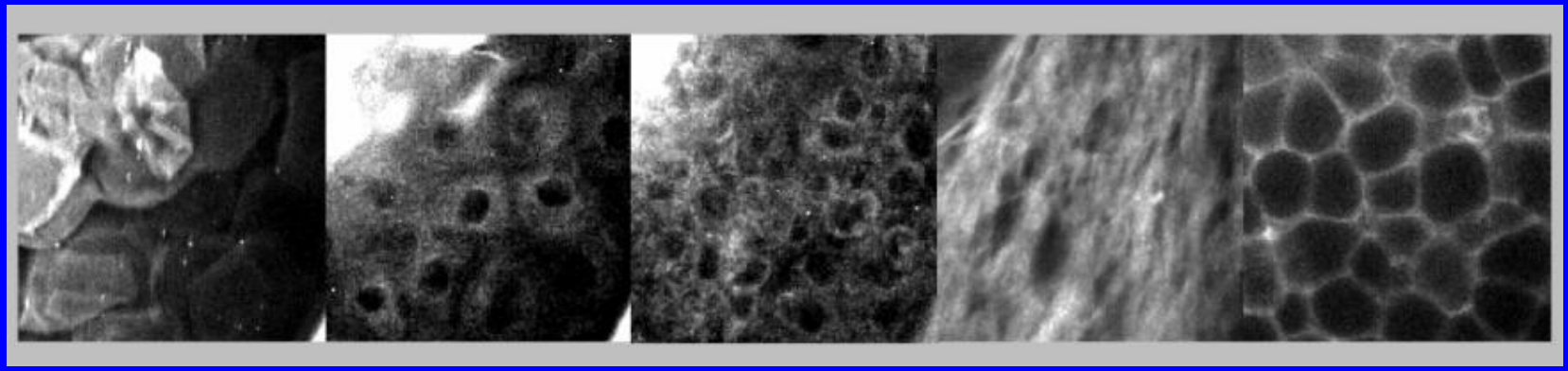

In collaboration with I. Kochevar, Wellman Labs, MGH and B. Masters

IN VIVO IMAGING OF NEURONAL DEVELOPMENT

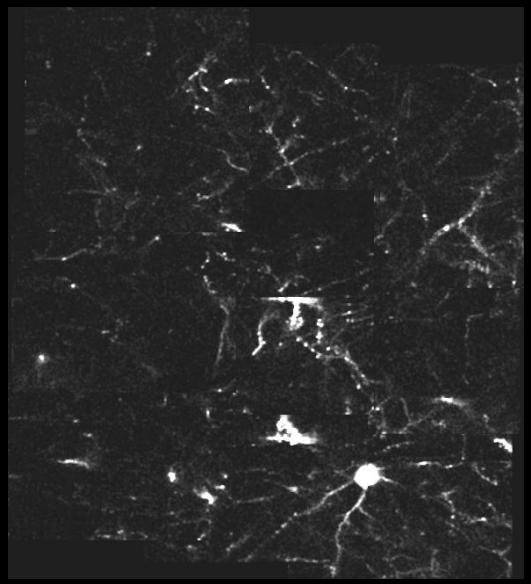

Z-Stack, Individual Slices

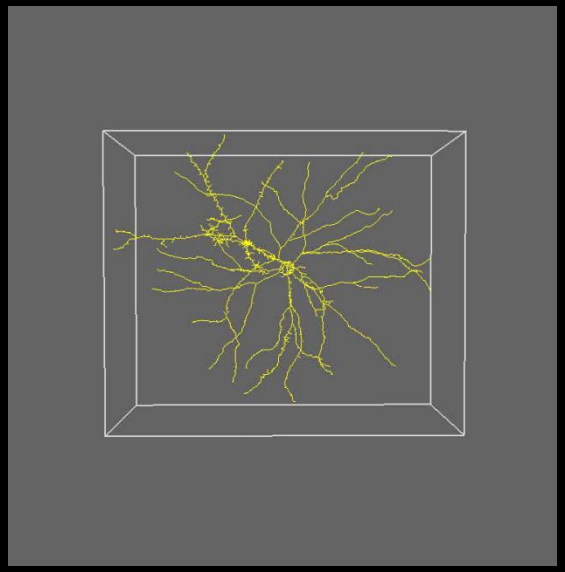

Computational Model of Dendrite Branches

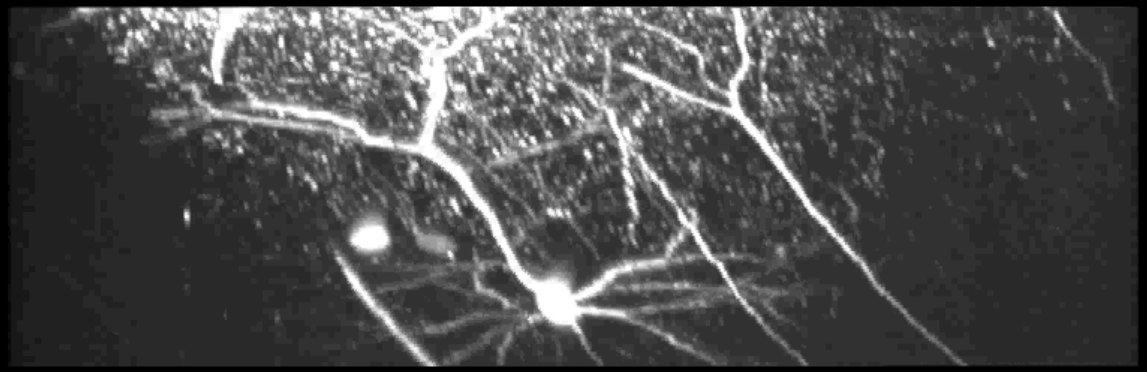

Reconstructed 3-D View

In collaboration with Wei Lee & Elle Nevidi, MIT

Fluorophores used in two-photon microscopy

Most conventional fluorophores can be used in two-photon microscopes. As a guideline, fluorophores can be excited in two-photon mode at twice their one-photon absorption wavelength. However, it should be recognize that this "twice wavelength" rule is only a rough approximation because one- and two-photon absorption processes have different quantum mechanical selection rules. Today, the two-photon excitation spectra of many fluorophores have been measured. In general, a fluorophore's two-photon excitation spectrum, scaled to half the wavelength, can be very different from its one-photon counterpart (See Xu et al, 1995 , PNAS).

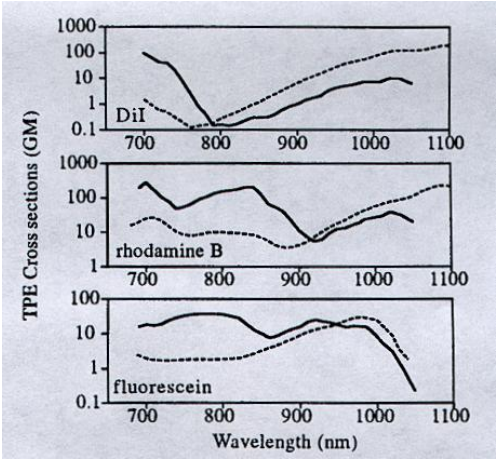

Equally important, fluorophores designed for one-photon excitation is not optimized for two-photon excitation. Therefore, effort involved in the design of fluorophores with significantly high two-photon cross section is essential (Albota et al., 1998, Science).

Two-photon cross sections of some common fluorophores, η_2 is the fluorescence quantum efficiency under two-photon excitation (Xu, 1996; Xu, 1997; Chen, 1997)

Fluorophores	**Excitation Wavelength (nm)**	**$\eta_2\delta$ (10^{-50} cm^4 s /photon)**	**δ (10^{-50} cm^4 s /photon)**
1. Extrinsic Fluorophores			
Rhodamine B	840	-	210 ± 55
Fluorescein (pH~11)	782	-	38 ± 9.7
Fura-2 (free)	700	11	
Fura-2 (with Ca^{2+})	700	12	
Indo-1 (free)	700	4.5 ± 1.3	12 ± 4
Indo-1 (high Ca)	700	1.2 ± 0.4	2.1 ± 0.6
Bis-MSB	691	6.0 ± 1.8	6.3 ± 1.8
Dansyl	700	1	
Dansyl Hydrazine	700	0.72 ± 0.2	
DiI	700	95 ± 28	
Couramin 307	776	19 ± 5.5	
Cascade Blue	750	2.1 ± 0.6	
Lucifer Yellow	860	0.95 ± 0.3	
DAPI	700	0.16 ± 0.05	
BODIPY	920	17 ± 4.9	
2. Intrinsic Fluorophores			
GFP wild type	~800		~6
GFP S65T	~960		~7
NADH	~700		~0.02
FMN	~700		~0.8
Phycoerythrin	1064		322± 110

3D Multiple Particle Tracking with Video Rate Two-Photon Microscopy

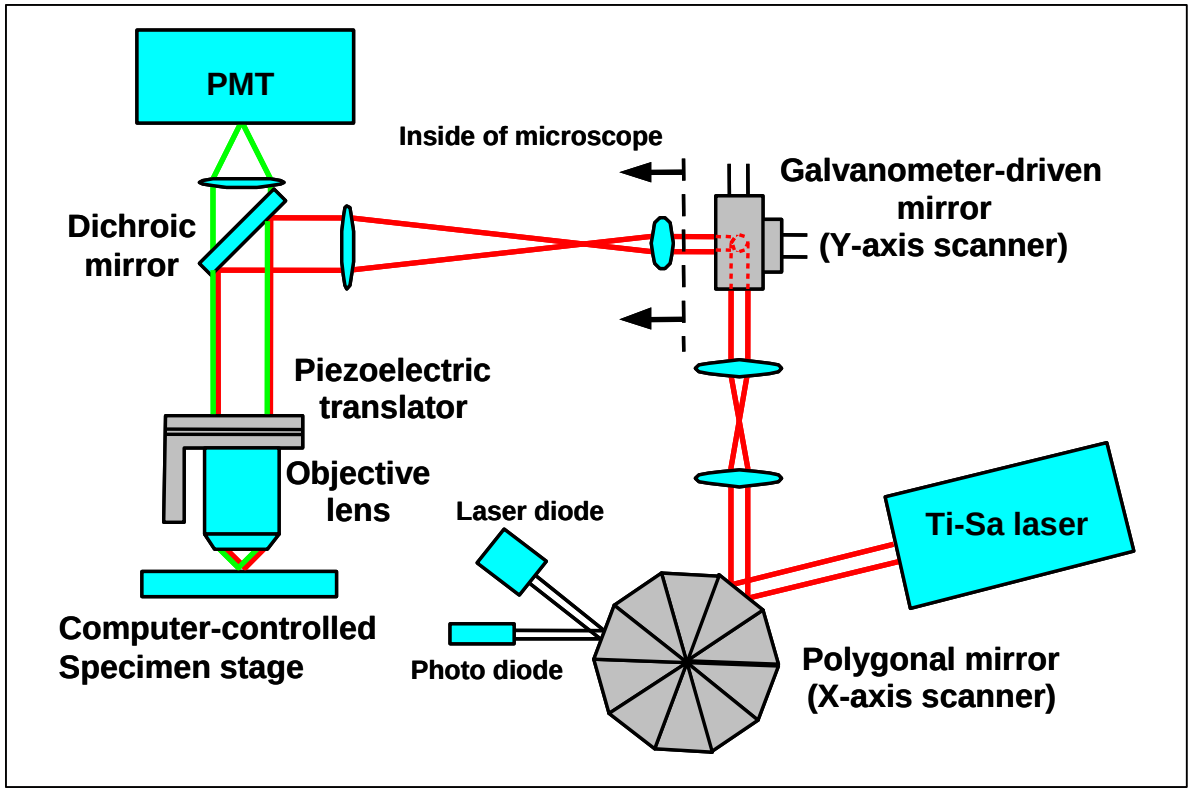

In collaboration with Ki Hean Kim (MIT)

Imaging of myocyte contraction -- R6G labeled mitochondria

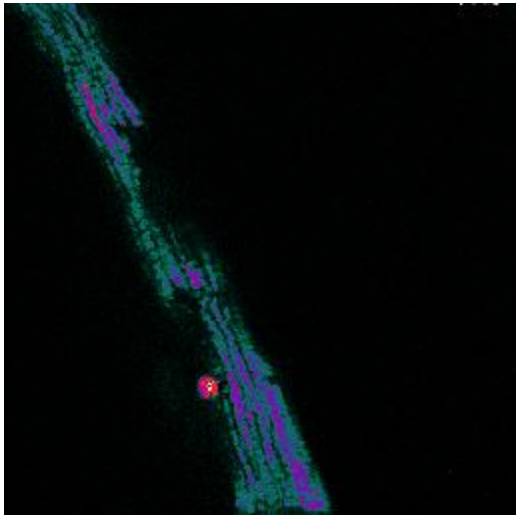

In collaboration with J. Lammerding, H. Huang, K. Kim, R. Kamm, R. Lee (MIT and Brigham & Women's Hospital)

3D Quantification of Blood Flow in Solid Tumors

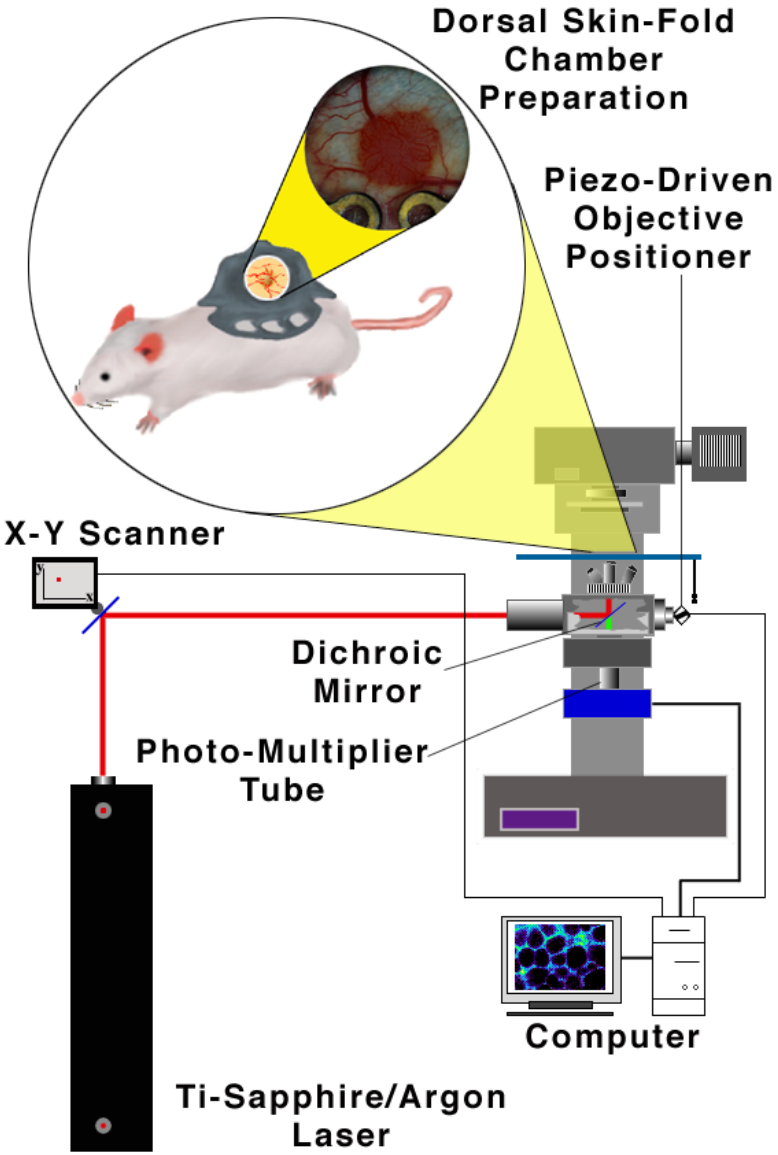

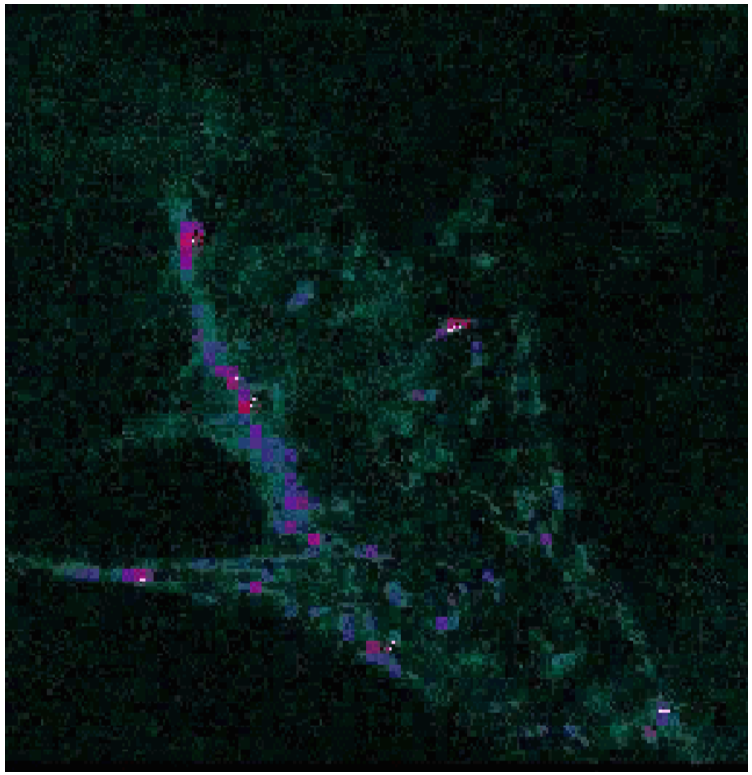

In collaboration with Rakesh Jain, MGH

MMM Ray Tracing

2-Photon Microscope – multi foci scanning

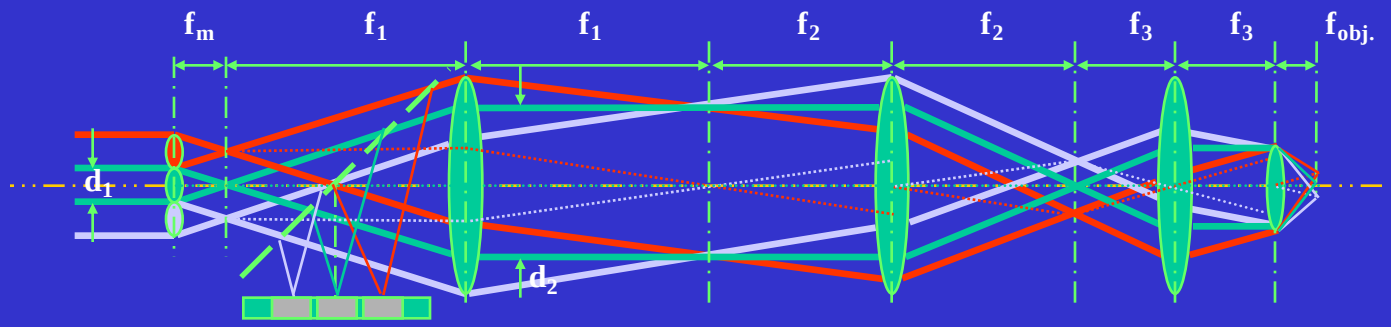

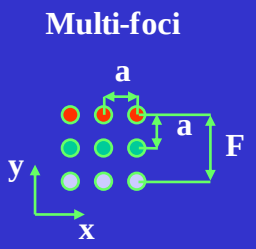

CCD

Resonant-mirror-position

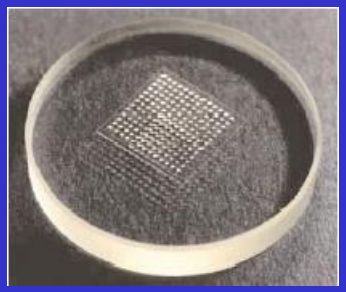

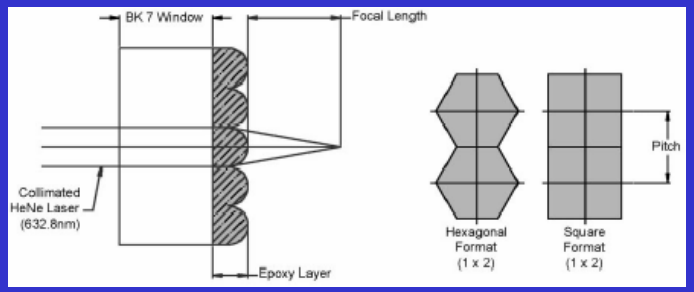

Fixed micro-lens array for Resonant-mirror setup

In collaboration with Karsten Bahlmann (MIT), Mike Kirber (BU Medical Center)

MAPMT-based MMM

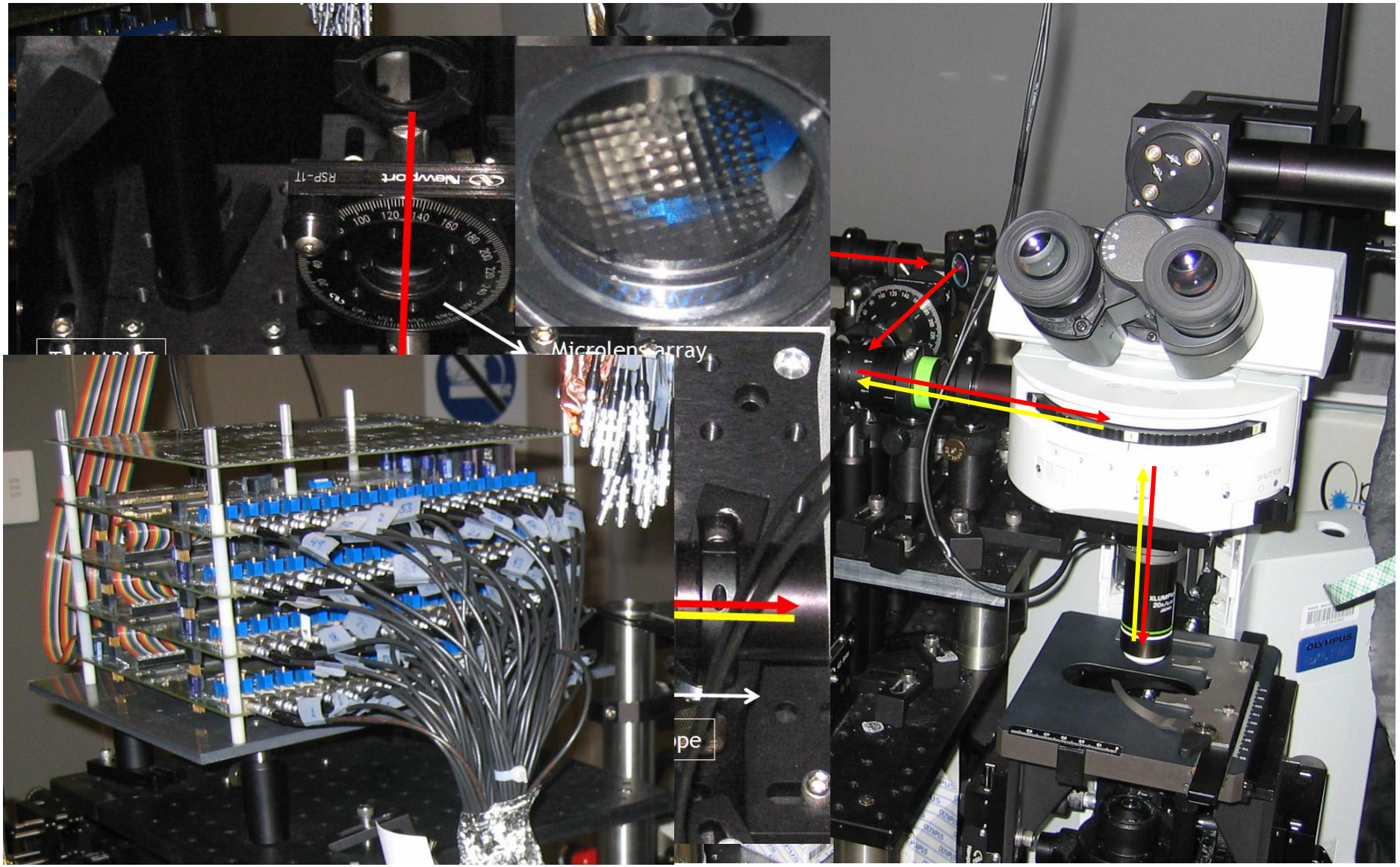

Spontaneous contraction of cardiac myocyte cells labeled with fluo3

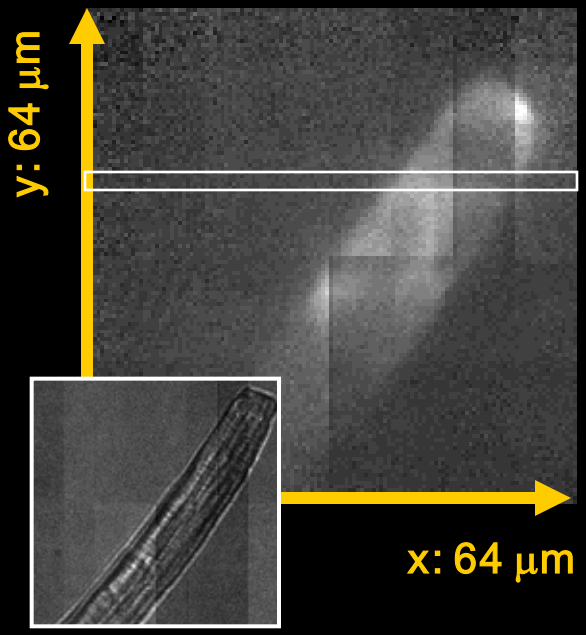

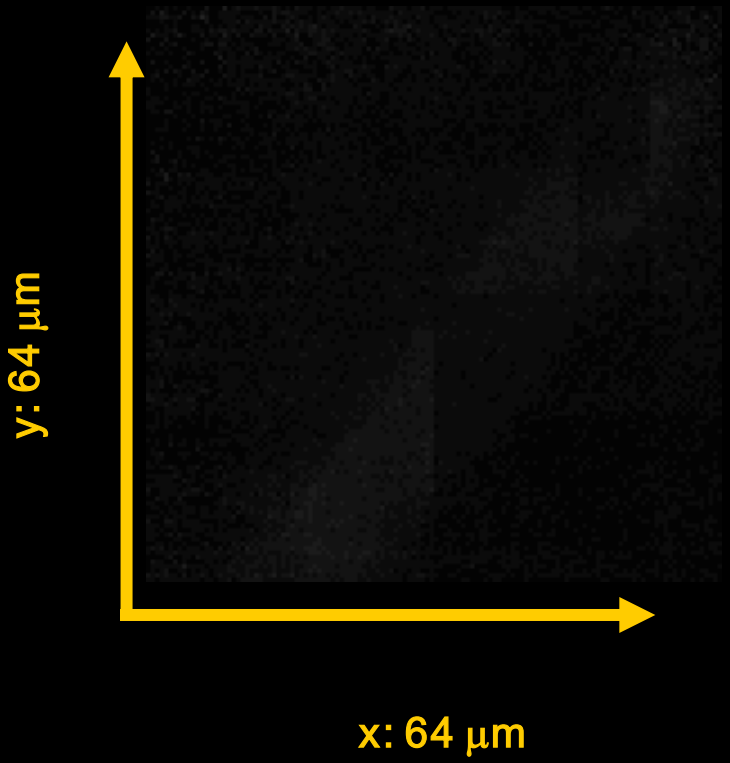

800 images at 640 frames/sec : 1,25 sec sequence

QUANTIFYING AND UNDERSTANDING GENETICALLY INDUCED CARDIAC HYPERTROPY

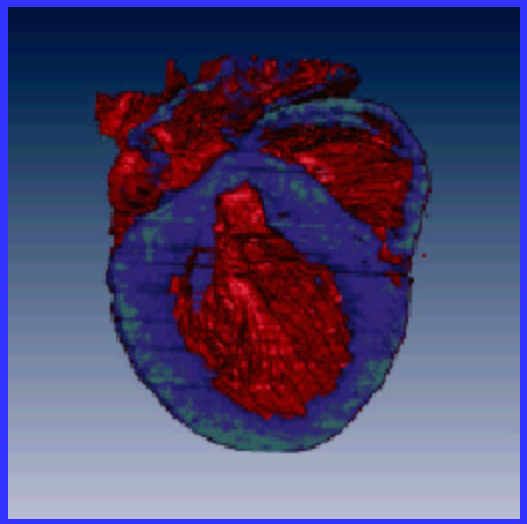

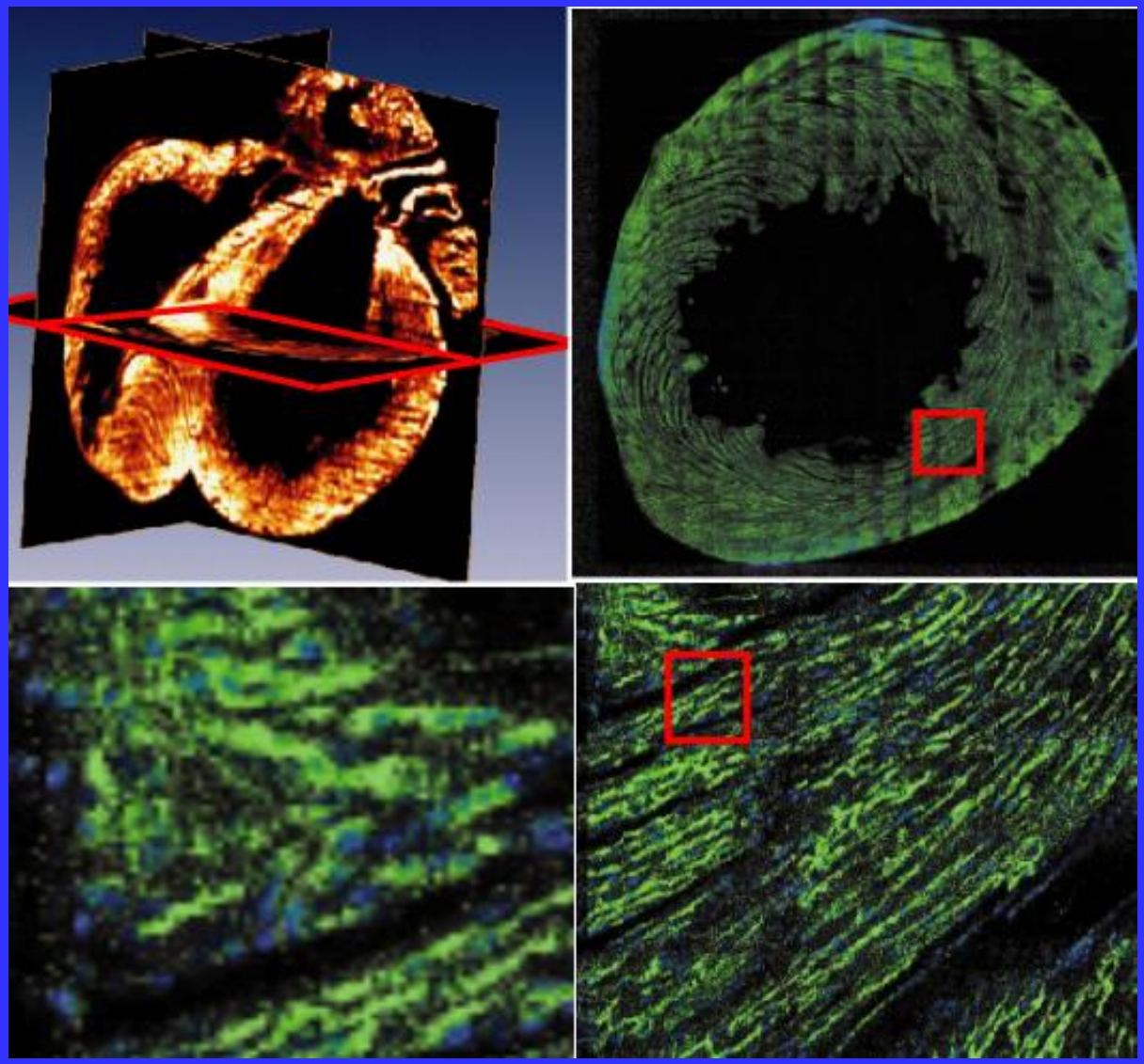

Macroscopic View of Whole Mouse Heart with Microscopic Subcellular Image Resolution

SECOND HARMONIC GENERATION (SHG)

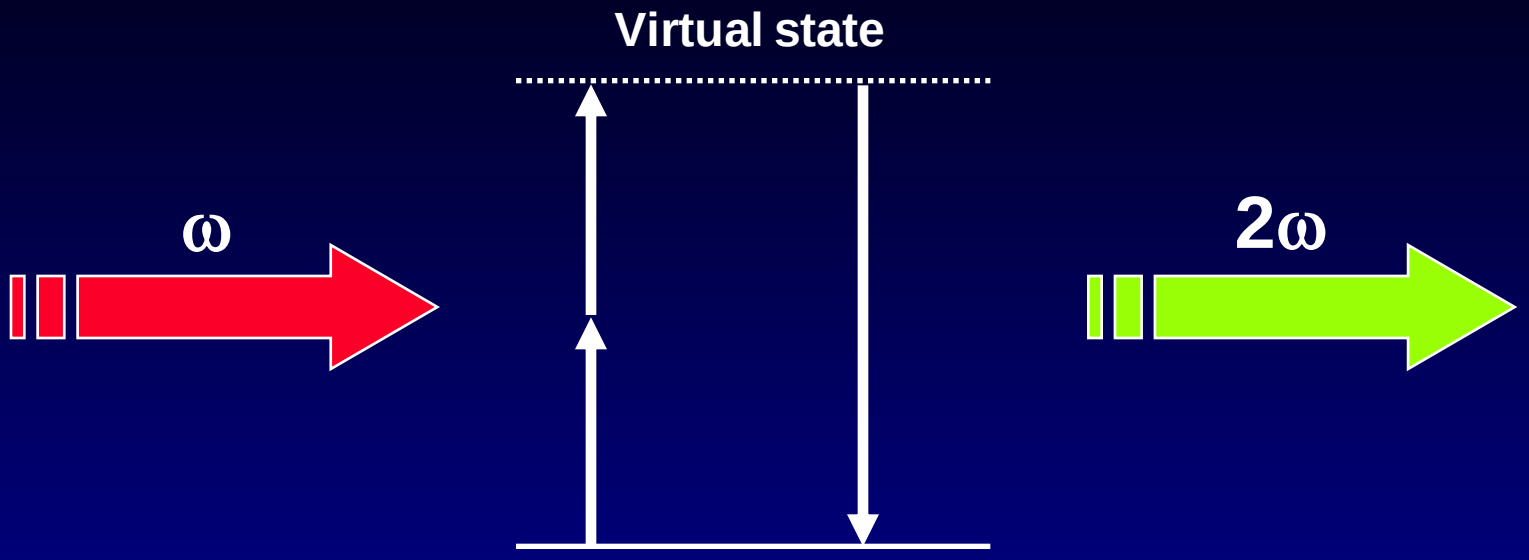

- Coherent process resulting from induced nonlinear polarization:

$$P = \varepsilon_0\left(\chi^{(1)}E + \chi^{(2)}EE + ...\right)$$

- 2nd order susceptibility vanishes in centrosymmetric media
- No transition to higher electronic state
- Phase of SH wave is deterministic with respect to the incident field
- Complementary to multiphoton excitation

SHG IN BIOLOGY

- **Early demonstrations:**
  - **Fine (1971), Freund (1986)**
- **Subcellular and membrane imaging:**
  - **Campagnola (1999), Moreaux (2000)**
- **Imaging of bulk connective tissue:**
  - **Freund and Deutsch (1986)**
  - **Guo (1997), Campagnola (2002), Brown (2003), Sun (2003)**
- **Quantitative SHG measurement:**
  - **Kim (1999,2000), Stoller (2003)**

SHG MICROSCOPY

- Intrinsic 3D sectioning capability due to nonlinear excitation process
- Sensitive to noncentrosymmetric media such as lipid bilayers, structural proteins
- Reduced photodamage, photobleaching
- Complementary to multiphoton fluorescence microscopy

Review of Second Harmonic Generation
(Materials follow discussion of Jerome Mertz web site)

Two useful concepts of light and electromagnetic field

(1) Accelerating charges produce light

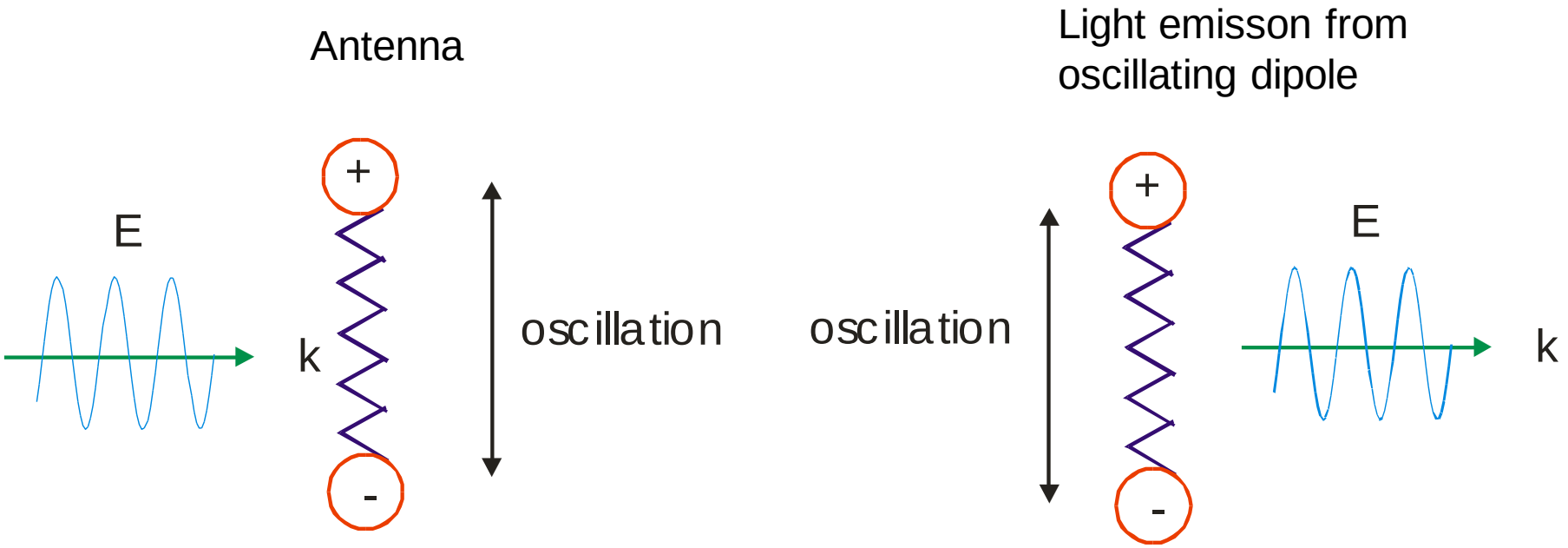

(2) Dielectric materials are made up of molecules; some of this molecules are polarizable

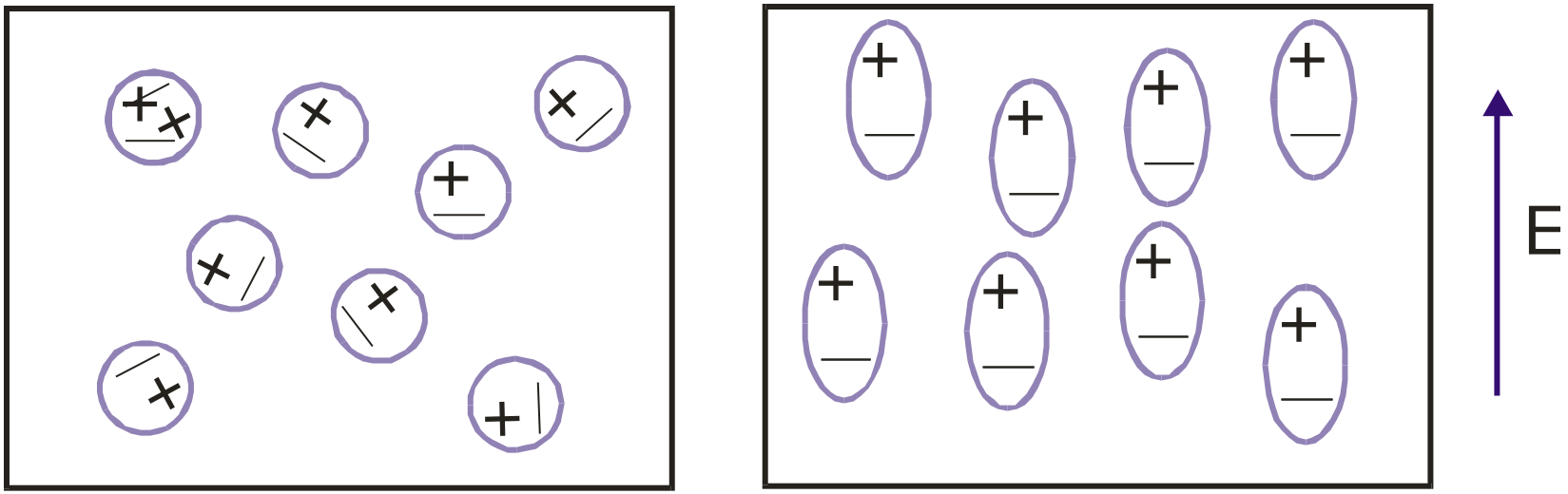

Molecular Emission Under Strong EM Field
Hyper-Rayleigh Scattering

Symmetric molecule

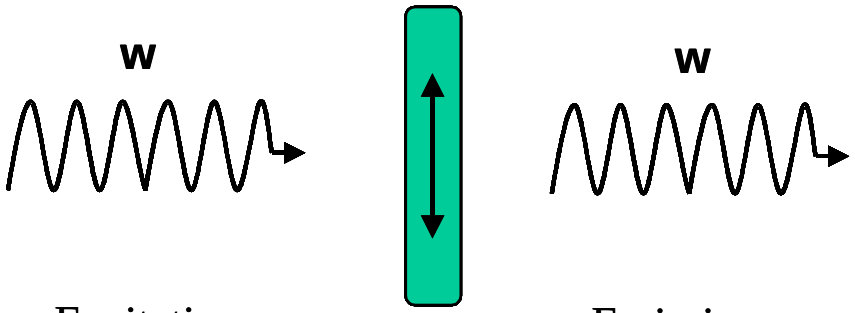

Asymmetric molecule

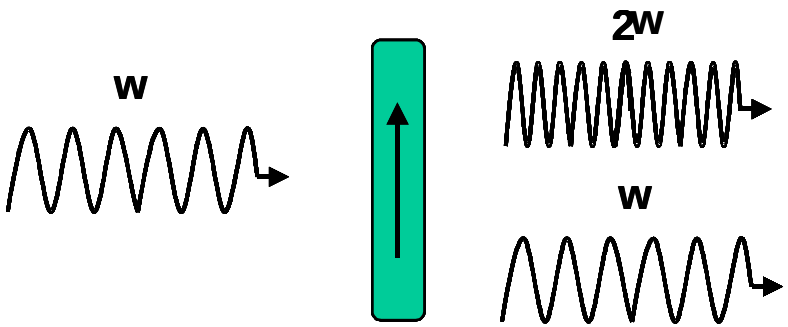

Light Emission From Two Molecules

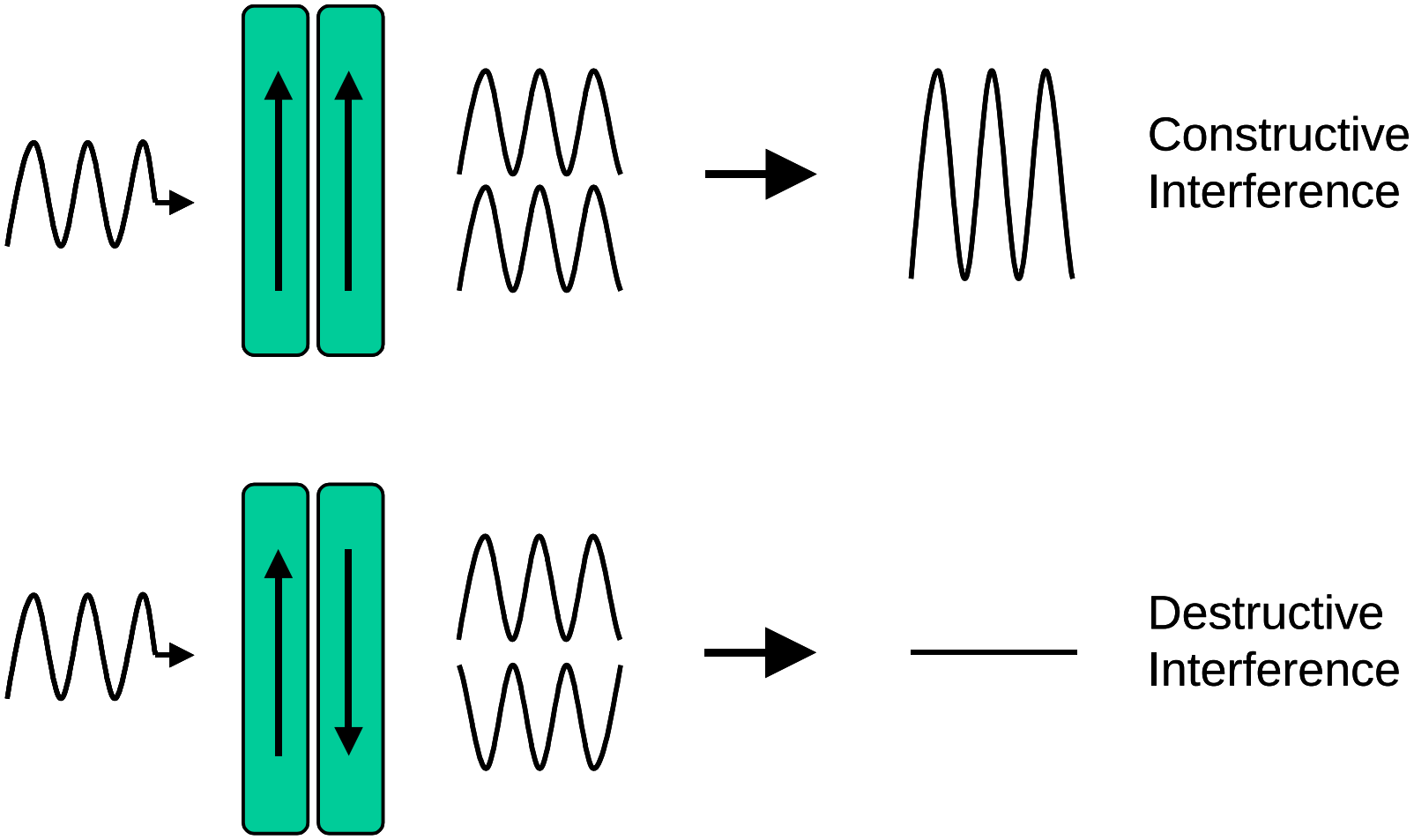

Scattered light is coherent

Emission intensity depends on molecular orientation and interference

Light Emission From a Collection of Molecules

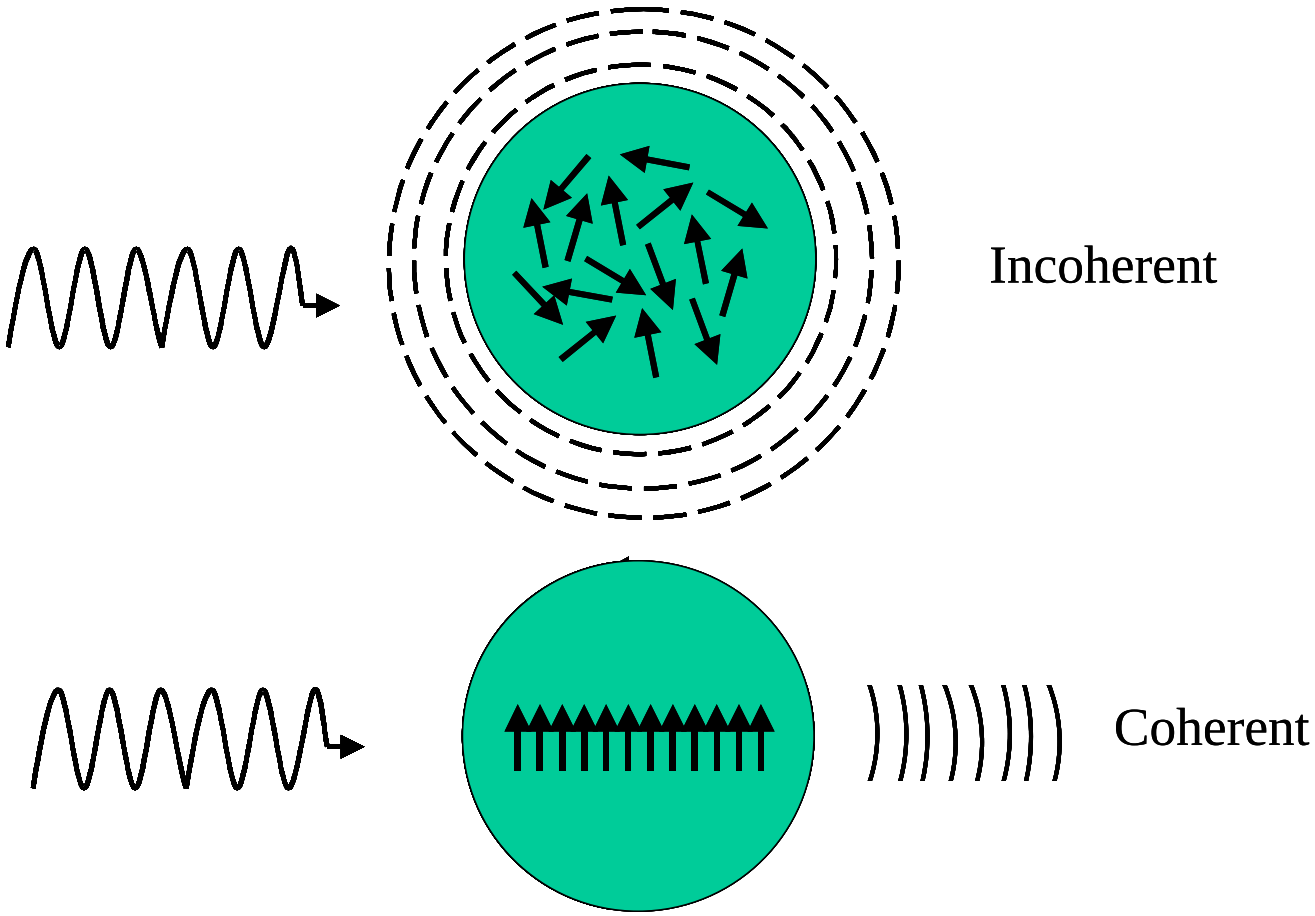

Coherent sum of hyper Rayleigh scattered light is second harmonic generation
Second harmonic emission is DIRECTIONAL because of phase matching condition

SHG From Fish Scale

Data are either extracted from:

Campagnola, Biophys J, 2002

Millard, Biophys J, 2004

Muscle and Extracellular Matrix Structure Of Mouse Lower Leg

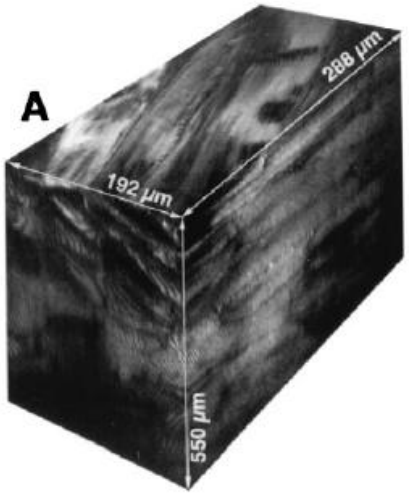

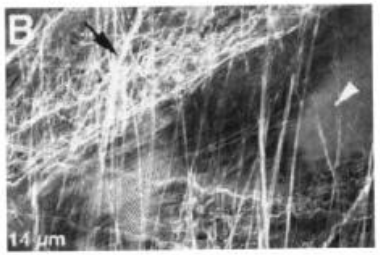

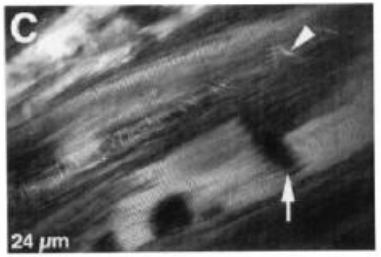

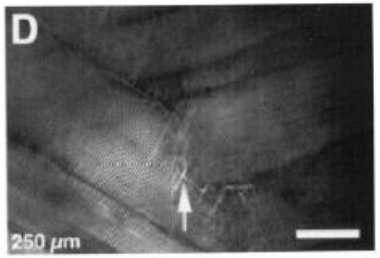

A Comparison of Myofilaments of Normal and Mutant Nematode

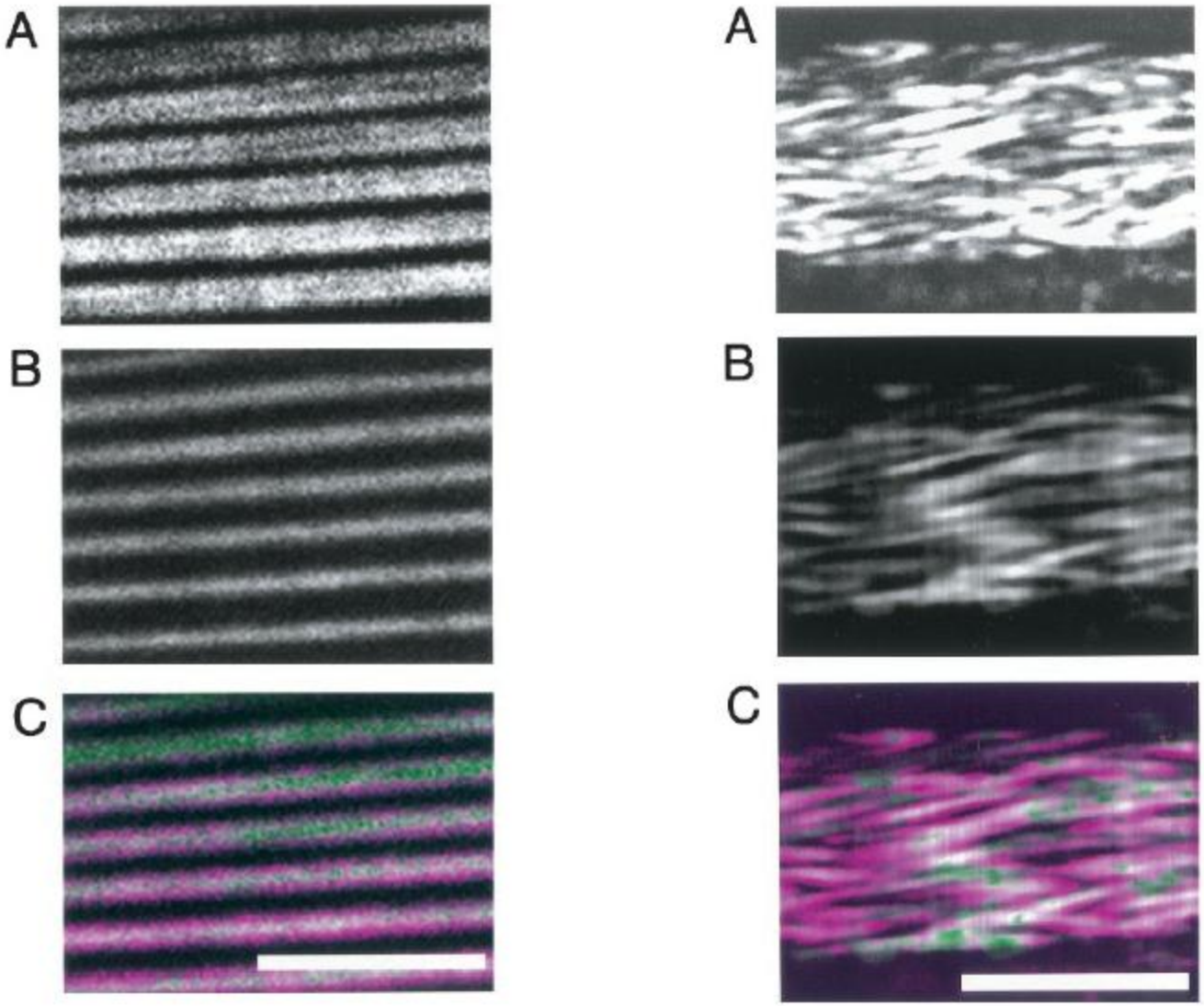

SHG Imaging of C. Elegans Embryo

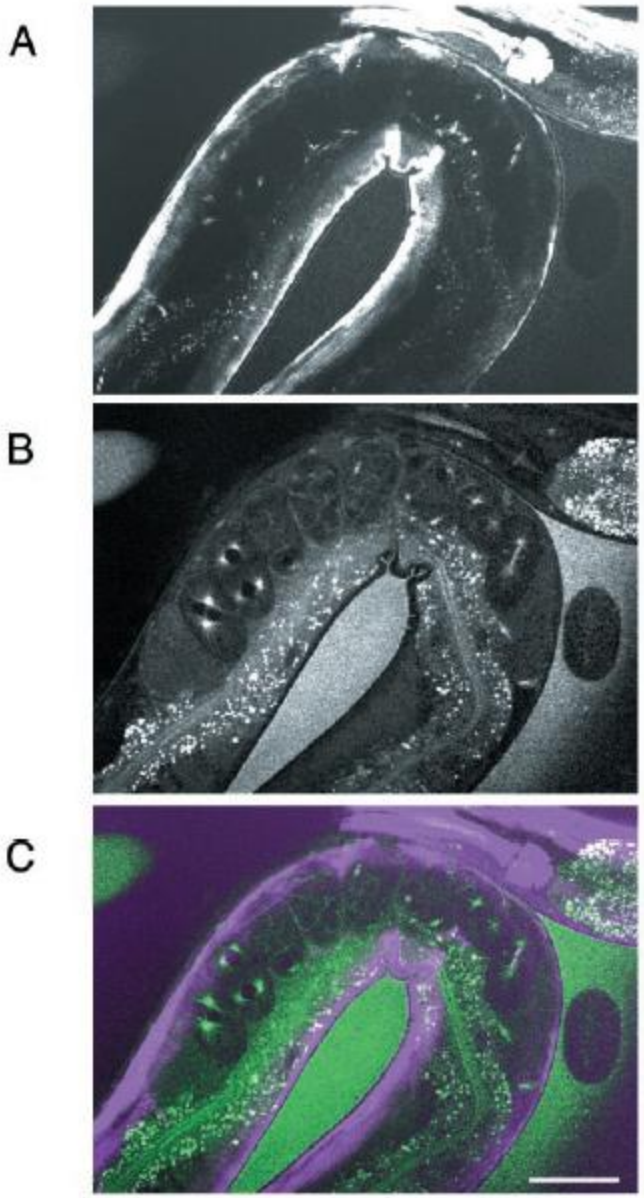

SHG and Fluorescence (GFP) Imaging of Microtubule

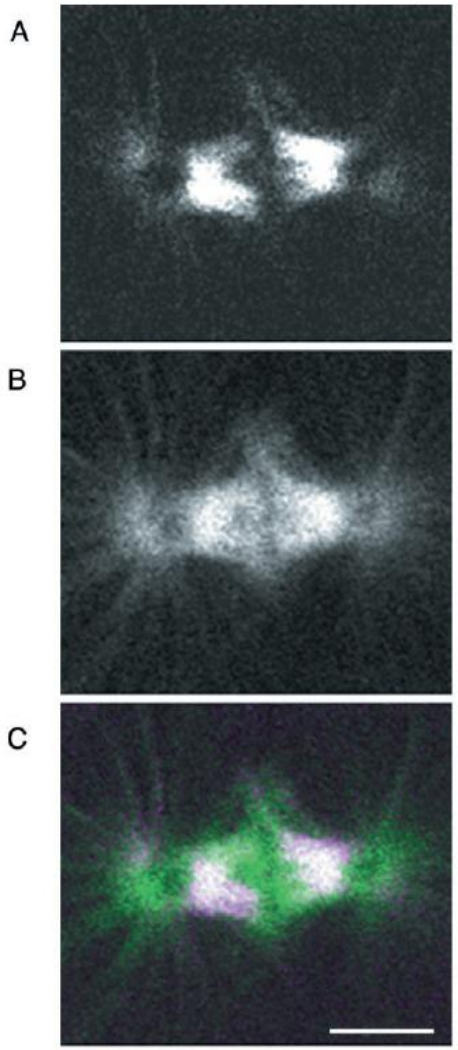

SHG Spectra of Specimen Studied and Its Excitation Wavelength Dependences

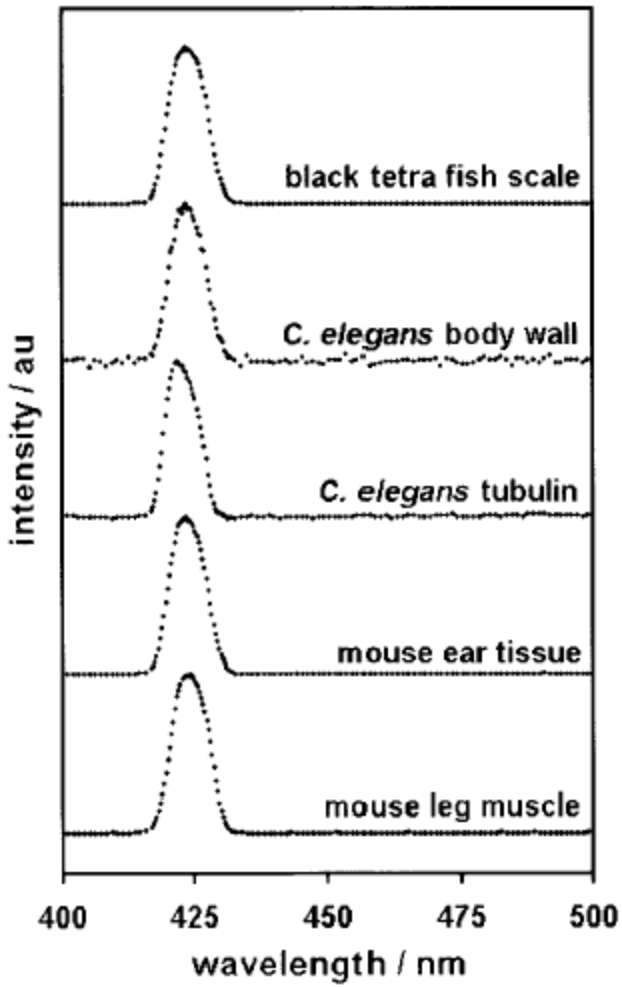

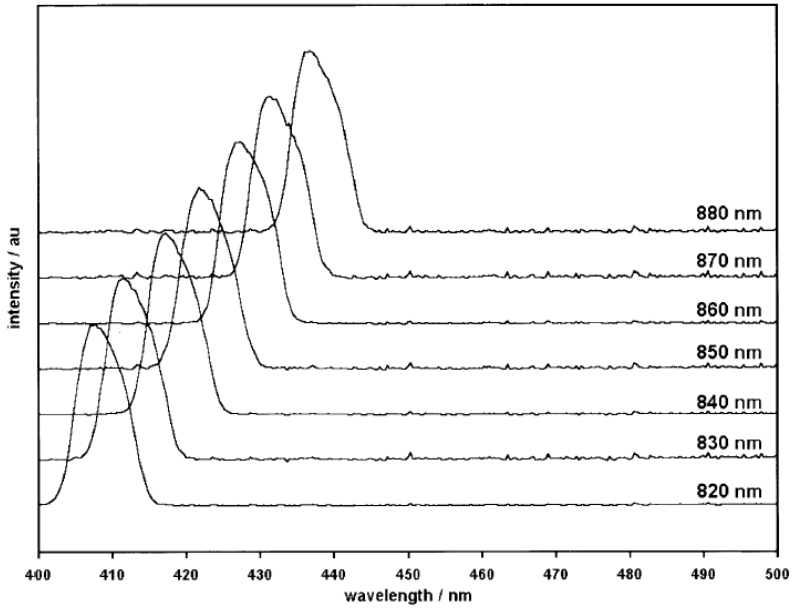

Excitation Polarization Dependence of SHG

A

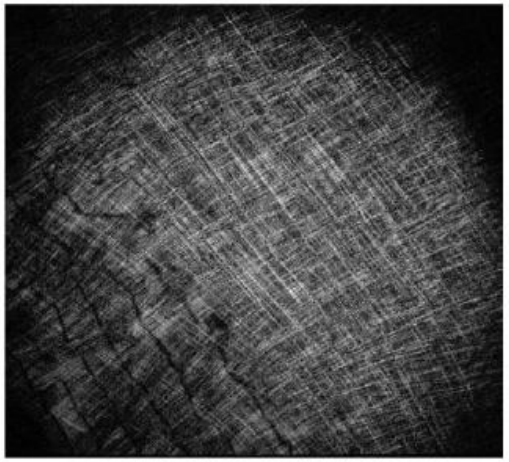

B

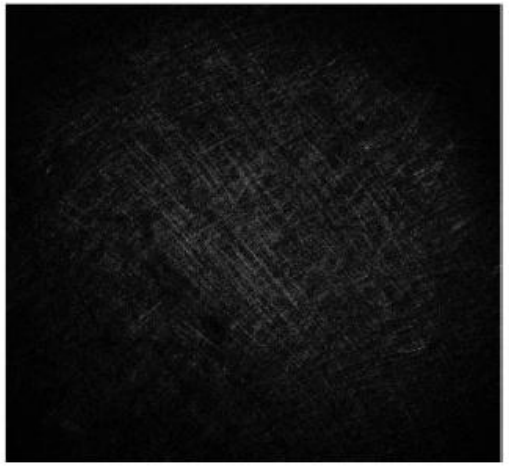

SHG Does Not Generate Photobleaching

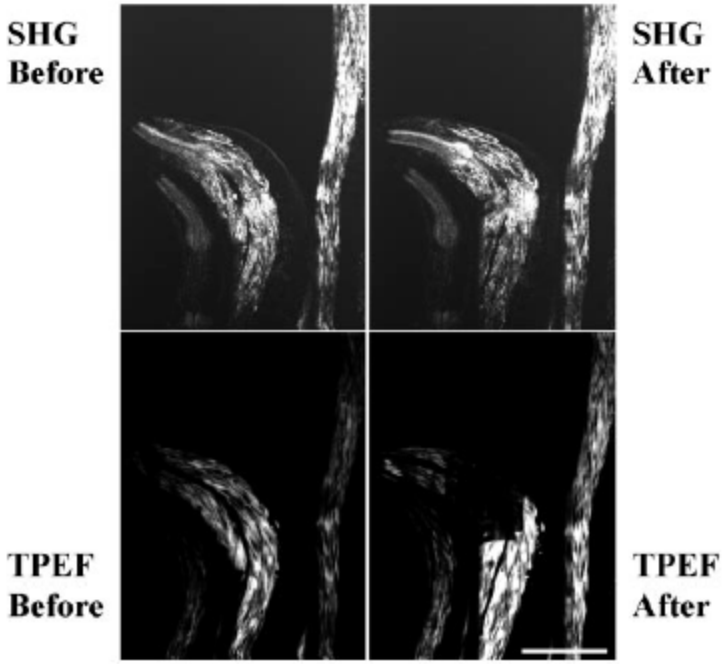

State of the Art Membrane Potential Measurement

Patch Clamp – Nehr & Sackmann, 1991 Physiology Nobel

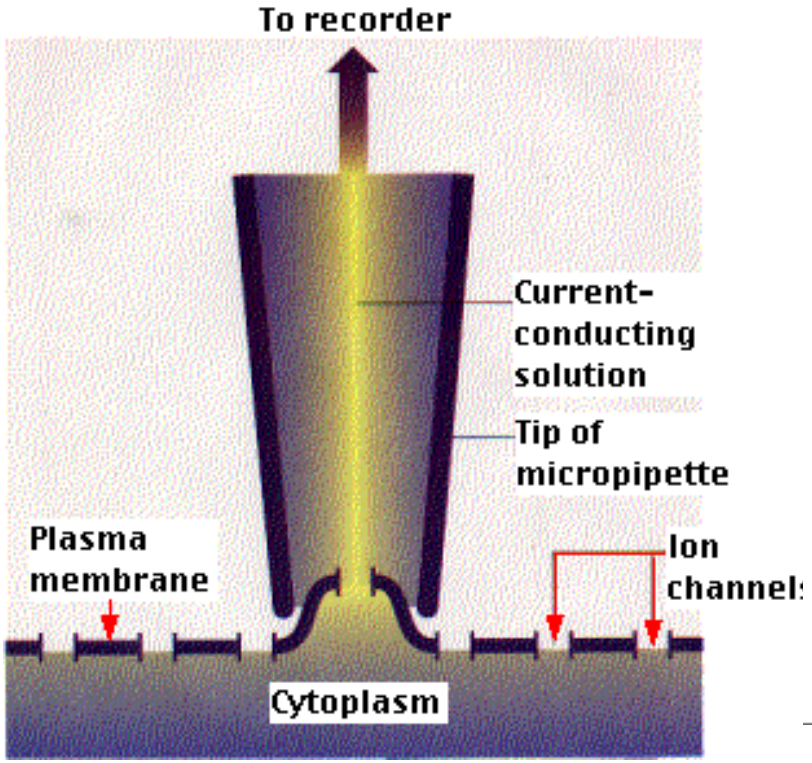

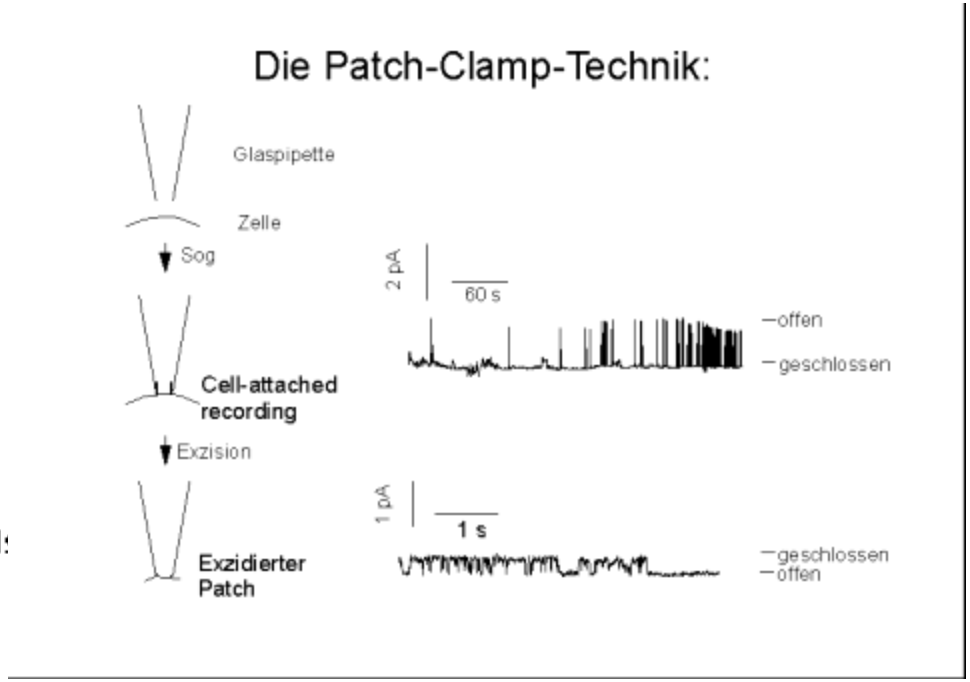

users.rcn.com

www.vetmed.uni-giessen.de

The need for Potential Measurement Beyond Single Channel

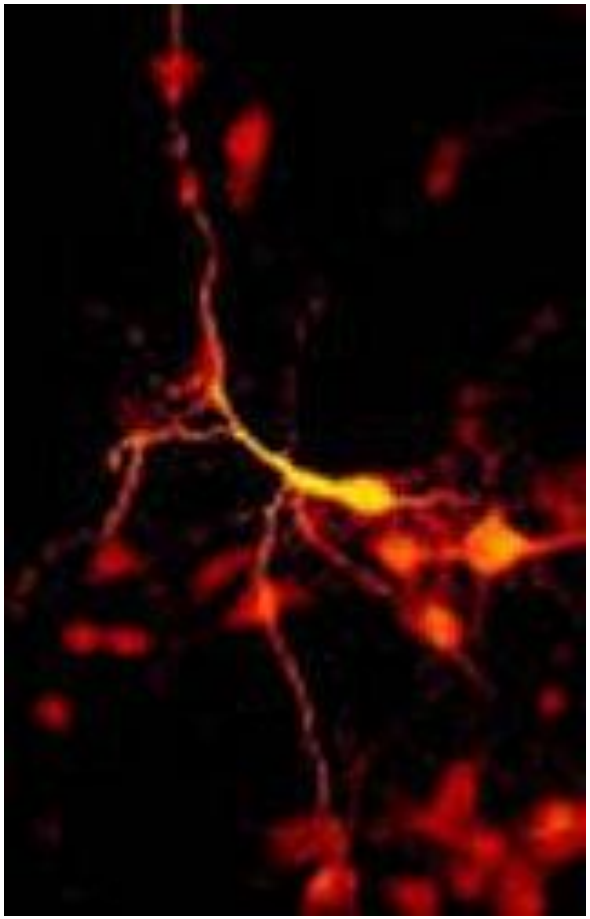

http://www1.med.uc.edu/

Challenges in Dynamic Membrane Potential Measurements

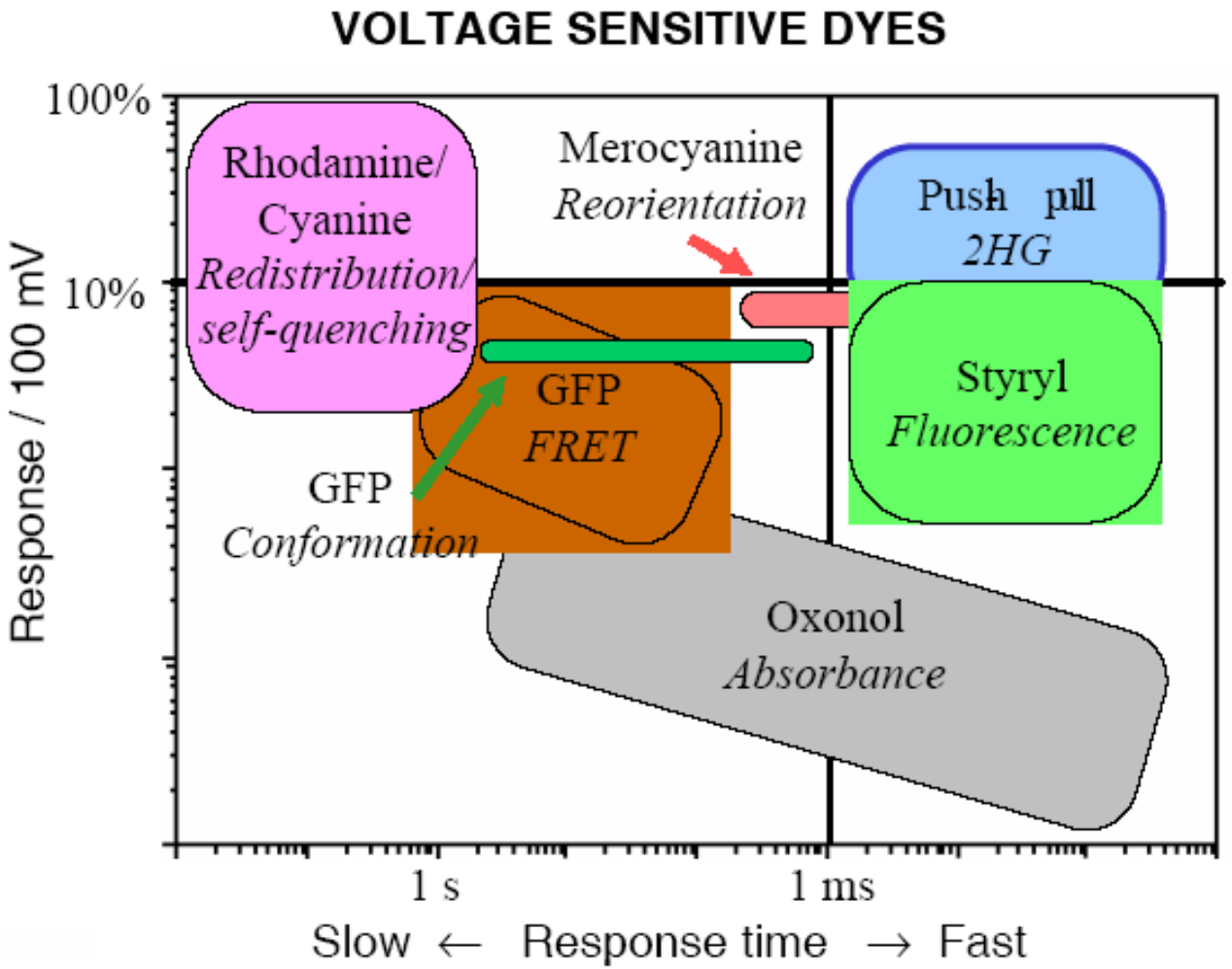

http://www.physio.espci.fr/shg.pdf

Second Harmonic Imaging Using Three Styry Probesl

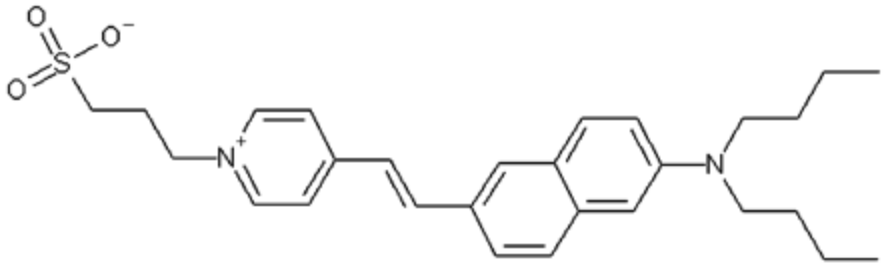

Di-4-ANEPPS

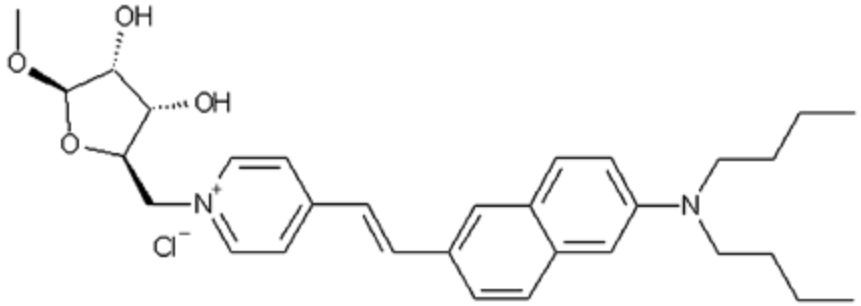

Di-4-ANEPMRF

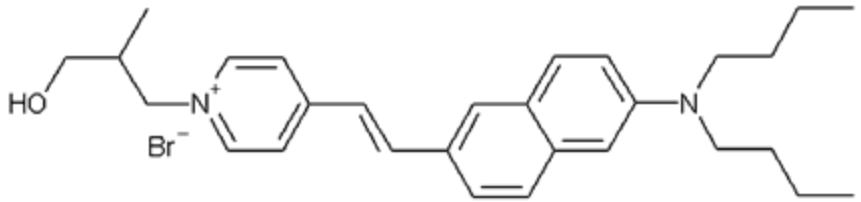

Di-4-ANEPMPOH

Measurement Instrument Diagram

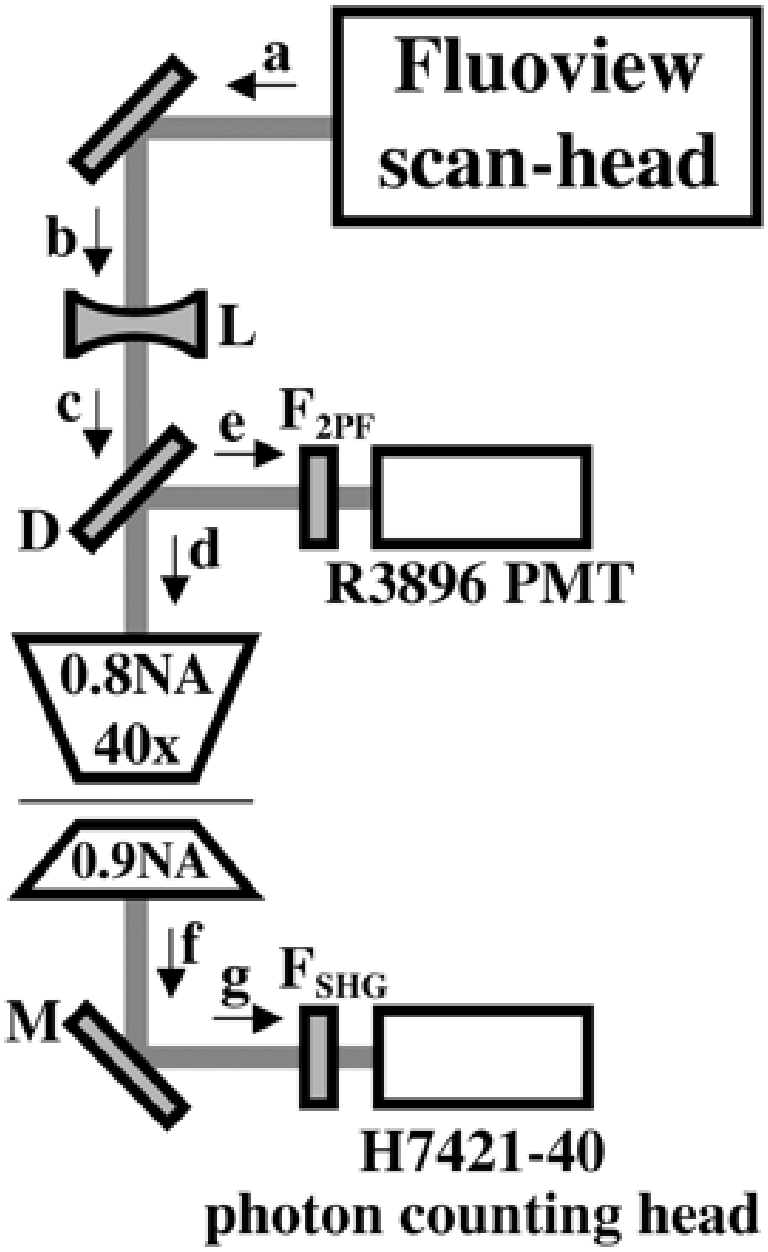

di-4-ANEPPS excited at 910 nm under alternative voltage

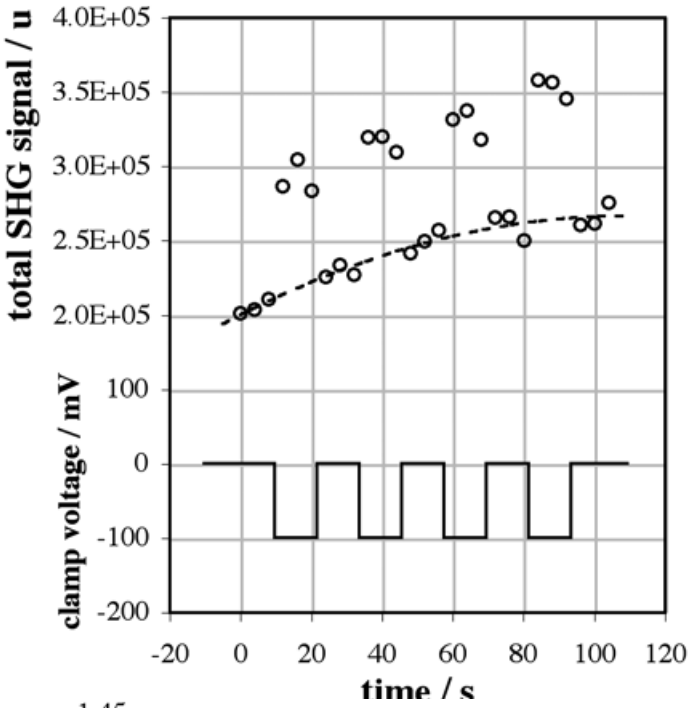

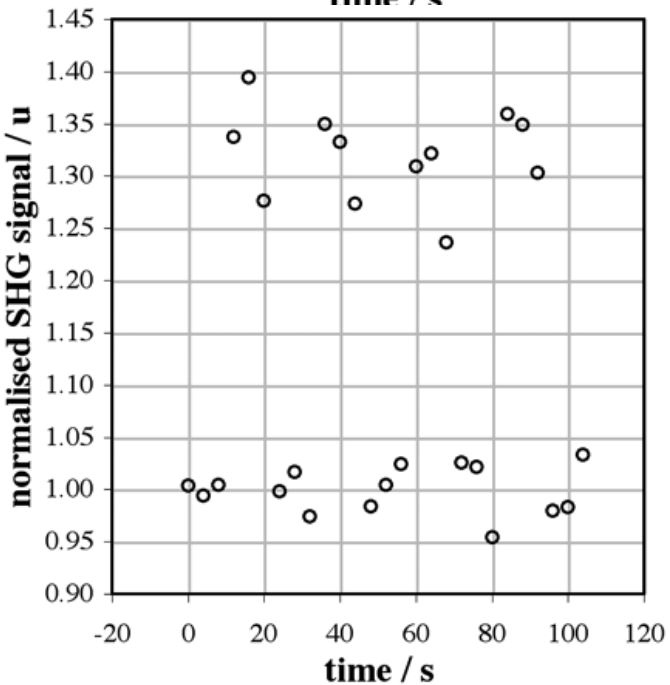

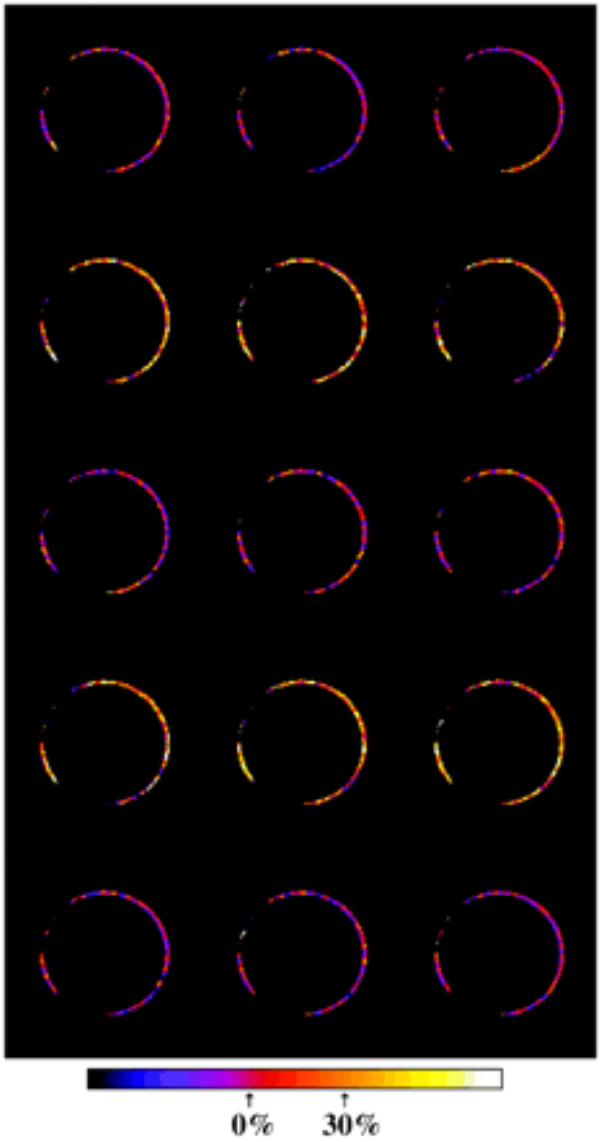

Quantifying Mechanotransduction Effects on Focal Adhesion Protein Interactions: A FLIM-FRET/FCS Study

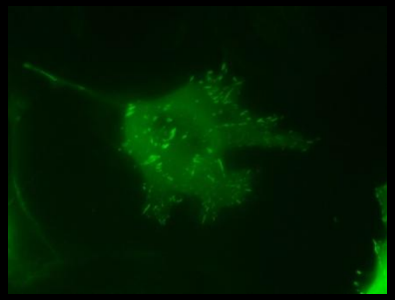

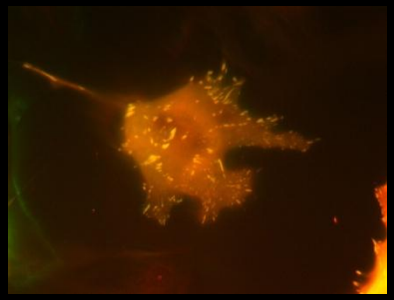

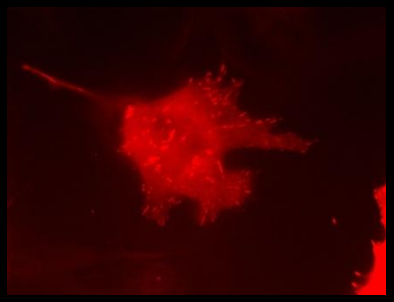

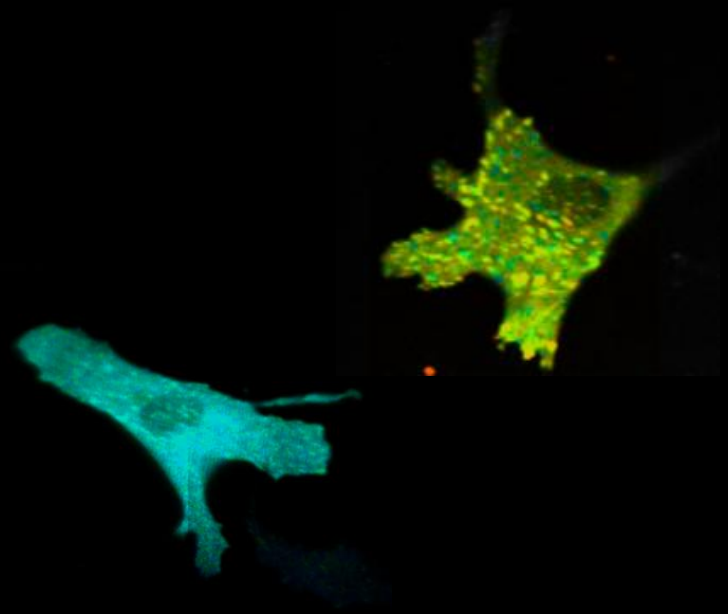

Massachusetts Institute of Technology

CSBi

WHITEHEAD·MIT BIOIMAGING CENTER

Mechanotransduction

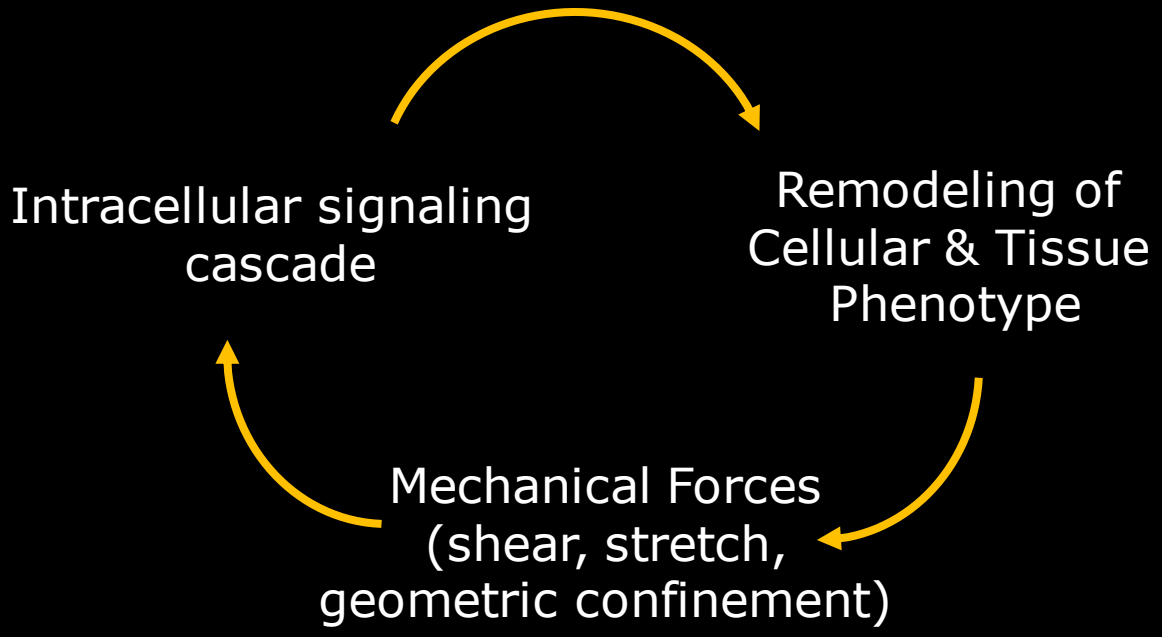

Cardiac Hypertrophy

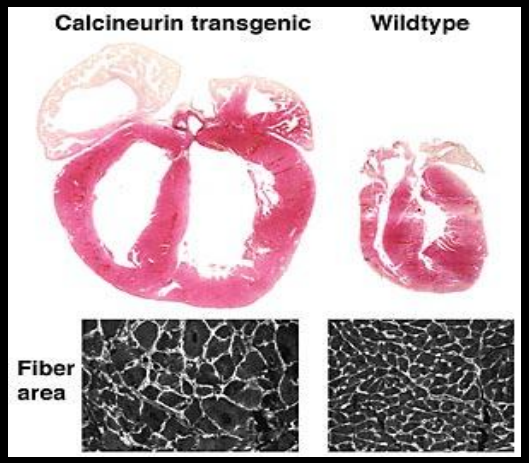

http://www.cincinnatichildrens.org

Arteriosclerosis

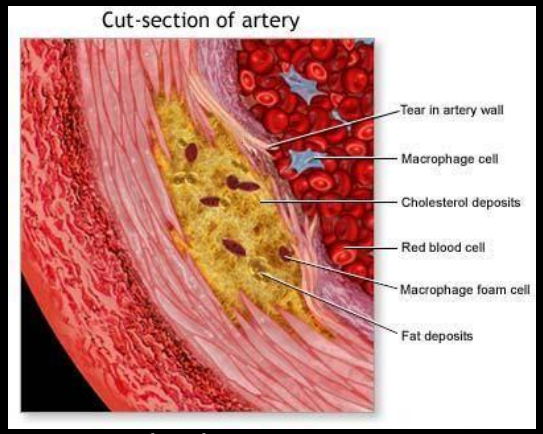

www.bodyrepairstore.com

Mechanotransduction Mechanisms

How Mechanical forces are mediated?

Shear flow modulation of membrane fluidity
Shear "compression" of glycocalyx layer
Mechanical force induced opening/closing of ion channels

Deformation of "structural" proteins linking cellular cytoskeleton & ECM

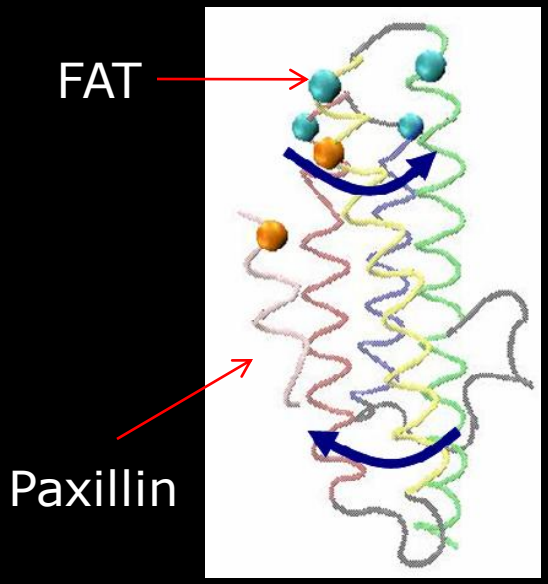

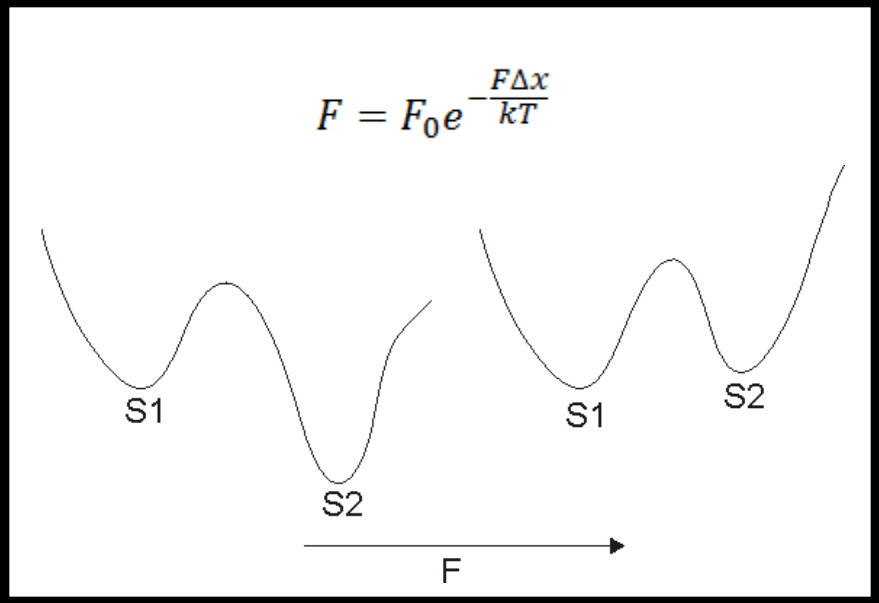

Focal adhesion complex

Focal adhesion complex serves as the adhesion sites of cells and mechano-signal transduction center of the cell

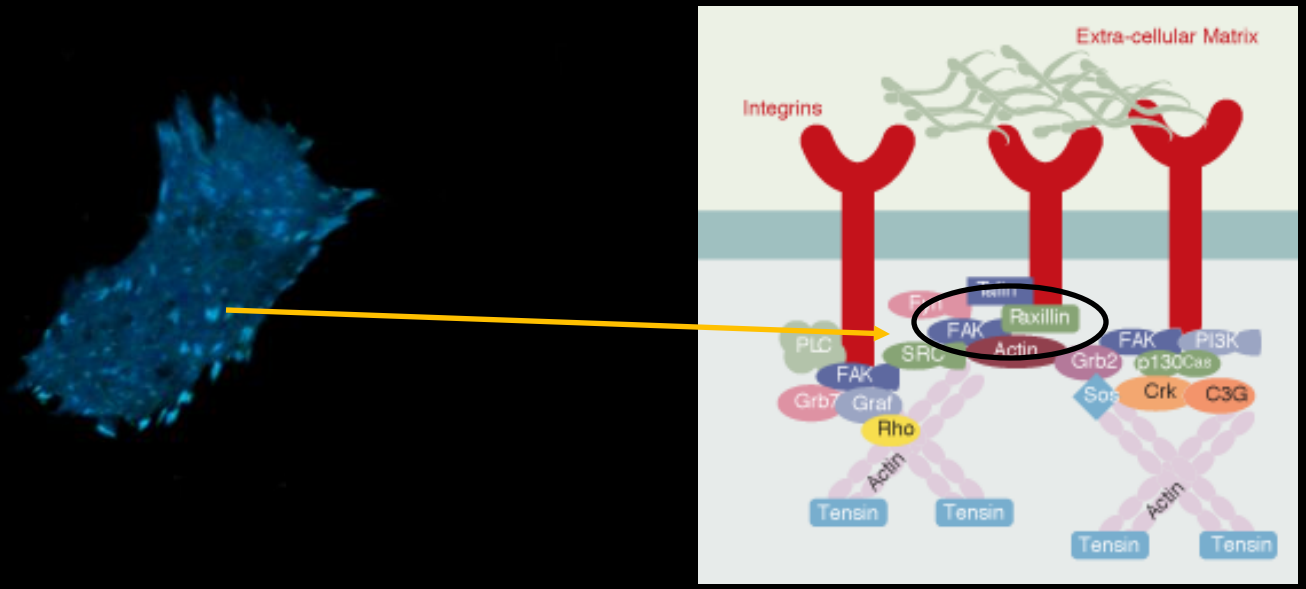

Quantification of Paxillin-Focal adhesion kinase interaction

Paxillin-FAT in endothelial cells

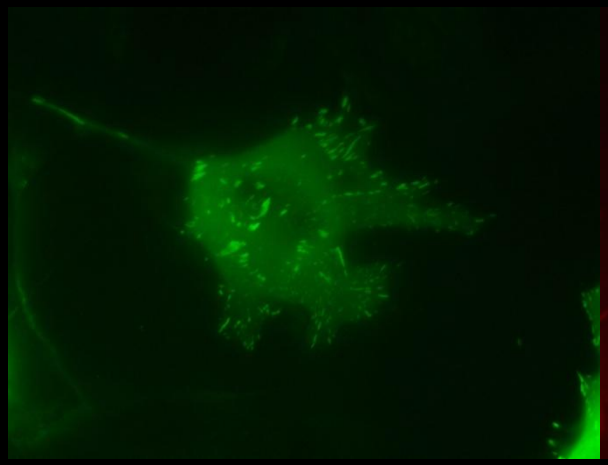

GFP-Paxillin

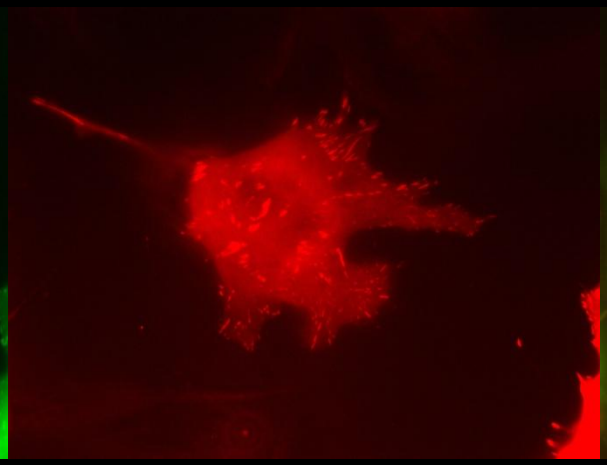

FAT-mCherry

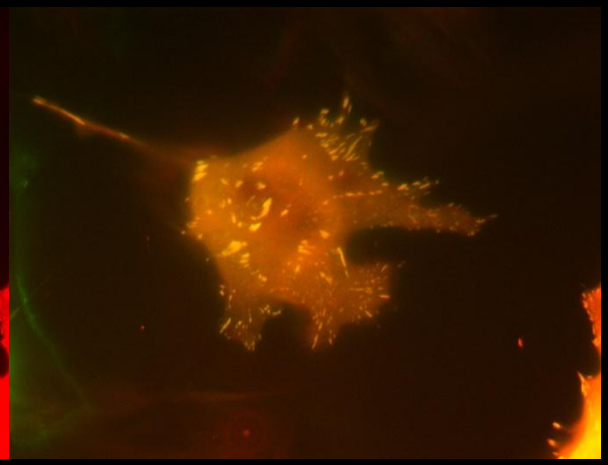

Spectral overlap

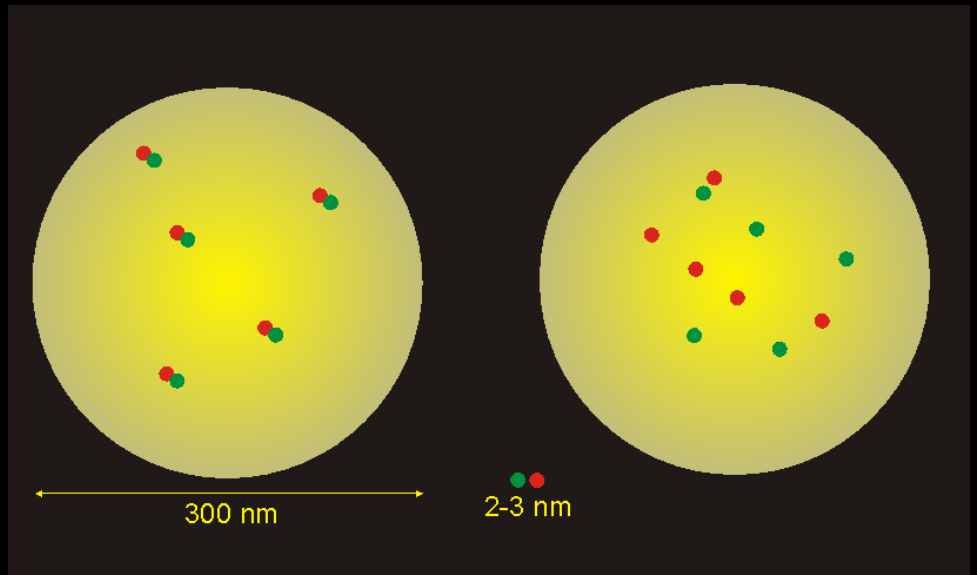

Fluorescence Resonance Energy Transfer (FRET)

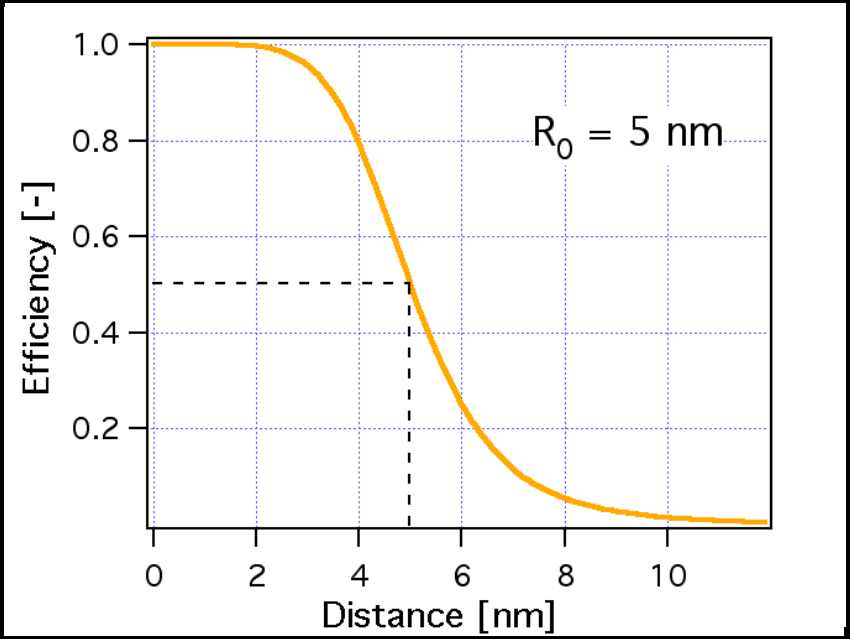

Dipole - dipole interaction

r^6 dependence

Efficiency

50% energy transfer

Förster distance

R_0 = 40 to 70 Å

Decrease donor intensity

Increase acceptor intensity

Decrease donor lifetime

$$E = \frac{R_0^6}{R_0^6 + r^6} = 1 - \frac{F_{DA}}{F_D}$$

$$R_0^6 = \frac{9000 \ln(10) \kappa^2 \phi_D}{128 \pi^5 N_A n^4} J \qquad \text{where, } J = \frac{\int F_D(\lambda) \varepsilon_A(\lambda) \lambda^4 d\lambda}{\int F_D(\lambda)}$$

Quantification of Mechanotransduction with Foster resonance energy transfer (FRET)

Src phosphorylation dynamics

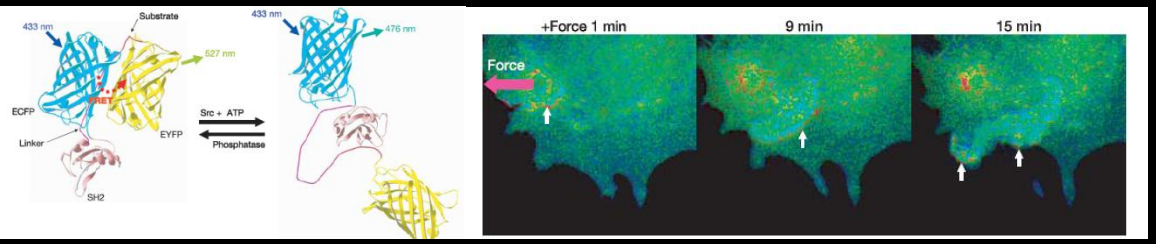

Wang et al., Nature 2005

MscL activation

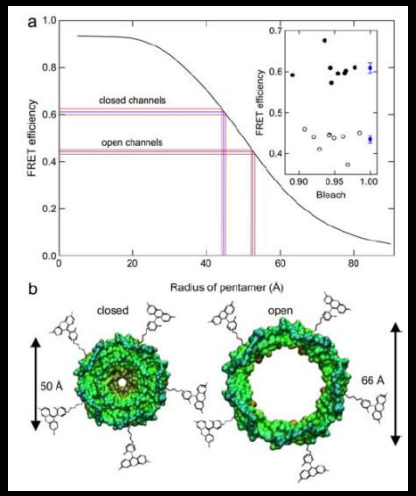

Corry et al., BJ 2005

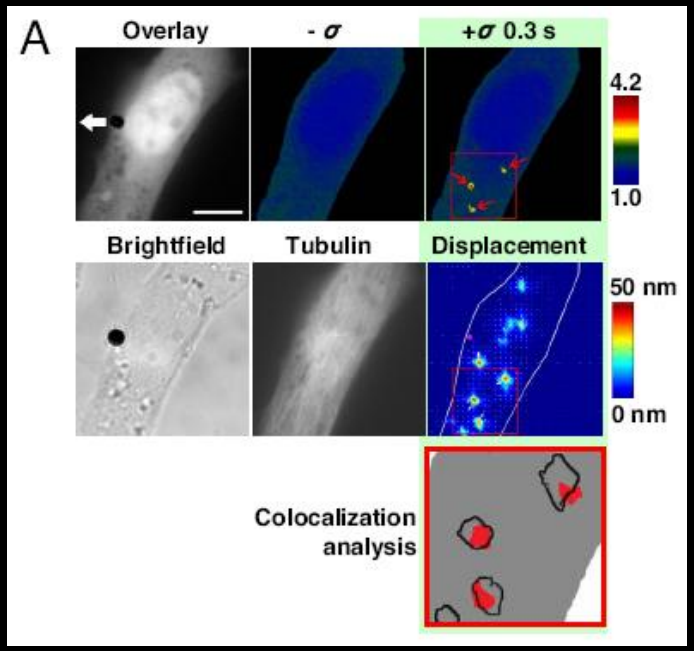

Na et al., PNAS 2008

GPCR conformation change

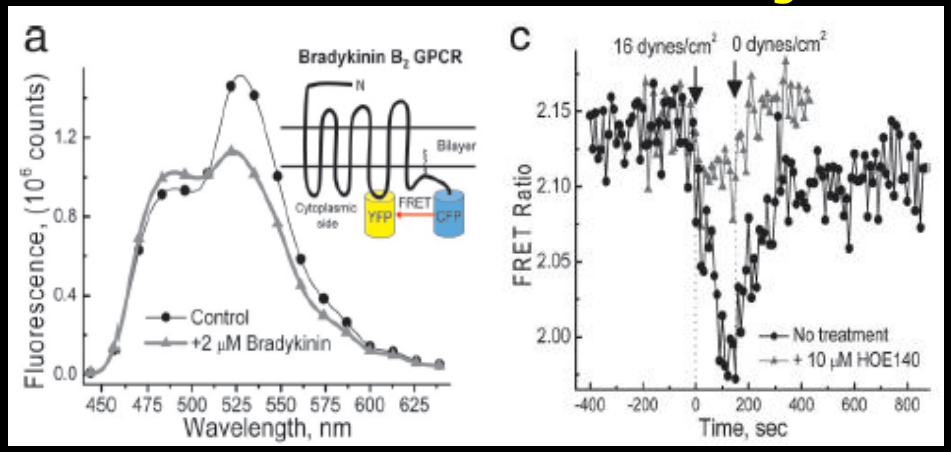

Chachivilis et al., PNAS 2008

Fluorescence Resonance Energy Transfer (FRET)

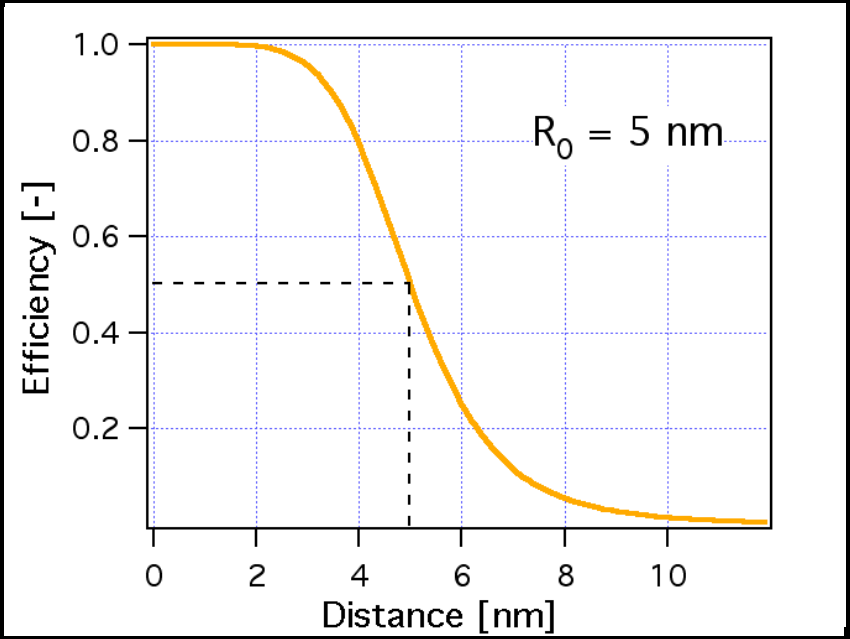

Dipole - dipole interaction

r^6 dependence

Efficiency

50% energy transfer

Förster distance

R_0 = 40 to 70 Å

Decrease donor intensity

Increase acceptor intensity

Decrease donor lifetime

$$E = \frac{R_0^6}{R_0^6 + r^6} = 1 - \frac{F_{DA}}{F_D}$$

$$E = \frac{R_0^6}{R_0^6 + r^6} = 1 - \frac{\tau_{DA}}{\tau_D}$$

$$R_0^6 = \frac{9000 \ln(10) \kappa^2 \phi_D}{128 \pi^5 N_A n^4} J$$

where, $J = \frac{\int F_D(\lambda) \varepsilon_A(\lambda) \lambda^4 d\lambda}{\int F_D(\lambda)}$

“Quantify” Signaling Pathway Using t-FRET

1. High receptor concentration, No ligand

2. High receptor concentration, Full ligand coverage

3. High receptor concentration, low ligand coverage

4. Low receptor concentration, low ligand coverage

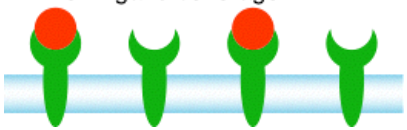

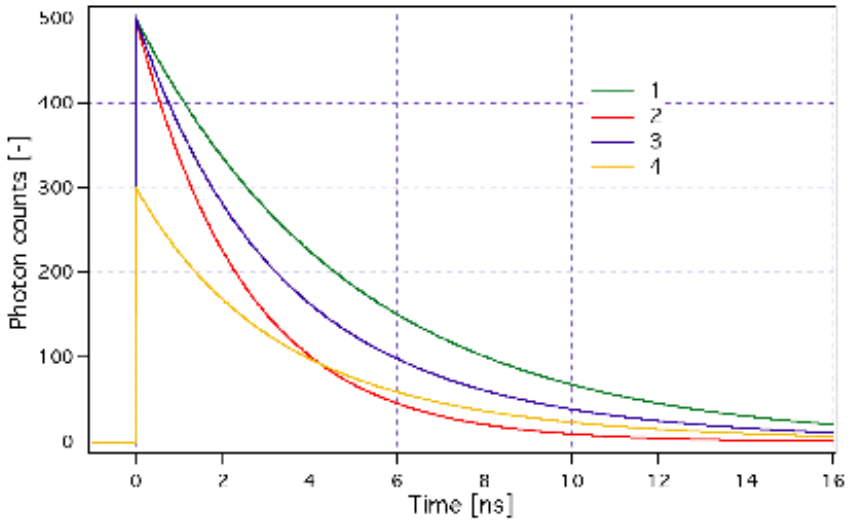

$$I_{\mathrm{i}}^{\mathrm{model}}(t) = \int_0^{\mathrm{t}} G(t-T) \times c_{2\mathrm{i}+1} \left(c_{2\mathrm{i}+2} \exp\left(-\frac{T}{c_1}\right) + (1 - c_{2\mathrm{i}+2}) \exp\left(-\frac{T}{c_2}\right)\right) \mathrm{d}T.$$

What can we quantify?

- Is there binding?

  Presence or absence of FRET

- What is the conformation of the bound molecule?

  FRET Efficiency: $E = \frac{R_0^6}{R_0^6 + r^6} = 1 - \frac{\tau_{DA}}{\tau_D}$

- What is the fraction of molecule bound?

  FRET ratio: $[P-F]/[P] = I_{P-F} / I_P$

- What is the thermodynamic constants of binding?

  Dissociation constant & Gibb's free energy

$$\ln K = -\frac{\Delta G}{kT} = \frac{[P][F]}{[P-F]}$$

Use fluorescence correlation spectroscopy to get [F]

Fluorescence Correlation Spectroscopy (FCS)

Poisson statistics: $\sigma_n^2 = \bar{n}$

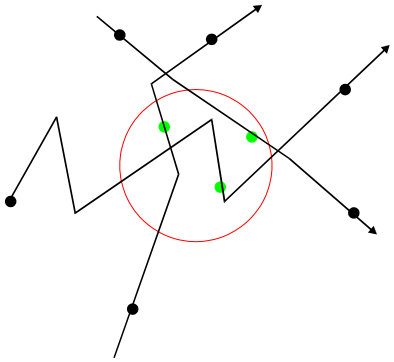

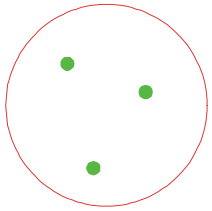

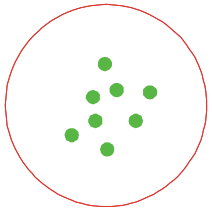

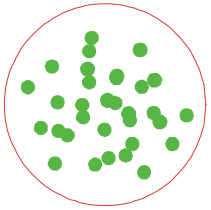

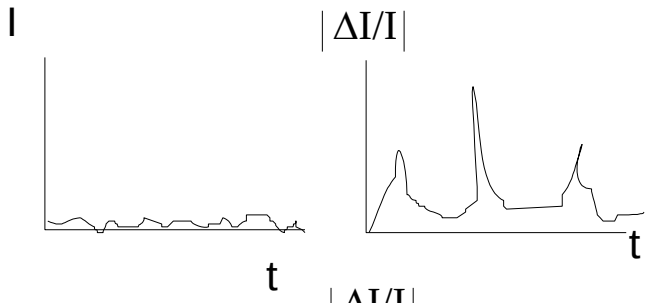

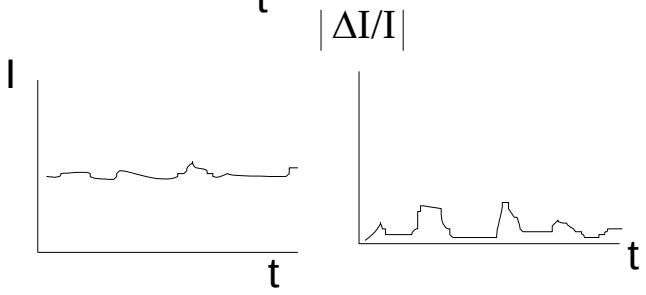

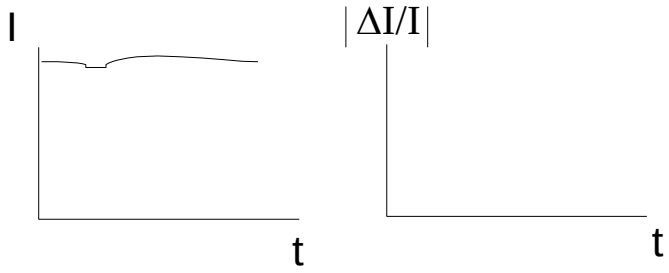

FAT and Paxillin Binding

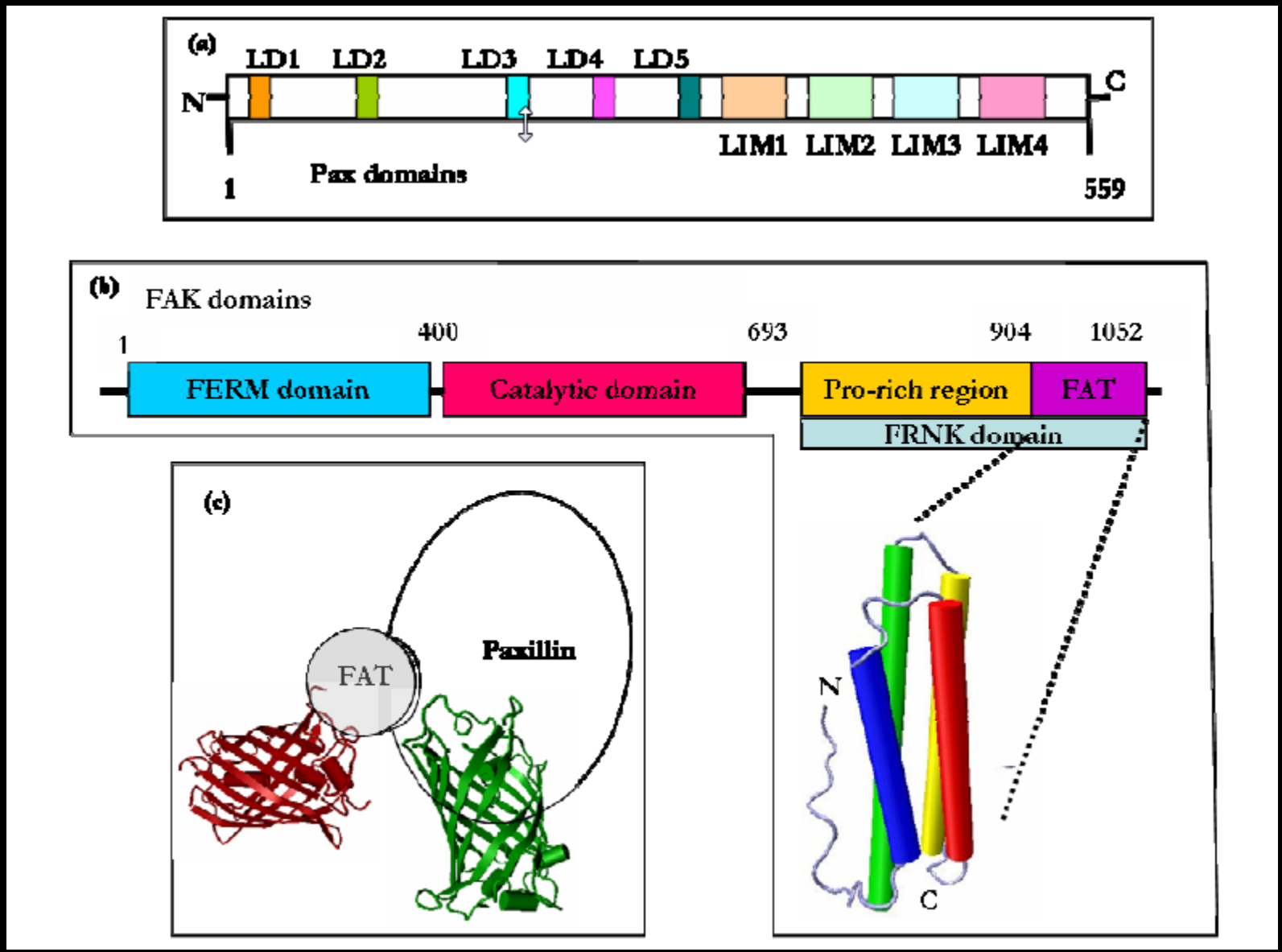

Thermodynamics of Pax/FAT Interaction

Bovine aortic endothelial cells (BAECs)

Co-transfected with Pax and FAT plasmids

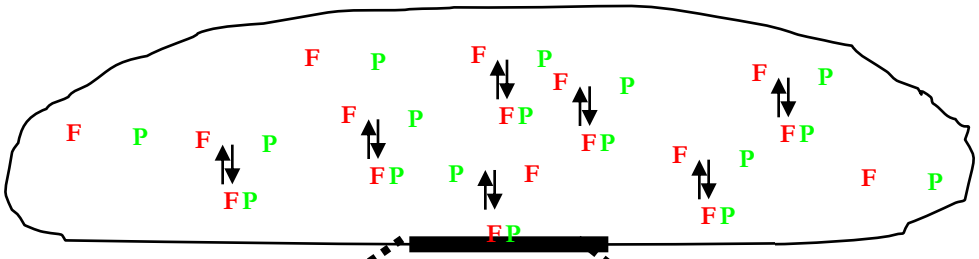

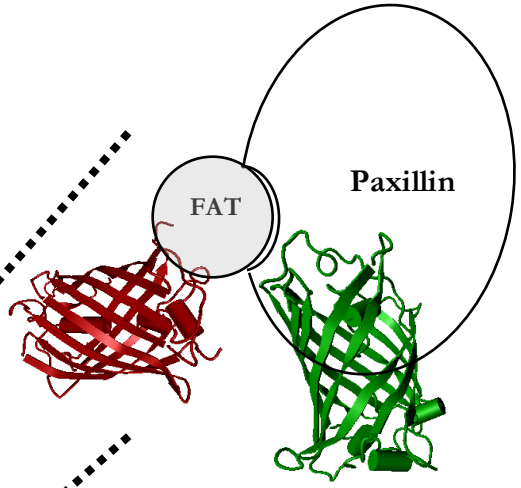

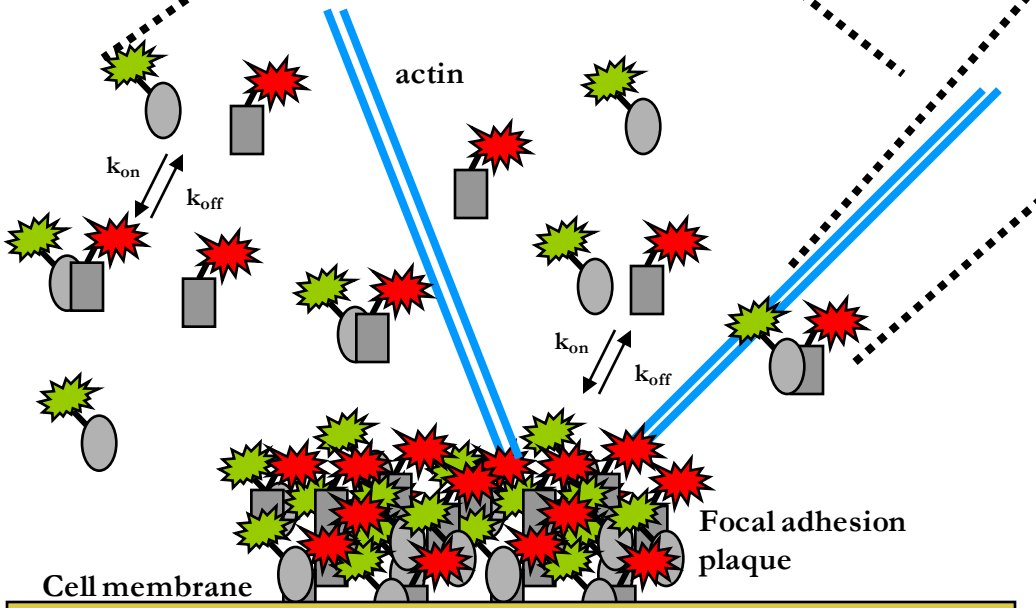

$$\text{FAT-mCh}_{\text{cyto}} + \text{GFP-Pax}_{\text{cyto}} \underset{k_{on}}{\overset{k_{off}}{\rightleftharpoons}} \text{FAT-mCh---GFP-Pax}_{\text{cyto}}$$

$$K_d = \frac{[\text{FAT}] * [\text{Pax}]}{[\text{FAT-Pax}]}$$

How to measure k_d & ΔG spectroscopically

$$K_d = \frac{[\text{FAT}] * [\text{Pax}]}{[\text{FAT-Pax}]}$$

For a given cell, measure concentrations or ratio of concentrations

$$\rightarrow \quad \frac{[\text{Pax}]}{[\text{FAT-Pax}]} = \frac{1}{1 - \text{FRETratio}}$$

$$\rightarrow \quad \eta = 1 - \frac{\text{FRETlifetime}}{\text{non-FRETlifetime}}$$

$\rightarrow$ B = Green molecule intensity/C_{gfp} = [Pax] +(1-η)[FAT- Pax]

$\rightarrow$ C = Red molecule intensity/C_{mc} = [FAT] + [FAT-Pax] + B/γ

C_{gfp} is the brightness of gfp, C_{mc} is the brightness of m-cherry,
γ is a parameter characterizing bleedthrough from the green to the red channel

Solve simultaneous equations to obtain K_d. Calculate Gibbs free energy, $\Delta G = RT \ln K_d$

In vitro systems exist to measure K_d for purified protein pairs e.g. isothermal titration calorimetry (ITC) and surface plasmon resonance (SPR) but no *in vivo* methods exist.

Typical FLIM-FRET & FCS data

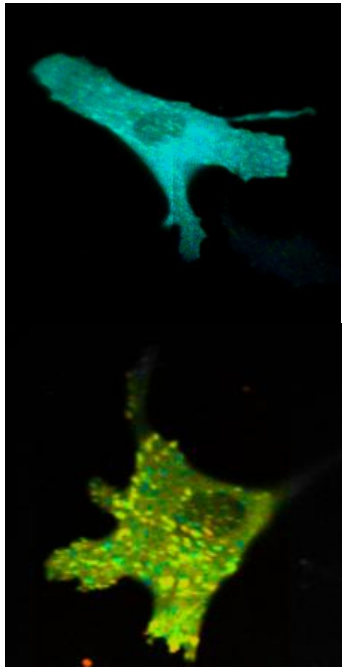

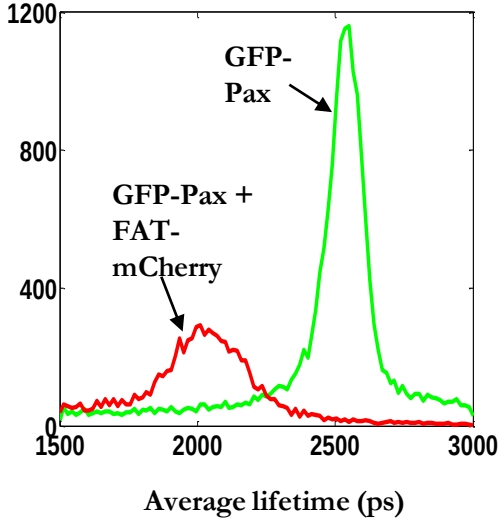

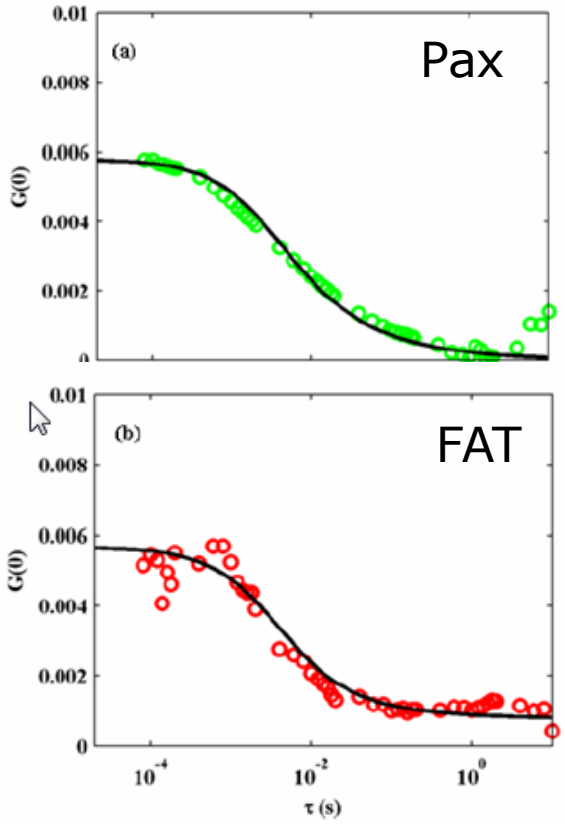

Quantification of a single cell

FRET

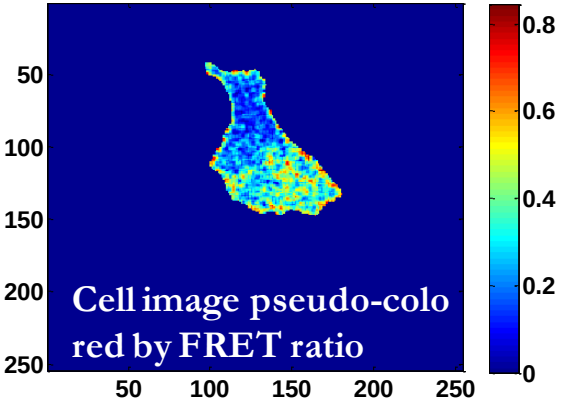

Fixed τ_1 = 2.6ns, fit τ_2 = 1.9ns

⇒ R ~ 56Å

$\eta = 1 - \tau_2/\tau_1 = 0.2692$

Solve simultaneous equations to obtain K_d

FRET / FLIM: $\dfrac{[\text{FAT-Pax}]}{[\text{Pax}] + [\text{FAT-Pax}]} = A$

FCS @ 890nm: [Pax] +(1-η)[FAT- Pax] = B

FCS @ 780nm: [FAT] + [FAT-Pax] + B/17 = C

FCS

Calibration	Red ch	Green ch
Intensity	0.3	5.2
Concentration	18.2 nM	21.8 nM

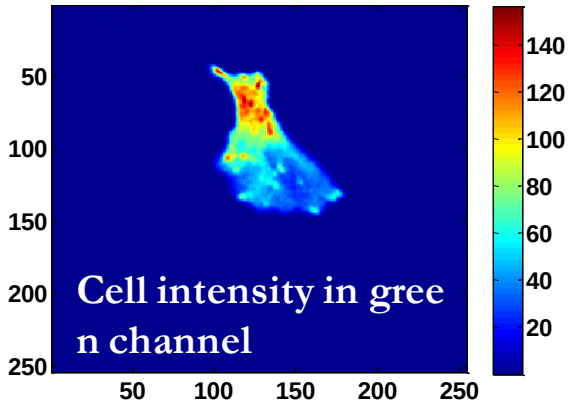

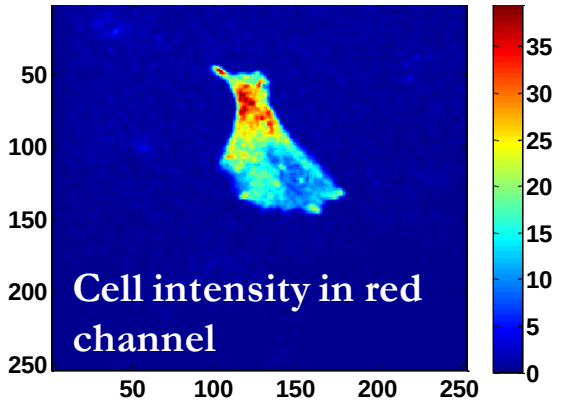

Thermodynamics of Pax/FAT Interaction in a single cell

Histogram of K_d for cytosolic region

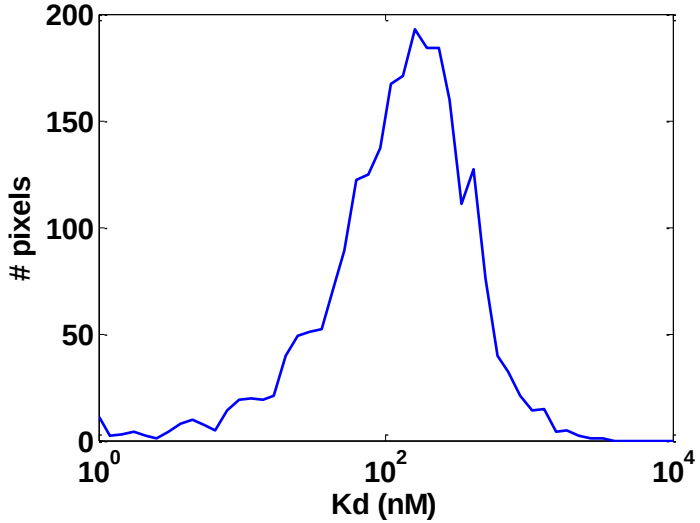

- Histogram peaks at K_d value ~200nM

$$K_d = \frac{[\text{FAT}] * [\text{Pax}]}{[\text{FAT-Pax}]}$$

$$[\text{FAT}] = K_d \frac{[\text{FAT-Pax}]}{[\text{Pax}]}$$

[FAT] vs [FAT-Pax]/[Pax]

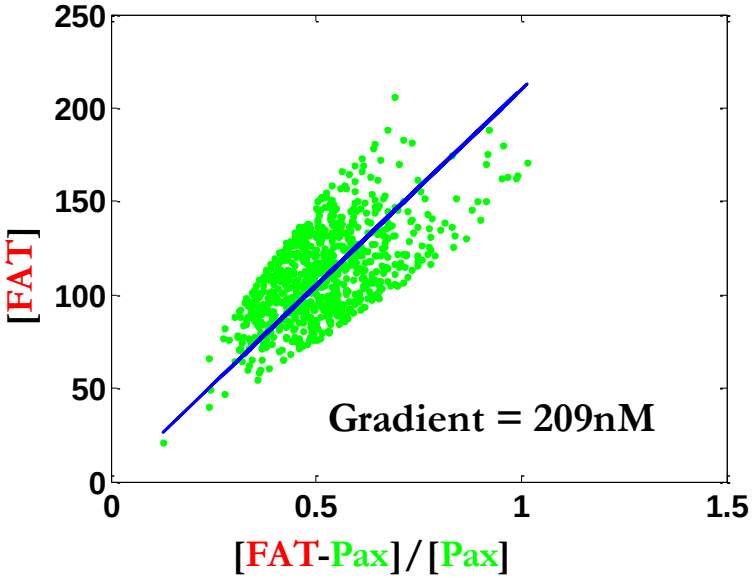

Pixels within 3 bins on either side of histogram peak

Linear fit result

Variation of ΔG across different cells

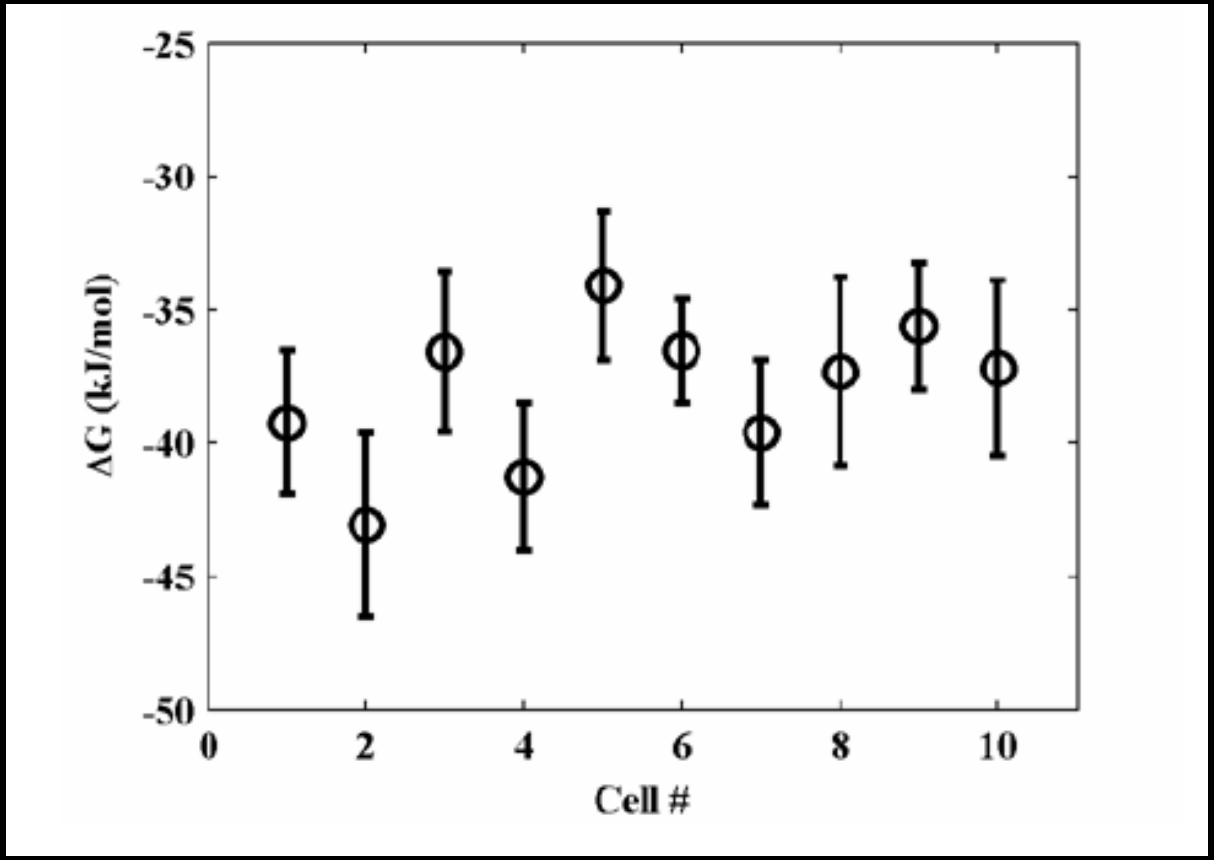

Measurement of 10 distinct cells over three days
Error bars are std dev in one cell

Compare k_d & ΔG with in vitro system

Spectroscopic measurement: K_d = 367 ± 33 nM (S.E. 10 cells)

In vitro results:

- Isometric Titration Calorimetry (ITC) *Gao et. al. J. Biol Chem. 2004*

K_d ~ 10 μM for FAT + 1 LD domain of Pax

- Surface Plasmon Resonance (SPR): *Thomas et. al. J. Biol Chem. 1999*

K_d ~ 4 μM for FAT + 1 LD domain of Pax

K_d ~ 300 – 600 nM for FAT + both LD domains of Pax that bind FAT

Paxillin-FAT interaction shows significant allosteric effect both in vivo & in vitro

Protein states in FAC vs cytosol?

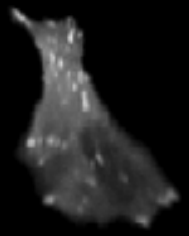

Pax intensity image

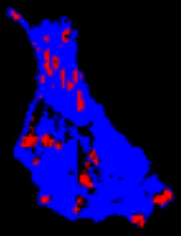

Segmentation Mask for FACs

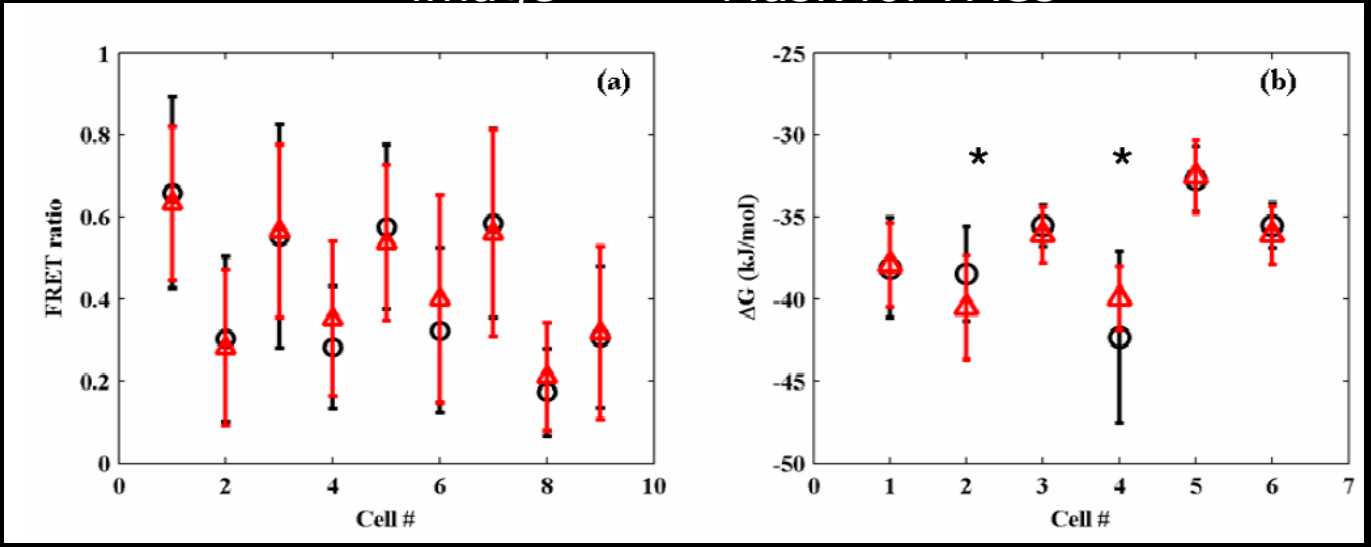

No significant differences in binding constants is observed FAC vs cytosol →paxillin-FAT mechanosensitivity is not via direct force induced protein deformation

Is paxillin-FAT binding mechno-sensitive?

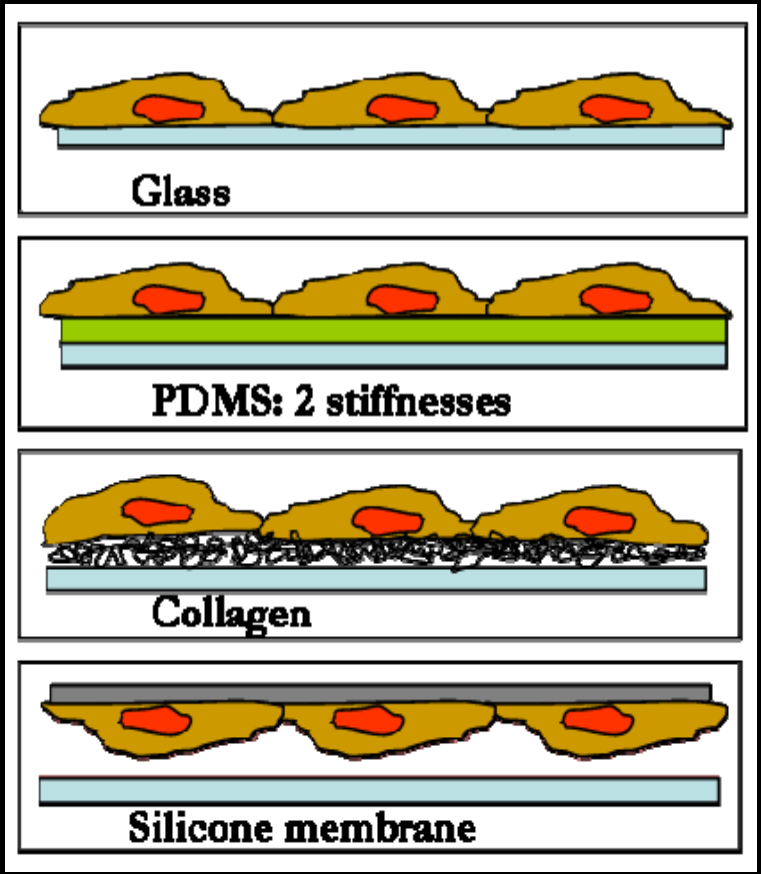

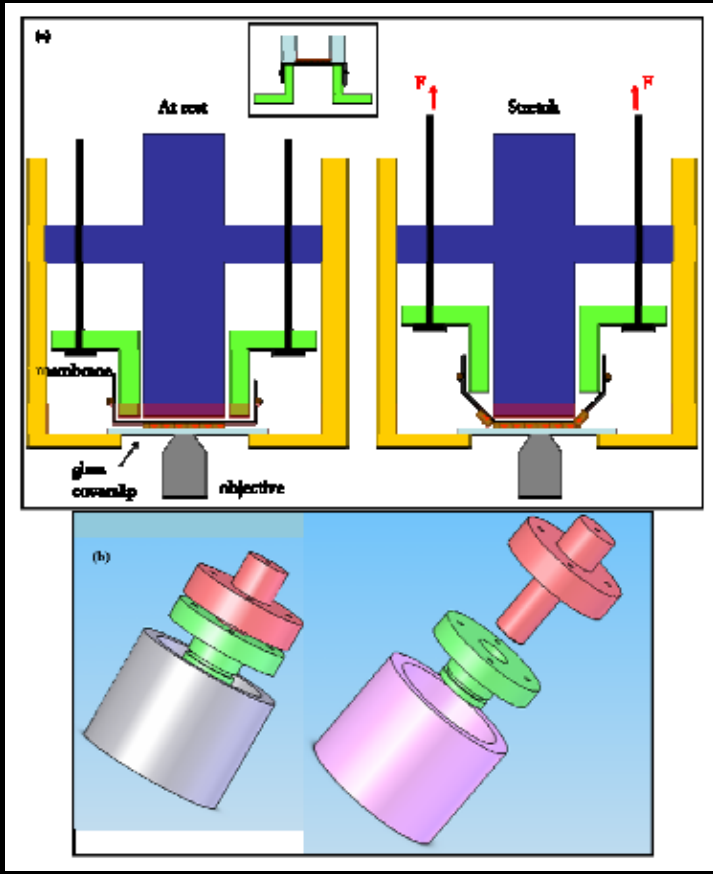

Vary substrate shear modulus

Apply bi-axial stretching (up to 10%)

Effect of Substrate Stiffness

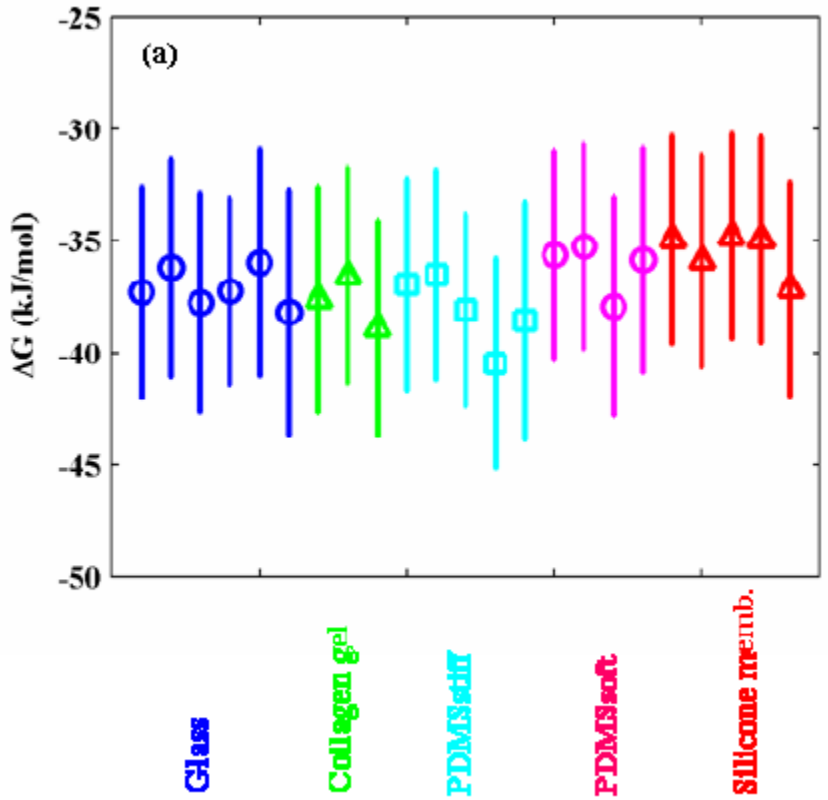

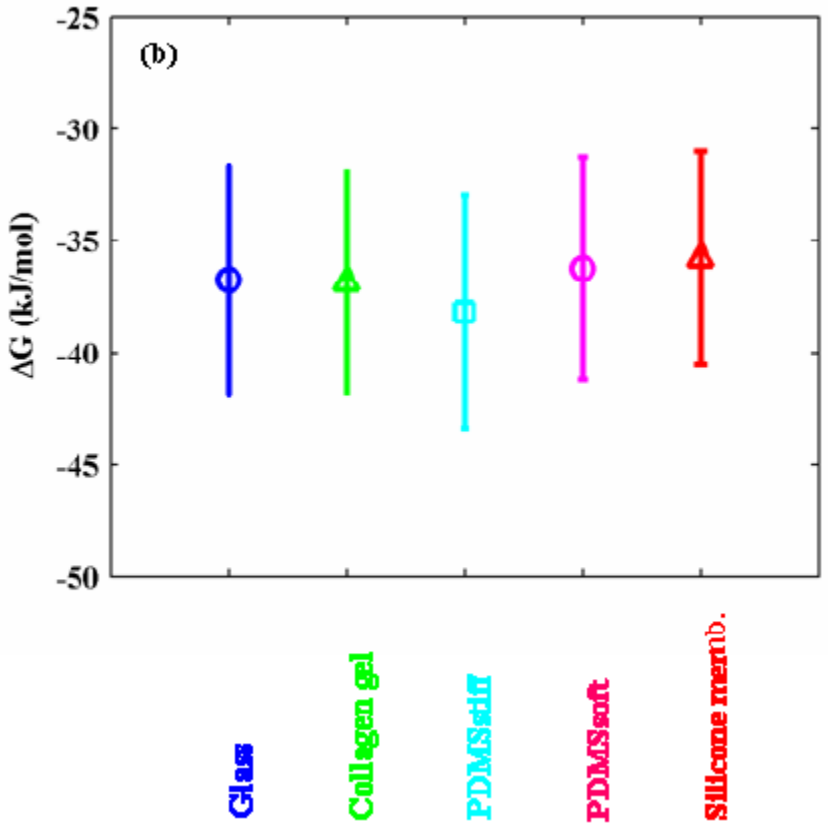

No significant differences in binding constants as a function of substrate stiffness

Effect of Bi-axial Stretch

Static Stretch

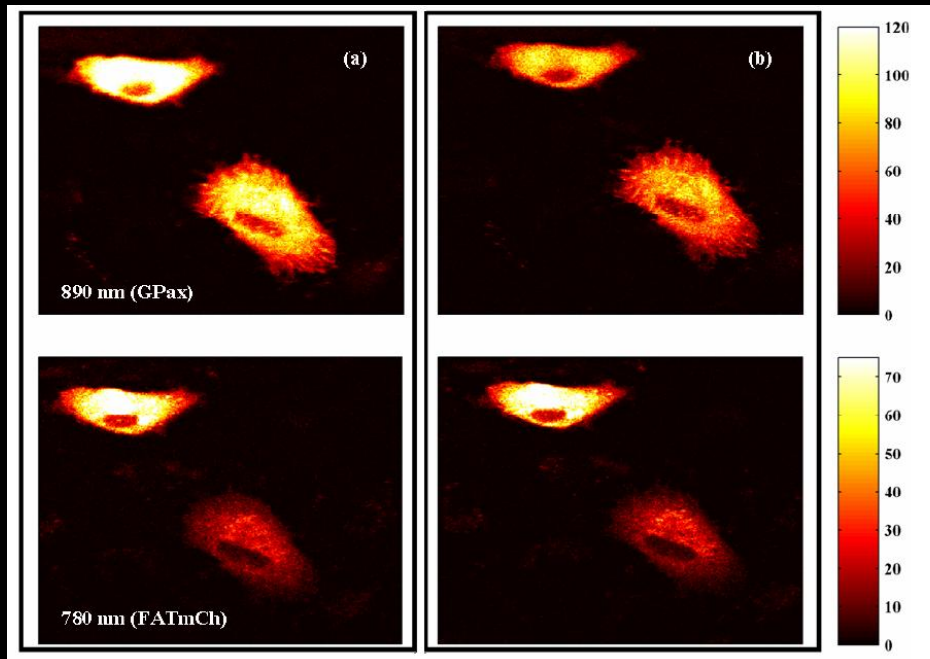

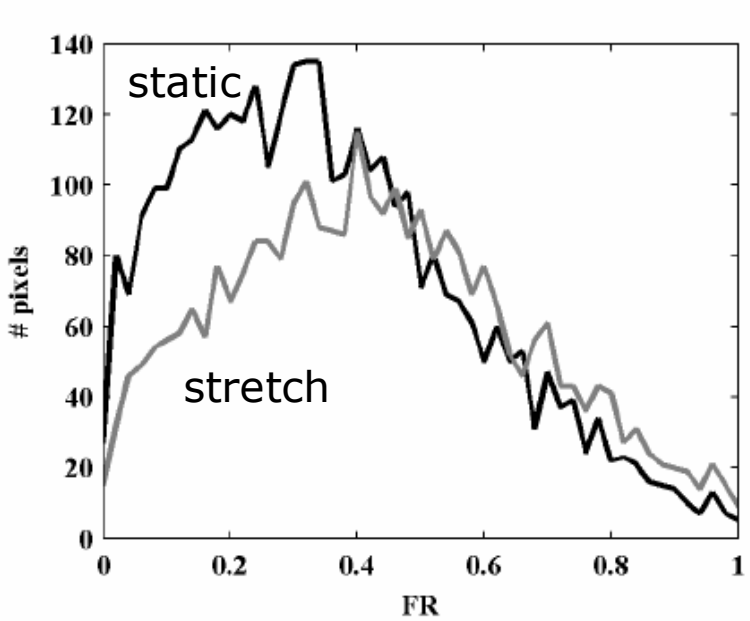

Shift in FRET Ratio distribution

FRET ratio increases → Larger fraction of paxillin is bound
FRET efficiency increase → Tighter binding and a GFP-mCherry distance reduction by 2A.

Bi-Axial Stretching Results for 5 cells

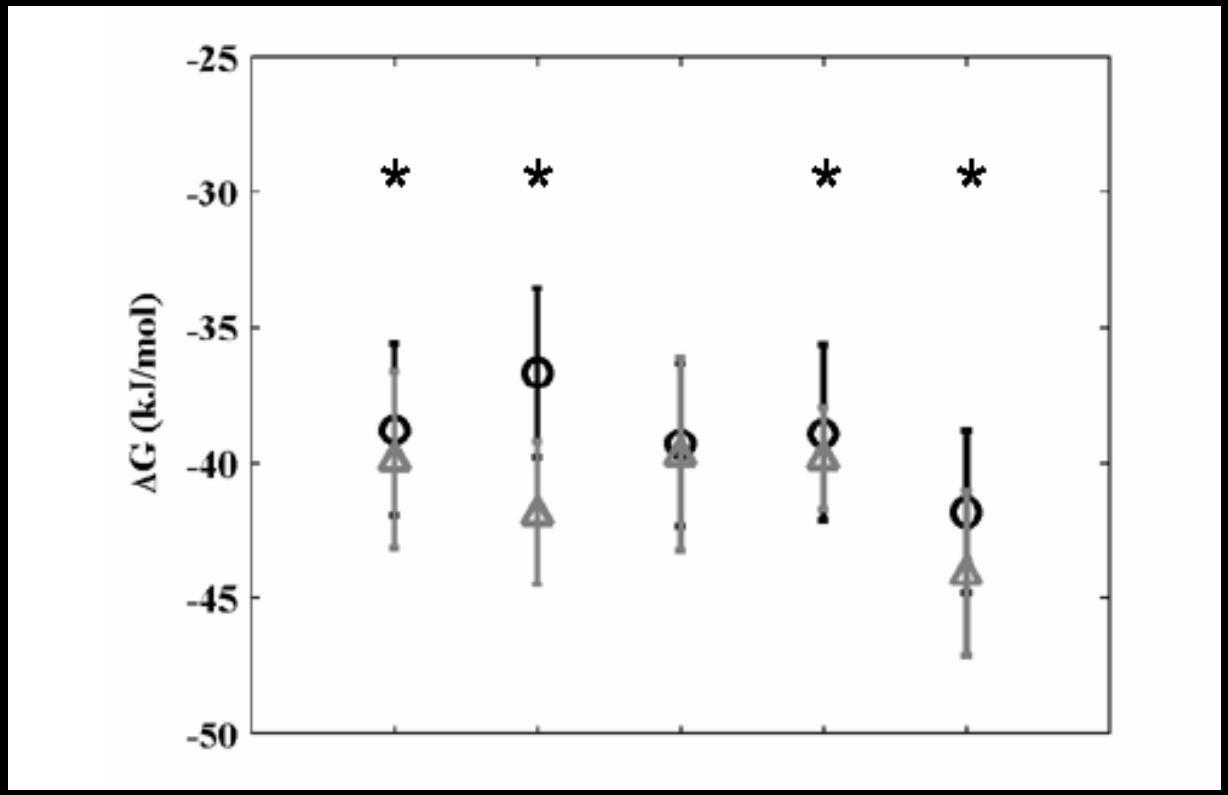

* indicates $p<0.05$

Chemical disruption to mechanotransduction

Cytochlastin D

Genistein

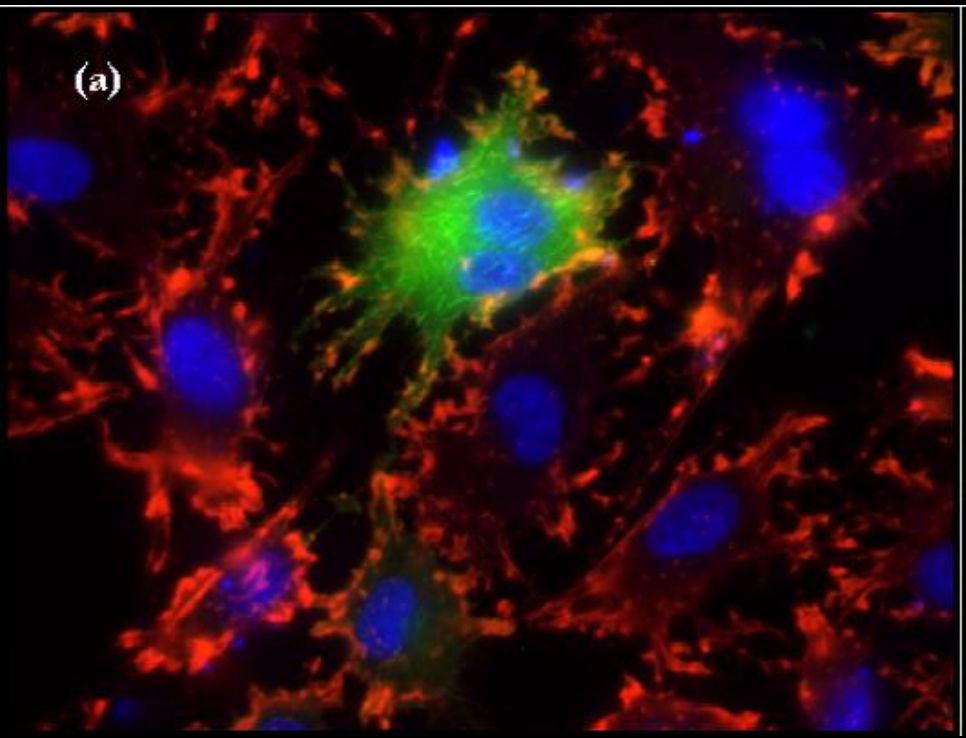

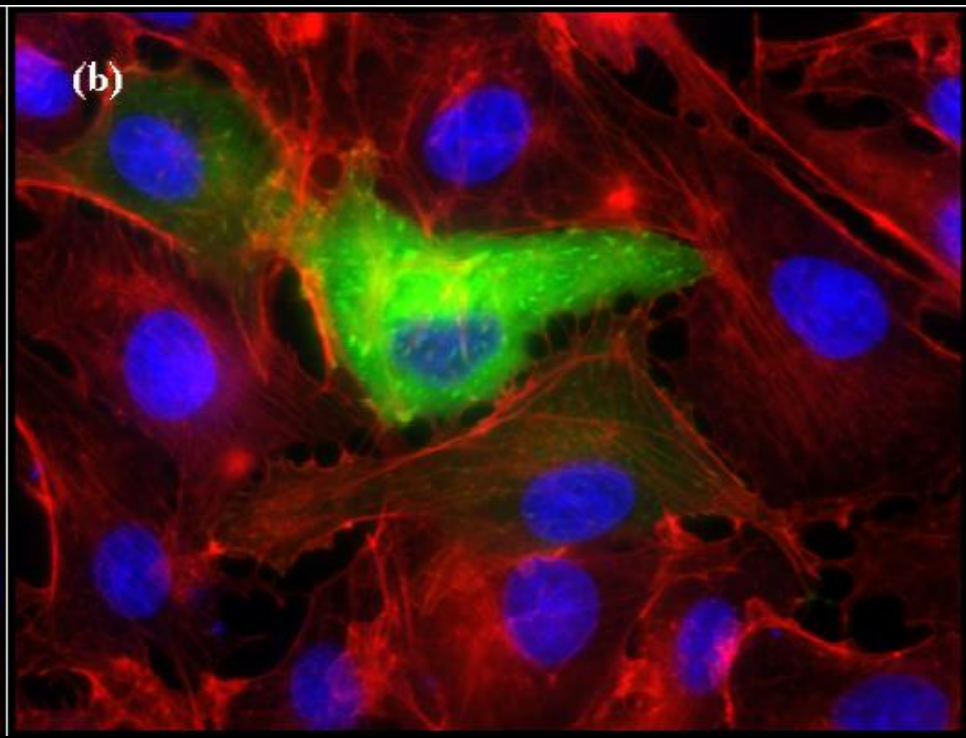

Blocks actin polymerization

Blocks protein tyrosine phosphorylation

Blocking of stretch responses

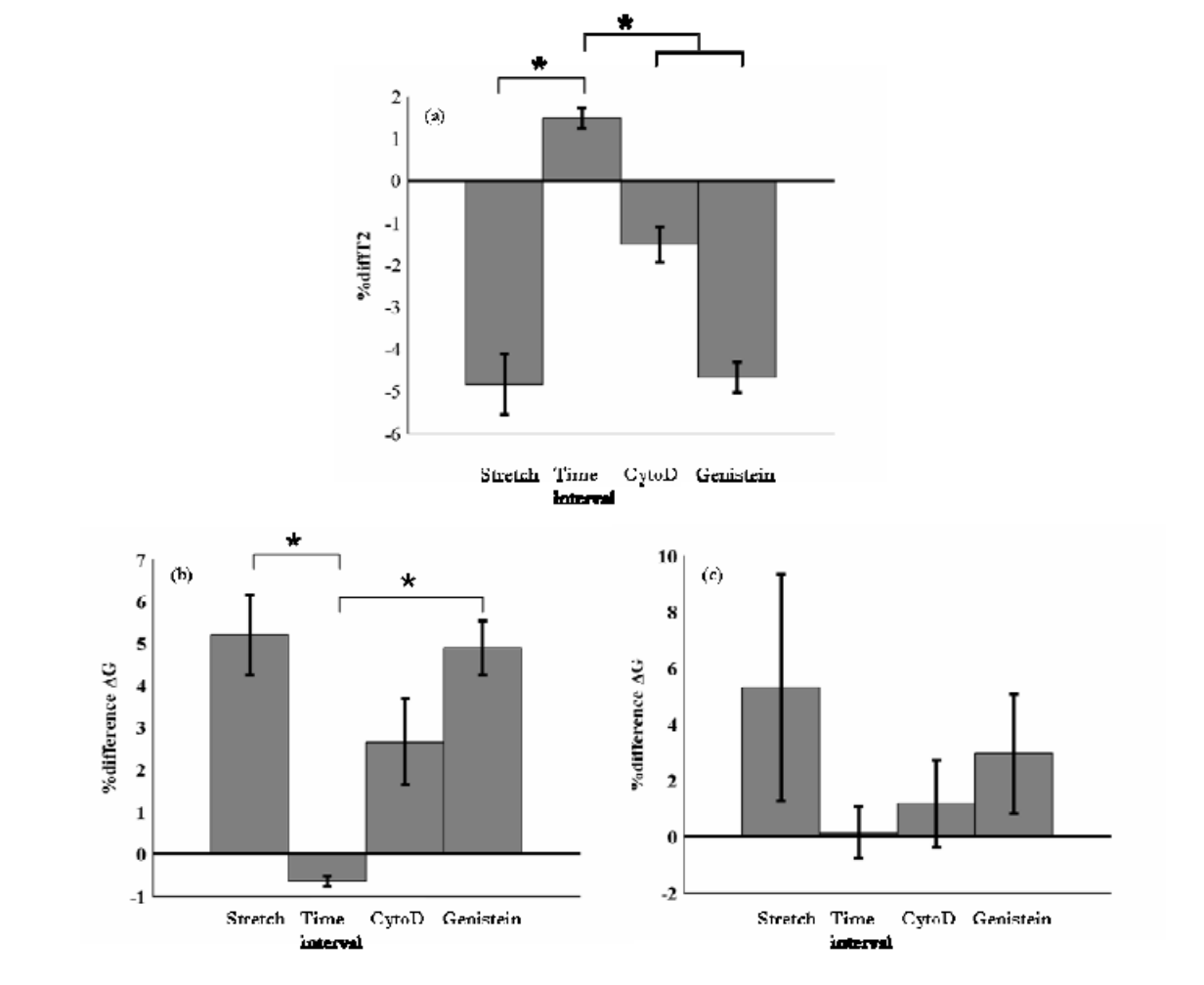

Disruption of actin cytoskeleton (via cytoD) reduces mechanotransduction
Blocking tryosine phosphorylation does not block mechanotransduction

Conclusion

Demonstrate measurement of intra-cellular protein dissociation constants via FLIM-FRET & FCS
(Aother option is FCCS: Ruan & Tetin, Anal. Biochem 2007
Bacia & Schwille, Nat. Prot,. 2007)

Pax-FAT has in vivo dissociation constant of 350 nM

GFP-mcherry is separated by 5.6 nm in bound complex

Pax-FAT binding appears to show allosteric effect in vivo

Binding constants for Pax-FAT is similar between FAC & cyotsol

10% bi-axial stretch results in tighter Pax-FAT binder with a 0.2 nm decrease in GFP-mcherry distance

Disruption of actin cytoskeletin blocks mechano-effect on Pax-FAT binding but blocking tryosine phosphorylation does not.

Future work

(1) Further elucidate mechanisms for paxillin-FAT mechano-sensitivity

(2) Studied other protein partners in the FAC (talin-vinculin)

Challenge: This binary mode of studying protein interaction is ultimately limited when many proteins, such as paxillin and FAK, Have 10s of bindin partners and allosteric effects may be significant (Slaughter et al., PNAS 2007)

(3) Understand tissue physiology/pathology based on models of cellular mechanotransduction pathways

Challenge: Single cell behavior in 2D cell culture is not a good predictor for behavior (both individual & collective) in 3D tissues.

Acknowledgement

Dr. Nur Aida Abdul Rahim, MIT

Prof. Roger Kamm, MIT